Freie Universität Berlin

Ball Packings
and
Lorentzian Discrete Geometry

by

陈 浩
CHEN, Hao

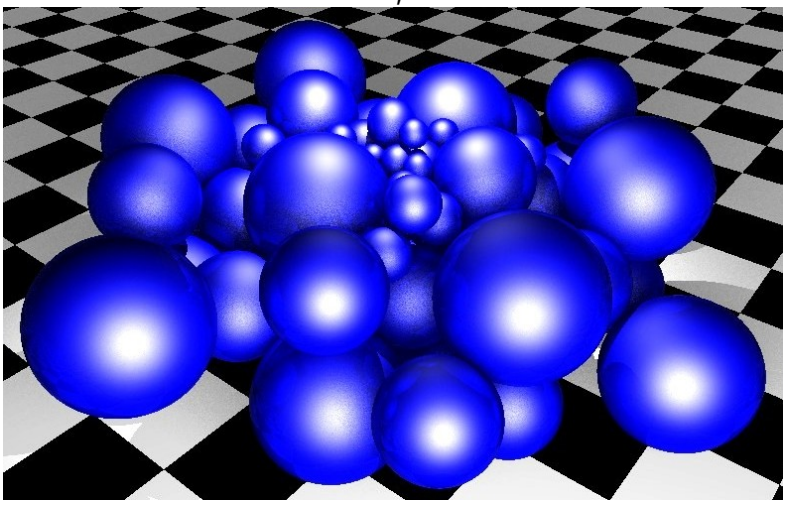

A thesis submitted in partial fulfilment of the requirements
for the degree of Doctor of Mathematics

in the
Institut für Mathematik
Fachbereich Mathematik und Informatik
Freie Universität Berlin

Berlin
July 28, 2014

Supervisor and first reviewer:
Prof. Günter M. Ziegler

Second reviewer:
Prof. Christophe Hohlweg

Date of defense:
June 11, 2014

Institut für Mathematik
Freie Universität Berlin

To my wife.

Summary

While the tangency graphs of disk packings are completely characterised by Koebe–Andreev–Thurston's disk packing theorem, not so much is known about the combinatorics of ball packings in higher dimensions. This thesis tries to make a contribution by investigating some higher dimensional ball packings.

The key idea throughout this thesis is a correspondence between balls in Euclidean space and space-like directions in Lorentz space. This allows us to interpret a ball packing as a set of points in the projective Lorentz space.

Our investigation starts with Descartes' configuration, the simplest ball packing studied in this thesis. It serves as the basic element for further constructions. Then we explicitly construct some small packings whose tangency graph can be expressed as graph joins, and identify some graph joins that are not the tangency graph of any ball packing. With the help of these examples, we characterise the tangency graphs of Apollonian ball packings in dimension 3 in terms of the 1-skeletons of stacked polytopes. Partial results are obtained for higher dimensions.

Boyd–Maxwell packings form a large class of ball packings that are generated by inversions, generalising Apollonian packings. Motivated by their appearance in recent studies on limit roots of infinite Coxeter systems, we revisit Boyd–Maxwell packings. We prove that the set of limit roots is exactly the residual set of Boyd–Maxwell packings. Furthermore, we describe the tangency graph of a Boyd–Maxwell packing in terms of the corresponding Coxeter complex, and complete the enumeration of Coxeter groups generating these packings. We then propose a further generalization, which may exist in much higher dimensions.

Motivated by a result of Benjamini and Schramm, we also study ball packings whose tangency graph is a higher dimensional grid graph. We give a loose bound on the size of such grid graphs that admit a ball packing.

Acknowledgement

I'm grateful to my supervisor, Günter M. Ziegler, for his guidance and trust. Without your encouragement, I could not imagine how my transition from physics to mathematics would go. To my co-author, Jean-Philippe Labbé, who showed me Figure 3.1(a), which led me to the topic of Coxeter group. Working along with you has been a great pleasure. I'm thankful to George Maxwell, for his great availability to check the enumeration results in the Appendix. To Igor Rivin, Yaokun Wu, Richard Klitzing, and the reviewer of this thesis, Christophe Hohlweg. Some ideas in this thesis emerged from the discussions with you. I'm also thankful to Boris Springborn, Vivien Ripoll, and my mentor, Stefan Felsner, for very inspiring discussions. To my collegues in the discrete geometry workgroup, especially Raman Sanyal, Karim Adiprasito, Louis Theran, Bernd Gonska, Ivan Izmestiev, Cesar Cellabos, Christian Stump, Emerson Leon, Moritz Firsching for very helpful discussions and suggestions. I would also like to acknowledge Elke Pose and Dorothea Kiefer, who helped me with all the paper work.

I would like to express my gratitute to my wife for her support and understanding. She allows me to think about mathematics when she is shopping. To my parents, who support me even though they don't understand anything of my research. To Robert and Christine Bozza. You treated me as a son during my stay in France. I would like to thank my teachers in Ecole Polytechnique. Because of you, I failed an exam of mathematics for the first time in my life, and decided to switch my major from physics to mathematics. It's still you who made this transition possible. I'm especially thankful to Jean-Pierre Bourguignon for his encouragement and continued support. To Jürgen Jost from MPI for Mathematics in Sciences, for his guidance and supervision during my first research project. I would also like to thank MPI for Colloid and Interface, where my wife works. I was allowed to stay in the library and write many of the manuscripts.

My doctoral research is supported by the Deutsche Forschungsgemeinschaft within the Research Training Group 'Methods for Discrete Structures' (GRK 1408).

Contents

Introduction

A ball packing is a collection of balls in Euclidean space with disjoint interiors. The tangency graph of a ball packing takes the balls as vertices and the tangency relations as edges.

For disk packings, i.e. ball packing in dimension 2, the tangency graphs are completely characterized by Koebe–Adreev–Thurston's disk packing theorem. In higher dimensions, studies have been focused on congruent ball packings, i.e. every ball has the same size. The main problem is to find the densest packing. However, not so much is known about the tangency graph of non-congruent ball packings. In other words, we have no systematic way to tell if a given graph is the tangency graph of a ball packing. Among the few works dealing with higher dimensional non-congruent ball packings, there are Kuperberg and Schramm [54] on the average degree, Alon [3] on the minimum degree, Cooper and Rivin [28] on rigidity, Miller et al. [66] on separator properties, Benjamini and Schramm [7] on lattice graphs, and Maehara [57] on chromatic number, etc. We will review these work in Section 1.3.1.

This thesis tries to make a contribution to the knowledge and understanding of higher dimensional ball packings. The key idea throughout the thesis is a representation of balls as space-like directions in Lorentz space, see Sections 1.2.2 and 1.3. In such a representation, the tangency relations between balls are indicated by the Lorentz distances between normalized space-like vectors. This allows us to reformulate problems about ball packings in the language of Lorentzian discrete geometry.

The thesis is organized as follows. In Chapter 1, we define our main object of study, introduce important notions and techniques, and review previous studies that are relevent to the study of ball packings. The remaining of the thesis is devoted to the following classes of ball packings.

We start Chapter 2 with Descartes' configurations. In dimension d, a Descartes' configuration is a collection of $d+2$ pairwise tangent balls. The tangency graph of a Descartes' configuration is a complete graph. This packing is simple yet exhibits interesting properties. In particular, Descartes theorem and its generalizations in higher dimensions reveal strong relations between the curvatures and centers of the balls in a Descartes' configuration. Descartes' configurations, and a generalization by Boyd (see

Section 2.1.2), serve as basic elements for the constructions of many packings studied in this thesis.

In Section 2.2, we study some small ball packings whose tangency graph can be expressed as graph joins. These constructions give an intuition on the difference between disk packings and higher dimensional ball packings. Furthermore, we identify some graph joins that are not the tangency graphs of any ball packing in a given dimension. These graphs are therefore forbidden induced subgraphs for the tangency graphs of ball packings.

An Apollonian packing is constructed from a Descartes' configuration by repeatedly introducing new balls to form new Descartes' configurations. In dimension 2, the tangency graph of an Apollonian disk packing is the 1-skeleton of a stacked 3-polytope. In Section 2.3, we compare tangency graphs of Apollonian packings to 1-skeletons of stacked polytopes in higher dimensions. Based on our results on graph joins, we obtain a forbidden induced graph characterisation for Apollonian ball packings in dimension 3. For even higher dimensions, partial results are obtained.

Apollonian packings can be generated by inversions. Boyd–Maxwell packings, developed by Boyd in 1973 [12], form a large class of packings that are generated by inversions, including Apollonian packings as special cases. Maxwell [62] related these packings to Lorentzian Coxeter systems. Motivated by recent studies on limit roots, we revisit Boyd–Maxwell packings in Chapter 3, and prove that the set of limit roots is exactly the residual set of the corresponding Boyd–Maxwell packings. This is joint work with Jean-Philippe Labbé. Furthermore, we describe the tangency graphs of these packings in terms of Coxeter complexes, see Section 3.3. We also complete the enumeration of Coxeter groups that generate Boyd–Maxwell packings. The algorithm and the complete list is given in Appendix A.

Inspired by recent studies of limit roots, we propose in Section 3.4 two further generalizations of Boyd–Maxwell packings. One of them concerns non-packing ball clusters, similarly generated as Boyd–Maxwell packings. The other extends Maxwell's work to degenerate Lorentzian Coxeter systems. The latter produces a large family of examples in much higher dimensions for infinite ball packings generated by inversions..

Chapter 4 is independent to the previous Chapters. Motivated by a result of Benjamini and Schramm [7] on the ball packing of infinite lattice graphs, we study ball packings whose tangency graphs are finite grid graphs in higher dimensional space. We give a loose bound on the size of such grid graphs, and explicitly construct some small examples.

Chapter 1

Representing balls in Lorentz space

1.1 Balls

Balls are perhaps one of the most common objects in mathematics. In this thesis, we also consider balls of infinite radius or negative radius, so the definition of a ball is slightly different from the usual one. In this section, we define basic notions like balls and spheres, and relations between balls such as tangency, disjointness and overlapping. We also introduce various ways of coordinating balls.

1.1.1 What is a ball?

We work in the d-dimensional extended Euclidean space $\hat{\mathbb{R}}^d = \mathbb{R}^d \cup \{\infty\}$. Let $\|\cdot\|$ denote the Euclidean norm, and $\langle \cdot, \cdot \rangle$ denote the Euclidean inner product.

Definition 1.1.1. A *d-ball* of *curvature* κ is one of the following sets:

- $\{\mathbf{x} \in \hat{\mathbb{R}}^d \mid \|\mathbf{x} - \mathbf{c}\| \leq 1/\kappa\}$ if $\kappa > 0$;
- $\{\mathbf{x} \in \hat{\mathbb{R}}^d \mid \|\mathbf{x} - \mathbf{c}\| \geq -1/\kappa\} \cup \{\infty\}$ if $\kappa < 0$;
- $\{\mathbf{x} \in \hat{\mathbb{R}}^d \mid \langle \mathbf{x}, \hat{\mathbf{n}} \rangle \geq b\} \cup \{\infty\}$ if $\kappa = 0$.

In the first two cases, the point $\mathbf{c} \in \mathbb{R}^d$ is called the *center* of the ball, and $1/\kappa$ is the *radius* of the ball. In the second case, the ball is considered to have negative radius. In the last case, a closed half-space is considered as a ball of infinite radius, the unit vector $\hat{\mathbf{n}}$ is called the *normal vector*, and $b \in \mathbb{R}$. The boundary of a d-ball is called a $(d-1)$-*sphere*. It is a $(d-1)$-dimensional hyperplane if the ball is of curvature 0. In this thesis, balls and spheres are denoted by sans-serif upper-case letters, such as B and S.

For a ball $\mathsf{B} \subset \hat{\mathbb{R}}^d$, the *curvature–center coordinates*, introduced by Lagarias, Mallows and Wilks in [55], is defined as follows:

$$\mathbf{m}(\mathsf{B}) = \begin{cases} (\kappa, \kappa\mathbf{c}) & \text{if } \kappa \neq 0; \\ (0, \hat{\mathbf{n}}) & \text{if } \kappa = 0. \end{cases}$$

Here, the term "coordinate" is an abuse of language, since the curvature-center coordinates do not uniquely determine a ball when $\kappa = 0$. A real global coordinate system would be the *augmented curvature–center coordinates* [55]

$$\tilde{\mathbf{m}}(\mathsf{B}) = (\bar{\kappa}, \mathbf{m}(\mathsf{B}))$$

where $\bar{\kappa}$ is the curvature of the ball obtained by inversion of B in the unit sphere. In this thesis, the curvature-center coordinates $\mathbf{m}(\mathsf{B})$ are good enough for our use.

1.1.2 Tangency and Separation

Our main concern is the tangency relation between balls. Two balls are said to be *disjoint* if their intersection is empty. Two balls are said to be *tangent* at a point $\mathbf{t} \in \hat{\mathbb{R}}^d$ if $\mathbf{t}$ is the only element of their intersection. We call $\mathbf{t}$ the *tangency point*, which can be the infinity point ∞ if it involves two balls of curvature 0. Two balls *overlap* if their interiors intersect.

Let B_1 and B_2 be two balls in $\hat{\mathbb{R}}^d$ centered at $\mathbf{c}_1$ and $\mathbf{c}_2$ with curvatures κ_1 and κ_2, respectively. The *separation* $\delta(\mathsf{B}_1, \mathsf{B}_2)$ is designed to indicate the tangency relation between B_1 and B_2. If neither of the two balls is of curvature 0, the *separation* is defined as (compare [12, Equation (2)])

$$\delta(\mathsf{B}_1, \mathsf{B}_2) = (\kappa_1^2\kappa_2^2\|\mathbf{c}_1 - \mathbf{c}_2\|^2 - \kappa_1^2 - \kappa_2^2)/2\kappa_1\kappa_2. \tag{1.1}$$

Otherwise, if $\kappa_1 \neq 0$ but $\kappa_2 = 0$, assume that B_2 is a half-space defined by $\langle \mathbf{x}, \hat{\mathbf{n}} \rangle \geq b$. Then the separation is defined as (compare [12, Equation (3)])

$$\delta(\mathsf{B}_1, \mathsf{B}_2) = \kappa_1(b - \langle \mathbf{c}_1, \hat{\mathbf{n}} \rangle) \tag{1.2}$$

Note that $b - \langle \mathbf{c}_1, \hat{\mathbf{n}} \rangle$ is the signed distance from $\mathbf{c}_1$ to the hyperplane defining B_2. If $\kappa_1 = \kappa_2 = 0$, both B_1 and B_2 are half-spaces. Let θ be the angle between the defining hyperplanes, then the separation is defined as

$$\delta(\mathsf{B}_1, \mathsf{B}_2) = -\cos(\theta) \tag{1.3}$$

Equations (1.2) and (1.3) can be derived by taking the limit of (1.1) as the curvatures

tend to 0. If κ_1 and κ_2 are *not both* negative, one verifies that

$$\delta(\mathsf{B}_1, \mathsf{B}_2) \begin{cases} > 1 & \text{if } \mathsf{B}_1 \text{ and } \mathsf{B}_2 \text{ are disjoint;} \\ = 1 & \text{if } \mathsf{B}_1 \text{ and } \mathsf{B}_2 \text{ are tangent;} \\ < 1 & \text{if } \mathsf{B}_1 \text{ and } \mathsf{B}_2 \text{ overlap;} \\ = 0 & \text{if } \mathsf{B}_1 \text{ and } \mathsf{B}_2 \text{ intersect orthogonally.} \end{cases}$$

So the separation function indicates the tangency relation as expected.

Möbius transformations are conformal automorphisms of $\hat{\mathbb{R}}^d$. A Möbius transformation can be decomposed into inversions in spheres, see [18, Theorem 3.9]. A Möbius transformation map balls into balls while preserving tangency relations. The separation function is invariant under Möbius transformations. The group of Möbius transformations on $\hat{\mathbb{R}}^d$ is called *Möbius group*, denoted by $\mathrm{Möb}(d)$.

Fix $d+2$ balls $\mathsf{B}_1, \ldots, \mathsf{B}_{d+2}$. Boyd [12, 14] defines the *polyspherical coordinates* of a ball B as follows,

$$\mathbf{p}(\mathsf{B}) = (\delta(\mathsf{B}, \mathsf{B}_1), \ldots, \delta(\mathsf{B}, \mathsf{B}_{d+2})).$$

Remark 1.1.2. Note that if B_i is the half-space $\mathbf{x}_i \leq 0$ for $1 \leq i \leq d$, then $\delta(\mathsf{B}, \mathsf{B}_i)$ coincides with the $(i+1)$-th entry of the curvature-center coordinate $\mathbf{m}(\mathsf{B})$.

1.2 Lorentzian representation of balls

In this section, we recall basic notions of Lorentz space, and introduce a correspondence between balls in Euclidean space and space-like directions in Lorentz space. This correspondence is the key idea throughout the thesis.

1.2.1 Lorentz space

A d-dimensional *Lorentz space* $(V, \mathcal{B})$ is a d-dimensional vector space V associated with a bilinear form $\mathcal{B}$ of signature $(d-1, 1)$. That is, for any basis $(\mathbf{e}_1, \ldots, \mathbf{e}_d)$ of V, the matrix $(\mathcal{B}(\mathbf{e}_i, \mathbf{e}_j))_{ij}$ is nonsingular with $d-1$ positive eigenvalues and one negative eigenvalue.

Let $(V, \mathcal{B})$ be a Lorentz space. A vector $\mathbf{x} \in V$ is *space-like* (resp. *time-like, light-like*) if $\mathcal{B}(\mathbf{x}, \mathbf{x})$ is positive (resp. negative, zero). A subspace $U \subseteq V$ is *space-like* if its non-zero vectors are all space-like, *light-like* if U contains some non-zero light-like vector but no time-like vector, or *time-like* if U contains some time-like vector. Two vectors $\mathbf{x}, \mathbf{y} \in V$ are said to be orthogonal if $\mathcal{B}(\mathbf{x}, \mathbf{y}) = 0$. For a non-zero vector $\mathbf{x} \in V$, we define its orthogonal hyperplane

$$H_{\mathbf{x}} = \{\mathbf{y} \in V \mid \mathcal{B}(\mathbf{x}, \mathbf{y}) = 0\}.$$

We see that $H_{\mathbf{x}}$ is space-like (resp. light-like, time-like) if $\mathbf{x}$ is time-like (resp. light-like, space-like). For a subspace $U \subseteq V$, its orthogonal companion is defined as

$$U^{\perp} = \{\mathbf{y} \in V \mid \mathcal{B}(\mathbf{y}, \mathbf{x}) = 0 \text{ for all } \mathbf{x} \in U\}.$$

Note that if U is light-like, light-like vectors in U are also contained in $U^{\perp}$, and $U + U^{\perp}$ is not the whole space V.

The set of light-like vectors $Q = \{\mathbf{x} \in V \mid \mathcal{B}(\mathbf{x}, \mathbf{x}) = 0\}$ forms a cone called the *light cone*. The following is a very useful fact about Lorentz spaces.

Proposition 1.2.1 ([18, Theorem 2.3])**.** *Let $(V, \mathcal{B})$ be a Lorentz space and let $\mathbf{x}, \mathbf{y} \in Q$ be two light-like vectors. Then $\mathcal{B}(\mathbf{x}, \mathbf{y}) = 0$ if and only if $\mathbf{x} = c\mathbf{y}$ for some $c \in \mathbb{R}$.*

The light cone without origin $Q \setminus \{0\}$ has two components. Fix a time-like vector $\mathbf{z}$ and call it the *direction of past*. The space-like hyperplane $H_{\mathbf{z}}$ separates the space V into two parts, each contains one component of the light cone. We say that a vector $\mathbf{x}$ is *future-directed* (resp. *past-directed*) if $\mathcal{B}(\mathbf{x}, \mathbf{z}) > 0$ (resp. < 0). Consequently, the two components of the light cone are respectively future- and past-directed. The direction of past $\mathbf{z}$, as indicated by the name, is past-directed.

The *projective Lorentz space* $\mathbb{P}V$ is the space of 1-dimensional subspaces of V. For a non-zero vector $\mathbf{x} \in V \setminus \{0\}$, let $\widehat{\mathbf{x}} \in \mathbb{P}V$ denote the line passing through $\mathbf{x}$ and the origin. For a set $X \subset V$, we define the corresponding projective set

$$\widehat{X} := \{\widehat{\mathbf{x}} \in \mathbb{P}V \mid \mathbf{x} \in X\}.$$

For example, the projective light cone is denoted by $\widehat{Q}$. We also use $\mathsf{conv}(\widehat{X})$ to denote the projective convex cone $\widehat{\mathrm{cone}(X)}$.

Fix a vector $\mathbf{z}$, we can identify $\mathbb{P}V$ with the affine hyperplane $H^1_{\mathbf{z}} = \{\mathbf{x} \mid \mathcal{B}(\mathbf{x}, \mathbf{z}) = 1\}$ plus a *projective hyperplane at infinity*. For a vector $\mathbf{x} \in V$, we represent $\widehat{\mathbf{x}} \in \mathbb{P}V$ by the vector $\mathbf{x}/\mathcal{B}(\mathbf{x}, \mathbf{z}) \in H^1_{\mathbf{z}}$ if $\mathcal{B}(\mathbf{x}, \mathbf{z}) \neq 0$, or some point at infinity if $\mathcal{B}(\mathbf{x}, \mathbf{z}) = 0$. In fact, if $\mathcal{B}(\mathbf{x}, \mathbf{z}) \neq 0$, $\widehat{\mathbf{x}}$ is identified with the intersection of $H^1_{\mathbf{z}}$ and the straight line passing through $\mathbf{x}$ and the origin. In this sense, the projective light cone $\widehat{Q}$ is identified to the cross section of Q by the affine hyperplane $H^1_{\mathbf{z}}$. If $\mathbf{z}$ is time-like, then the affine picture of $\widehat{Q}$ is closed and projectively equivalent to a sphere, and its interior can be seen as the Kleinian model for hyperbolic space.

A linear transformation on V that preserves the bilinear form $\mathcal{B}$ is called a *Lorentz transformation*. The group of Lorentz transformations that preserve the future-directed light cone is called *orthochronous Lorentz group*, denoted by $O^+_{\mathcal{B}}(V)$.

The rest of this section is devoted to a correspondence between balls and vectors in Lorentz space. This is however not the first appearance of Lorentz space in discrete geometry. We refer the readers to [68] for a survey about applications of Lorentz space in combinatorics and discrete mathematics.

1.2.2 Space-like directions and balls

Given a *space-like* vector $\mathbf{x}$ in the Lorentz space $(V, \mathcal{B})$, the *normalized vector* $\overline{\mathbf{x}}$ of $\mathbf{x}$ is given by

$$\overline{\mathbf{x}} = \mathbf{x}/\sqrt{\mathcal{B}(\mathbf{x}, \mathbf{x})}$$

It lies on the one-sheet hyperboloid $\mathcal{H} = \{\mathbf{x} \in V \mid \mathcal{B}(\mathbf{x}, \mathbf{x}) = 1\}$. Note that $\widehat{\mathbf{x}} = \widehat{-\mathbf{x}}$ is the same point in $\mathbb{P}V$, but $\overline{\mathbf{x}}$ and $\overline{-\mathbf{x}}$ are two different vectors in opposite directions in V.

There is a classical correspondence between space-like directions in $(d+2)$-dimensional Lorentz space $(V, \mathcal{B})$ and balls in $\hat{\mathbb{R}}^d$, see for instance [18, Section 2.2; 42, Section 1.1; 62, Section 2]. Given a space-like vector $\mathbf{x}$, the intersection of $\widehat{Q}$ with the projective half-space $\widehat{H}^-_{\mathbf{x}} = \{\widehat{\mathbf{x}}' \in \mathbb{P}V \mid \mathcal{B}(\mathbf{x}, \mathbf{x}') \leq 0\}$ is a closed ball (spherical cap) on $\widehat{Q}$. We denote this ball by $\mathsf{B}(\mathbf{x})$. After a stereographic projection, $\mathsf{B}(\mathbf{x})$ becomes a ball in $\hat{\mathbb{R}}^d$. In Figure 1.1, for a past-directed normalized vector $\overline{\mathbf{x}}$, we show the corresponding projective vector $\widehat{\mathbf{x}}$, orthogonal hyperplane $H_{\mathbf{x}}$ and the ball $\mathsf{B}(\mathbf{x}) \subset \widehat{Q}$.

If the bilinear form $\mathcal{B}$ is in the *standard form*

$$\mathcal{B}(\mathbf{e}_i, \mathbf{e}_j) = \begin{cases} 1 & \text{if } i = j > 0; \\ -1 & \text{if } i = j = 0; \\ 0 & \text{if } i \neq j, \end{cases}$$

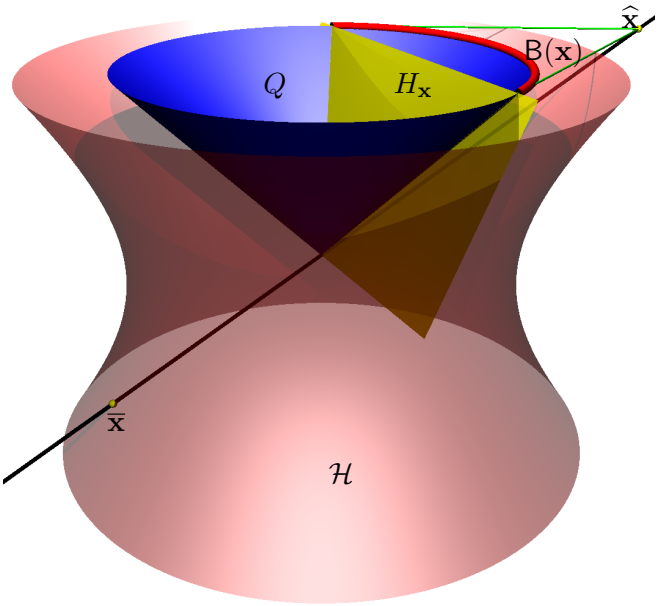

Figure 1.1: Correspondence between balls and space-like directions

then for a ball of positive finite radius r centered at $\mathbf{c} \in \mathbb{R}^d$, an explicit formula for the corresponding normalized vector is (compare [18, Equation (2.6)])

$$\overline{\mathbf{x}} = \left(\frac{1 + \|\mathbf{c}\|^2 - r^2}{2r}, \frac{1 - \|\mathbf{c}\|^2 + r^2}{2r}, \frac{\mathbf{c}}{r} \right) \tag{1.4}$$

Then the opposite normalized vector $-\overline{\mathbf{x}}$ corresponds to the ball of negative radius $-r$ with the same center. For an infinite-radius ball $\{\mathbf{x} \in \hat{\mathbb{R}}^d \mid \langle \mathbf{x}, \hat{\mathbf{n}} \rangle \geq b\}$, by taking $\mathbf{c} = (b+r)\mathbf{n}$ and let r tends to ∞, we obtain the following formula for the corresponding normalized vector:

$$\overline{\mathbf{x}} = (b, -b, \mathbf{n}) .$$

One verifies that $-\mathcal{B}(\overline{\mathbf{x}}, \overline{\mathbf{x}}')$ equals the separation $\delta(\mathsf{B}(\mathbf{x}), \mathsf{B}(\mathbf{x}'))$. Consequently, for two space-like vectors $\mathbf{x}$ and $\mathbf{x}'$, if they are *not both* future-directed, we have

- $\mathsf{B}(\mathbf{x})$ and $\mathsf{B}(\mathbf{x}')$ are disjoint if $\mathcal{B}(\overline{\mathbf{x}}, \overline{\mathbf{x}}') < -1$;
- $\mathsf{B}(\mathbf{x})$ is tangent to $\mathsf{B}(\mathbf{x}')$ if $\mathcal{B}(\overline{\mathbf{x}}, \overline{\mathbf{x}}') = -1$;
- $\mathsf{B}(\mathbf{x})$ and $\mathsf{B}(\mathbf{x}')$ overlap if $\mathcal{B}(\overline{\mathbf{x}}, \overline{\mathbf{x}}') > -1$;

The invariance of the separation function δ under Möbius transformations is reflected in the Lorentz space as the invariance of the bilinear form under Lorentz transformations. Indeed, the Möbius group $\mathrm{Möb}(d)$ is isomorphic to the orthochronous Lorentz group $O_{\mathcal{B}}^{+}(V)$ [18, Corollary 3.3].

1.2.3 Light-like vectors and kissing balls

In this part, we summarize some results from [20]. Fix a d-ball as the reference ball, then *kissing balls* are d-balls that are tangent to the reference ball. Without loss of generality, we may assume that the reference ball is a half-space $x_1 \leq 0$. These balls have been considered by Maehara and Noha [58] as "solid balls on a table".

Using the Lorentzian representation of balls introduced in the previous part, let $\overline{\mathbf{y}}$ be the normalized vector representing the reference ball, then the kissing balls are represented by normalized vectors

$$\{\overline{\mathbf{x}} \in \mathcal{H} \mid \mathcal{B}(\overline{\mathbf{x}}, \overline{\mathbf{y}}) = -1\}.$$

One verifies that these normalized vectors also lie on the cone

$$\{\overline{\mathbf{x}} \in V \mid \mathcal{B}(\overline{\mathbf{x}} + \overline{\mathbf{y}}, \overline{\mathbf{x}} + \overline{\mathbf{y}}) = 0\}. \tag{1.5}$$

In [20], we develop a distance geometry for *kissing spheres* (boundary of kissing balls). A Möbius invariant distance δ_K is defined for kissing spheres, such that two kissing

spheres are disjoint if their distance $\delta_K > 1$, tangent if $\delta_K = 1$, and intersect if $\delta_K < 1$. Two kissing spheres of distance 0 are tangent to the reference ball at the same point. Note that the triangular inequality does not hold for this distance function, so δ_K is not a metric.

Let $\mathsf{S}_1, \ldots, \mathsf{S}_n$ be n kissing spheres tangent to a d-dimensional reference ball. A powerful tool in the study of distance geometry is the distance matrix $\mathbf{D}$, defined by $\mathbf{D}_{ij} = \delta_K(\mathsf{S}_i, \mathsf{S}_j)^2$. It turns out that the distance matrix for a set of kissing spheres has a Lorentz signature (up to the sign), therefore generalizes Euclidean distance geometry. More specifically, for a set of kissing spheres with respect to a d-dimensional reference ball, the distance matrix is of rank $(d+1)$ and has exactly one positive eigenvalue. This allows us to represent kissing spheres in $(d+1)$-dimensional Lorentz space as vectors on the light cone, as we observed in Equation (1.5). For an explicit formula, see [20, Equation (8)].

This correspondence is not new. If we regard the half-space $x_0 \geq 0$ as the Poincaré half-space model for the n-dimensional hyperbolic space, then the kissing spheres are the horospheres. It is classical in hyperbolic geometry that horospheres can be identified to vectors in the lightcone, see for instance [34]. Furthermore, in the projective model of Möbius geometry, points in Euclidean space are mapped to light-like directions in Lorentz space [18, Equation 2.3]. In our correspondence, the directions or the light-like vectors correspond to the tangency points in the same way. Moreover, we use the vector lengths to distinguish different kissing spheres with the same tangency point.

1.3 Ball packings and tangency graphs

Definition 1.3.1. A *d-ball packing* is a collection of d-balls in $\hat{\mathbb{R}}^d$ with disjoint interiors.

Remark 1.3.2. In the literature, the term "sphere packing" is more popular. However, the author thinks that "ball packing" is the correct term for modern mathematics. For the same reason, 2-dimensional ball packings are called "disk packings" instead of "circle packings".

For a ball packing $\mathscr{B}$, its *tangency graph* $G(\mathscr{B})$ takes the balls as vertices, and two vertices are connected if and only if the corresponding balls are tangent. The tangency graph is invariant under Möbius transformations.

Definition 1.3.3. A graph G is said to be *d-ball packable* if there is a d-ball packing $\mathscr{B}$ whose tangency graph is isomorphic to G. In this case, we say that $\mathscr{B}$ is a *d-ball packing of G*.

Any induced subgraph of a d-ball packable graph is also d-ball packable, so the class of ball packable graphs is closed under the induced subgraph operation.

By the correspondence introduced in Section 1.2.2, a ball packing $\mathscr{B}$ in $\hat{\mathbb{R}}^d$ can be represented by a set of space-like normalized vectors X. For an explicit construction:

1. Map the balls in $\mathscr{B}$ to spherical caps on a sphere $\mathbb{S}^d$ through a stereographic projection;
2. Identify $\mathbb{S}^d$ with the projective light cone of a $(d+2)$-dimensional Lorentz space;
3. Take X as the set of normalized vectors corresponding to the caps, as described in Section 1.2.2.

In such a representation, we have at most one future-directed vector, and $\mathcal{B}(\overline{\mathbf{x}}, \overline{\mathbf{x}}') \leq -1$ for any two vectors $\overline{\mathbf{x}}, \overline{\mathbf{x}}' \in X$, where the equality is achieved only if the corresponding balls are tangent. The packing corresponding to a pair of opposite vectors $\{\mathbf{x}, -\mathbf{x}\}$ consists of two balls sharing the same boundary. We say that this packing is *trivial*.

1.3.1 Previous works on ball packings

The tangency graphs of *disk packings* (i.e. 2-ball packing) is fully characterised by Koebe–Andreev–Thurston's packing theorem, which was first proved by Koebe [51], and rediscovered by Thurston [86].

Theorem 1.3.4 (Koebe–Andreev–Thurston theorem [51, 86])**.** *Every connected simple planar graph is disk packable. If the graph is a finite triangulated planar graph, then it is the tangency graph of a unique disk packing up to Möbius transformations.*

There are many other proofs of the disk packing theorem, see for instance [9, 26, 95] for variational principle approaches, and [82] for an inductive proof. There is a stronger formulation in terms of edge-tangent polytopes, see Section 2.4. Thurston conjectured that disk packings can be used to approximate conformal mappings. This was proved by Rodin and Sullivan [72]. Disk packings then find applications in combinatorics, geometry, probability theory, computer modelling and many other domains. Notable generalizations of disk packings include circle patterns that allow specified overlaps, graphs of higher genus and packing of convex shapes other than disks. For surveys on disk packings, we recommend [73, 74, 81, 82].

In higher dimensions, studies have been focused on packings of congruent balls (i.e. balls of same size). There are two major research problems: The *kissing number problem* asks for the number of non-overlapping unit balls that can be arranged to touch a fixed unit ball. This can be regarded as a special case of spherical codes, and will be discussed in Section 2.2.2. The *densest packing problem* asks for the largest density of a congruent ball packing (the balls have the same radius) in a given dimension. One of the most famous problem would be *Kepler conjecture*, which was proved by Hales and Ferguson with the help of computer programs [41]. For surveys, we recommend [27, 70].

However, not so much is known about tangency graphs of higher dimensional ball packings. Clearly, every graph can be embedded in 3-dimensional space, but not all of them are 3-ball packable. The simplest example would be the complete graph on six vertices. Even for congruent ball packings, recognition of tangency graphs is NP-hard in dimension 2 [15], 3 and 4 [44].

Despite the difficulties, many properties of tangency graph have been studied. Kuperberg and Schramm [54] studied the average degree of non-congruent 3-ball packings, which turns out to be slightly bigger than the kissing number. Bezdek and Reid [8] studied the number of edges, triangles and 4-cliques in the tangency graphs of 3-ball packings. Alon [3] construct explicitly a congruent ball packing in dimension d such that minimum degree of its tangency graph is $2^{\sqrt{d}}$. Miller et al. [66] generalize the planar separator theorem to the tangency graphs of higher dimensional ball packings. Maehara [57] investigate the chromatic number of three dimensional ball packings. The chromatic number of higher dimensional ball packings is also asked in [5] and on MathOverflow [17].

On the geometric side, Cooper and Rivin [28] studied the rigidity of 3-ball packings. Vasilis [90] generalizes the ring lemma to dimension 3. Ball packings can also be studied in hyperbolic spaces. Notably, Szirmai [83, 84, 85] studied horoball packings using Coxeter groups.

Many interesting small examples have also been investigated. The Descartes' configurations was generalized to higher dimensions by Soddy [78] and Gosset [37]. This packing plays an essential role in Chapter 2. The Soddy's hexlet [77] is a packing consisting of nine balls. Maehara and Oshiro [60] revisited this packing and discovered another packing consisting of eight balls. We will rediscover these packing in Section 2.2 while constructing many other examples in higher dimensions. Maehara and Oshiro [59] proved that 15 congruent balls suffice to form a trefoil knot.

Apollonian packings are a fractal objects that are important not only in geometry [10, 13], but also in group theory [39] and number theory [38]. In Section 2.3, we study the relation of finite Apollonian packings and stacked polytopes. Infinite Apollonian packings only exist in dimension 2 and 3. However, a generalisation by Boyd [12] and Maxwell [62] exists up to dimension 9. We will revisit this generalisation in Chapter 3, and propose a further generalisation which may exist in much higher dimensions. Benjamini and Schramm [7] proved that the $(d+1)$-dimensional infinite grid graph is not d-ball packable, which motivates our investigation in Chapter 4.

Chapter 2

Apollonian packings

This chapter is based on [21]. We start with Descartes' configurations, then study some packings of graph joins, and finally investigate the tangency graph of Apollonian packings. Except for some packings of graph joins, most packings in this chapter are built with Descartes' configurations. Their graphs are $(d+1)$-trees, i.e. chordal graphs whose maximal cliques are of the same size $d+2$, where d is the dimension of the balls. Furthermore, all the packings in this chapter are rigid. In other words, they are the unique ball packings with the same tangency graphs, up to Möbius transformations.

In Section 2.1, we study Descartes' configurations. They are the simplest packings in this thesis, and are used to construct Apollonian packings and some packings of graph joins. We introduce Descartes–Soddy–Gosset theorem and its generalizations, which is essential for the calculations in this chapter.

In Section 2.2, we construct ball packings for some graph joins, and identify some graph joins that are not packable in a given dimension. These constructions provide forbidden induced subgraphs for the tangency graphs of ball packings, which are helpful for intuition. In particular, Soddy's hexlet, a ball packing consisting of nine balls, plays an important role in the proofs later.

An Apollonian ball packing is constructed from a Descartes' configuration by repeatedly filling new balls into "holes". A stacked polytope is constructed from a simplex by repeatedly gluing new simplices onto facets. See Section 2.3.1 and 2.3.2 for formal definitions, respectively. There is a 1-to-1 correspondence between 2-dimensional Apollonian ball packings and 3-dimensional stacked polytopes. Namely, a graph can be realised by the tangency relations of an Apollonian disk packing if and only if it is the 1-skeleton of a stacked 3-polytope. However, this relation does not hold in higher dimensions.

Motivated by this correspondence, we investigate in Section 2.3 the relation between Apollonian packings and stacked polytopes in higher dimensions. The main result, Theorem 2.3.1, characterise stacked 4-polytopes whose 1-skeletons are 3-ball packable.

For higher dimensions, we propose Conjecture 2.3.16 following the pattern of dimension 2 and 3. We also prove that the tangency graph of an Apollonian ball packing must be the 1-skeleton of a stacked polytope, except in dimension 3 when the packing contains a Soddy's hexlet.

In this chapter, the ball packing is always in dimension d, while the dimension for other objects vary correspondingly. For example, the stacked polytope is always in dimension $d+1$.

2.1 Descartes' configurations

A *Descartes' configuration* in dimension d is a d-ball packing consisting of $d+2$ pairwise tangent balls. The tangency graph of a Descartes' configuration is the complete graph on $d+2$ vertices. This is the basic element for the construction of many ball packings in this thesis.

2.1.1 Descartes–Soddy–Gosset Theorem

The following relation was first established in dimension 2 by René Descartes in a letter [30] to Princess Elizabeth of Bohemia. It was generalized to dimension 3 by Soddy in the form of a poem [78], and to arbitrary dimension by Gosset [37].

Theorem 2.1.1 (Descartes–Soddy–Gosset Theorem)**.** *In dimension d, if a set $\mathscr{D} = \{\mathsf{B}_1, \dots, \mathsf{B}_{d+2}\}$ of $d+2$ balls form a Descartes' configuration, are κ_i are the curvature of B_i $(1 \le i \le d+2)$, then*

$$\sum_{i=1}^{d+2} \kappa_i^2 = \frac{1}{d}\Big(\sum_{i=1}^{d+2} \kappa_i\Big)^2 \tag{2.1}$$

Equivalently, $\mathbf{K}^\intercal \mathbf{Q}_{d+2} \mathbf{K} = 0$, where $\mathbf{K} = (\kappa_1, \cdots, \kappa_{d+2})^\intercal$ is the vector of curvatures, and $\mathbf{Q}_{d+2} := \mathbf{I} - \mathbf{e}\mathbf{e}^\intercal/d$ is a square matrix of size $d+2$, where $\mathbf{e}$ is the all-one column vector, and $\mathbf{I}$ is the identity matrix, both of size $d+2$. A more general relation on the curvature-center coordinates was obtained in [55]:

Theorem 2.1.2 (Generalized Descartes–Soddy–Gosset Theorem)**.** *In dimension d, if a set $\mathscr{D} = \{\mathsf{B}_1, \dots, \mathsf{B}_{d+2}\}$ of $d+2$ balls form a Descartes' configuration, then*

$$\mathbf{M}^\intercal \mathbf{Q}_{d+2} \mathbf{M} = \begin{pmatrix} 0 & 0 \\ 0 & 2\mathbf{I} \end{pmatrix} \tag{2.2}$$

where $\mathbf{M}$ is the curvature–center matrix *of the configuration, whose i-th row is $\mathbf{m}(\mathsf{B}_i)$.*

See also [55, Theorem 3.3] for a formula concerning augmented curvature–center matrix. One verifies that $\mathbf{Q}_{d+2}$ has Lorentz signature, i.e. it has $(d+1)$ positive

eigenvalues and one negative eigenvalue. Therefore, in the Lorentz space associated with a bilinear form induced by $\mathbf{Q}_{d+2}$, the curvature vector of a Descartes' configuration is on the light cone, while the vectors of other curvature-center coordinates are on a one-sheet hyperboloid.

Given a Descartes' configuration $\mathsf{B}_1, \cdots, \mathsf{B}_{d+2}$, we can construct another Descartes' configuration by replacing B_1 with an B_{d+3}, such that the curvatures κ_1 and κ_{d+3} are the two roots of (2.1), treating κ_1 as unknown. So we have the relation

$$\kappa_1 + \kappa_{d+3} = \frac{2}{d-1} \sum_{i=2}^{d+2} \kappa_i \tag{2.3}$$

We see from (2.2) that the same relation holds for all the entries in the curvature-center coordinates,

$$\mathbf{m}(\mathsf{B}_1) + \mathbf{m}(\mathsf{B}_{d+3}) = \frac{2}{d-1} \sum_{i=2}^{d+2} \mathbf{m}(\mathsf{B}_i) \tag{2.4}$$

These equations are essential for the calculations in the present section.

By recursively replacing B_i with a new ball B_{i+d+2} in this way, we obtain an infinite sequence of balls $\mathsf{B}_1, \mathsf{B}_2, \cdots$, in which any $d+2$ consecutive balls form a Descartes' configuration. This is *Coxeter's loxodromic sequences* of tangent balls [29].

2.1.2 Boyd's generalisation

Equation (2.1) and (2.2) are further generalized by Boyd [12] to arbitrary $d+2$ balls. For arbitrary $d+2$ balls $\mathsf{B}_1, \ldots, \mathsf{B}_{d+2}$ in $\hat{\mathbb{R}}^d$, the *separation matrix* $\mathbf{\Delta}$ is defined by

$$\mathbf{\Delta}_{ij} = \delta(\mathsf{B}_i, \mathsf{B}_j), \quad 1 \leq i, j \leq d+2$$

Assume that Δ is invertible, then for another d-ball B, we have [12, Equation (9)]

$$\mathbf{p}(\mathsf{B})^\intercal \mathbf{\Delta}^{-1} \mathbf{p}(\mathsf{B}) = -1,$$

where $\mathbf{p}(\mathsf{B})$ is the polyspherical coordinates of B with respect to $\mathsf{B}_1, \ldots, \mathsf{B}_{d+2}$ (see Section 1.1.2). With a clever choice of B, Boyd proved that [12, Equation (11)]

$$\mathbf{K}^\intercal \mathbf{\Delta}^{-1} \mathbf{K} = 0.$$

And the following relation is a consequence of Remark 1.1.2.

$$\mathbf{M}^\intercal \mathbf{\Delta}^{-1} \mathbf{M} = \begin{pmatrix} 0 & 0 \\ 0 & -\mathbf{I} \end{pmatrix}.$$

For a Descartes' configuration, we have $\mathbf{\Delta} = \mathbf{e}\mathbf{e}^\intercal - 2\mathbf{I} = (\frac{1}{2}\mathbf{Q}_{d+2})^{-1}$. So the Descartes–Soddy–Gosset theorem and its generalisations are covered by the work of Boyd as special cases. Based on these results, Boyd generalizes Apollonian packings [14], which leads to the topic of Chapter 3, Boyd–Maxwell packings.

2.2 Packing of some graph joints

Notations

In this chapter, we use G_n to denote any graph on n vertices, and use

P_n for the path on n vertices (therefore of length $n-1$);

C_n for the cycle on n vertices;

K_n for the complete graph on n vertices;

$\bar{K}_n$ for the empty graph on n vertices;

$\Diamond_d$ for the 1-skeleton of the d-dimensional orthoplex[1];

The *join* of two graphs G and H, denoted by $G \star H$, is the graph obtained by connecting every vertex of G to every vertex of H. Most of the graphs in this section will be expressed in term of graph joins. Notably, we have $\Diamond_d = \underbrace{\bar{K}_2 \star \cdots \star \bar{K}_2}_{d}$.

2.2.1 Graphs in the form of $K_d \star P_m$

The following theorem reformulates a result of Wilker [93]. A proof was sketched in [12]. Here we present a very elementary proof, suitable for our further generalization.

Theorem 2.2.1. *Let $d > 2$ and $m \geq 0$. A graph in the form of*

(i) *$K_2 \star P_m$ is 2-ball packable for any m;*

(ii) *$K_d \star P_m$ is d-ball packable if $m \leq 4$;*

(iii) *$K_d \star P_m$ is* not *d-ball packable if $m \geq 6$;*

(iv) *$K_d \star P_5$ is d-ball packable if and only if $d = 3$ or 4.*

Proof. (i) is trivial, since $K_2 \star P_m$ is planar.

For dimension $d > 2$, we construct a ball packing for the complete graph $K_{d+2} = K_d \star P_2$ as follows. The two vertices of P_2 are represented by two disjoint half-spaces A

[1] also called "cross polytope"

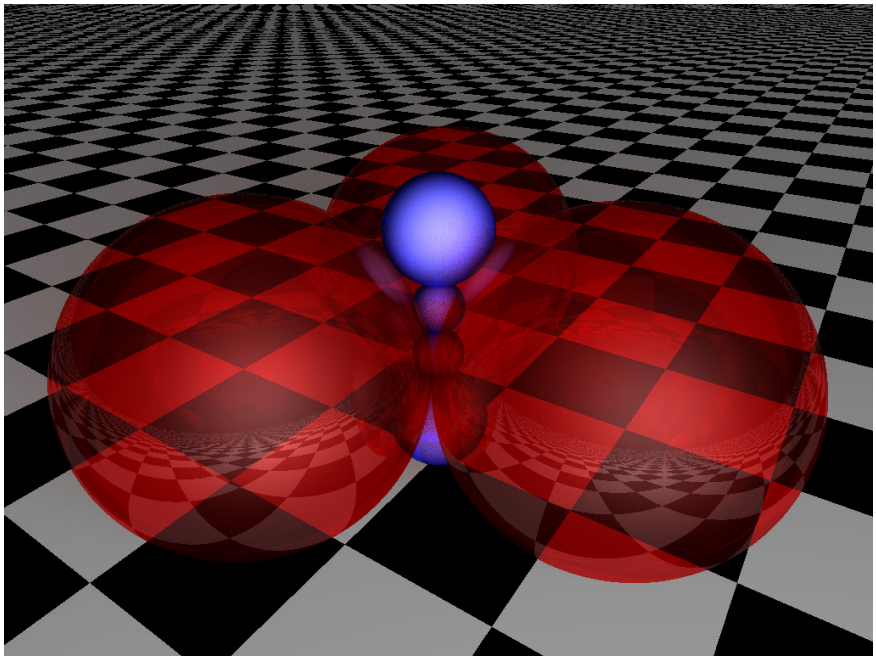

Figure 2.1: An attempt of constructing the 3-ball packing of $K_3 \star P_6$ results in $K_3 \star C_6$. Referring to the proof of Theorem 2.2.1, the red balls correspond to vertices in K_3, the blue balls are labeled by B, C, D, E from bottom to top. The upper half-space F is not shown. The image is rendered by POV-Ray.

and F at distance 2 apart (they are tangent at infinity), and the d vertices of K_d are represented by d pairwise tangent unit balls touching both A and F. Figure 2.1 shows the situation for $d = 3$, where red balls represent vertices of K_3. This is the unique packing of K_{d+2} up to Möbius transformations.

The centers of the unit balls defines a $(d-1)$-dimensional regular simplex. Let S be the $(d-2)$-dimensional circumsphere of this simplex. The idea of the proof is the following. Starting from $K_d \star P_2$, we construct the ball packing of $K_d \star P_m$ by appending new balls to the path, touching all the d unit balls representing K_d. The center of a new ball is at the same distance (1+ its radius) from the centers of the unit balls, so the new balls must center on a straight line passing through the center of S perpendicular to the hyperplane containing S. The construction fails when the sum of the diameters exceeds 2.

As a first step, we construct $K_d \star P_3$ by adding a new ball B tangent to A. By (2.3), the diameter of B is $2/\kappa_{\mathsf{B}} = (d-1)/d < 1$. Since B is disjoint from F, this step succeeded. Then we add a ball E tangent to F. It has the same diameter as B by symmetry, and they sum up to $2(d-1)/d < 2$. So the construction of $K_d \star P_4$ succeeded, which proves (ii).

We now add a ball C tangent to B. Still by (2.3), the diameter of C is

$$\frac{2}{\kappa_{\mathsf{C}}} = \frac{(d-1)^2}{d(d+1)}$$

If we sum up the diameters of B, C and E, we get

$$2\frac{d-1}{d} + \frac{(d-1)^2}{d(d+1)} = \frac{3d^2-2d-1}{d(d+1)} \tag{2.5}$$

which is smaller than 2 if and only if $d \leq 4$. Therefore the construction fails unless $d = 3$ or 4, which proves (iv).

For $d = 3$ or 4, we continue to add a ball D tangent to E. It has the same diameter as C. If we sum up the diameters of B, C, D and E, we get

$$2\left(\frac{d-1}{d} + \frac{(d-1)^2}{d(d+1)}\right) = 4\frac{d-1}{d+1} \tag{2.6}$$

which is smaller than 2 if and only if $d < 3$, which proves (iii). □

Remark 2.2.2. Figure 2.1 shows the attempt of constructing the ball packing of $K_3 \star P_6$ but results in the ball packing of $K_3 \star C_6$. This packing is called *Soddy's hexlet* [77]. It's an interesting configuration since the diameters of B, C, D and E sum up to exactly 3. This configuration is also studied by Maehara and Oshiro in [60].

Remark 2.2.3. Let's point out the main differences between the situation in dimension 2 and higher dimensions. For $d = 2$, a Descartes' configuration divides the space into 4 disconnected parts, and the radius of a circle tangent to the two unit circles of K_2 can be arbitrarily small. However, if $d > 2$, the complement of a Descartes' configuration is always connected, and the radius of a ball tangent to all the d balls of K_d is bounded away from 0. One verifies, by using the Descartes–Soddy–Gossett theorem, or from the circumradius of the regular simplex, that the radius of such a ball is at least $\frac{d-2}{d+\sqrt{2d^2-2d}}$, which tends to $\frac{1}{1+\sqrt{2}}$ as d tends to infinity.

2.2.2 Graphs in the form of $K_n \star G_m$

The following is a corollary of Theorem 2.2.1.

Corollary 2.2.4. *For $d = 3$ or 4, a graph in the form of $K_d \star G_6$ is not d-ball packable, with the exception of $K_3 \star C_6$. For $d \geq 5$, a graph in the form of $K_d \star G_5$ is not d-ball packable.*

Proof. Consider the graph $K_d \star G_m$, where $m = 6$ if $d = 3$ or 4, or $m = 5$ if $d > 4$. If G_m is not empty, we construct a packing of $K_d \star P_2$ with d unit balls and two

disjoint half-spaces, as in the proof of Theorem 2.2.1. Otherwise, we replace the upper half-space with a ball of an arbitrarily small curvature.

Since the centers of the balls of G_m are situated on a straight line, G_m can only be a path, a cycle C_m or a disjoint union of paths (possibly empty). The first possibility is ruled out by Theorem 2.2.1. The cycle is only possible when $d = 3$ and $m = 6$, in which case the ball packing of $K_3 \star C_6$ is Soddy's hexlet. There remains the case where G_m is a disjoint union of paths. As in the proof of Theorem 2.2.1, we try to construct the packing of $K_d \star G_m$ by introducing new balls, one above another on the straight line, touching all the unit balls representing K_d.

But this time, some ball is not allowed to touch the previous one. For such a ball, let r be its radius and h be the height (distance from the lower half-space) of its center. Since it touches all the unit balls, an elementary geometric calculation yields

$$(h + r)(2 - h + r) = 2(d - 1)/d.$$

The constant on the right hand side is the square of the circumradius of the $(d-1)$-dimensional regular simplex of edge length 2. On the left hand side, $h + r$ (resp. $h - r$) is the height of the highest (resp. lowest) point of the ball. We then observe that when we increase $h - r$ to avoid touching the previous ball, $h + r$ also increases, and any ball that is above it also has a higher value of $h + r$. Comparing to the proof of Theorem 2.2.1, we conclude that no matter how hard we try to keep the gaps small between non-touching balls, the last ball in G_m have to overlap the upper half-space (possibly replaced by a ball of small curvature). □

We now study some other graphs with the form $K_n \star G_m$ using kissing configurations and spherical codes. A *d-kissing configuration* is a packing of unit d-balls all touching another unit ball. The *d-kissing number* $k(d, 1)$ (the reason for this notation will be clear later) is the maximum number of balls in a d-kissing configuration. The kissing number is known to be 2 for dimension 1, 6 for dimension 2, 12 for dimension 3 [27], 24 for dimension 4 [67], 240 for dimension 8 and 196560 for dimension 24 [69]. We have immediately the following theorem.

Theorem 2.2.5. *A graph in the form of $K_3 \star G$ is d-ball packable if and only if G is the tangency graph of a $(d-1)$-kissing configuration.*

To see this, just represent K_3 by one unit ball and two disjoint half-spaces at distance 2 apart, then the other balls must form a $(d-1)$-kissing configuration. For example, $K_3 \star G_{13}$ is not 4-ball packable, $K_3 \star G_{25}$ is not 5-ball packable, and in general, $K_3 \star G_{k(d-1,1)+1}$ is not d-ball packable.

We can generalize this idea as follows. A *(d, α)-kissing configuration* is a packing of unit balls touching α pairwise tangent unit balls. The *(d, α)-kissing number* $k(d, \alpha)$

is the maximum number of balls in a (d, α)-kissing configuration. So the d-kissing configuration discussed above is actually the $(d, 1)$-kissing configuration, from where the notation $k(d, 1)$ is derived. Clearly, if G is the tangency graph of a (d, α)-kissing configuration, $G \star K_1$ must be the graph of a $(d, \alpha - 1)$-kissing configuration, and $G \star K_{\alpha-1}$ must be the graph of a d-kissing configuration. With a similar argument as before, we have

Theorem 2.2.6. *A graph in the form of $K_{2+\alpha} \star G$ is d-ball packable if and only if G is the tangency graph of a $(d-1, \alpha)$-kissing configuration.*

To see this, just represent $K_{2+\alpha}$ by two half-spaces at distance 2 apart and α pairwise tangent unit balls, then the other balls must form a $(d-1, \alpha)$-kissing configuration. As a consequence, a graph in the form of $K_{2+\alpha} \star G_{k(d-1,\alpha)+1}$ is not d-ball packable. The following corollary follows from the fact that $k(d, d) = 2$ for all $d > 0$.

Corollary 2.2.7. *A graph in the form of $K_{d+1} \star G_3$ is not d-ball packable.*

A $(d, \cos\theta)$-*spherical code* [27] is a set of points on the unit $(d-1)$-sphere such that the spherical distance between any two points in the set is at least θ. We denote by $A(d, \cos\theta)$ the maximal number of points in such a spherical code. Spherical codes generalize kissing configurations. The minimal spherical distance corresponds to the tangency relation, and $A(d, \cos\theta) = k(d, 1)$ if $\theta = \pi/3$. Corresponding to the tangency graph, the *minimal-distance graph* of a spherical code takes the points as vertices and connects two vertices if the corresponding points attain the minimal spherical distance. As noticed by Bannai and Sloane [6, Theorem 1], the centers of unit balls in a (d, α)-kissing configuration correspond to a $(d - \alpha + 1, \frac{1}{\alpha+1})$-spherical code after rescaling. Therefore:

Corollary 2.2.8. *A graph in the form of $K_{2+\alpha} \star G$ is $(d+\alpha)$-ball packable if and only if G is the minimal-distance graph of a $(d, \frac{1}{\alpha+1})$-spherical code.*

We give in Table 2.1 an incomplete list of $(d, \frac{1}{\alpha+1})$-spherical codes for integer values of α. They are therefore $(d + \alpha - 1, \alpha)$-kissing configurations for the α and d given in the table. The first column is the name of the polytope whose vertices form the spherical code. Some of them are from Klitzing's list of segmentochora [50], which can be viewed as a special type of spherical codes. Some others are inspired from Sloane's collection of optimal spherical codes [76]. For those polytopes with no conventional name, we keep Klitzing's notation, or give a name following Klitzing's method. The second column is the corresponding minimal-distance graph, if a conventional notation is available. Here are some notations used in the table:

- For a graph G, its *line graph* $L(G)$ takes the edges of G as vertices, and two vertices are adjacent if and only if the corresponding edges share a vertex in G.

- The *Johnson graph* $J_{n,k}$ takes the k-element subsets of an n-element set as vertices, and two vertices are adjacent whenever their intersection contains $k-1$ elements. Especially, $J_{n,2} = L(K_n)$.

- For two graph G and H, $G\square H$ denotes the *Cartesian product*.

We would like to point out that for $1 \leq \alpha \leq 6$, vertices of the uniform $(5-\alpha)_{21}$ polytope form an $(8, \alpha)$-kissing configuration. These codes are derived from the E_8 root lattice [6, Example 2]. They are optimal and unique except for the trigonal prism ($(-1)_{21}$ polytope) [4; 25, Appendix A]. There are also spherical codes similarly derived from the *Leech lattice* [6, Example 3; 24].

Table 2.1: Some $(d, \frac{1}{\alpha+1})$-spherical codes for integer α

spherical code	minimal distance graph	α	d
k-orthoplicial prism	$\Diamond_k \square K_2$	2	$k+1$
k-orthoplicial-pyramidal prism	$(\Diamond_k \star K_1)\square K_2$	2	$k+2$
rectified k-orthoplex	$L(\Diamond_k)$	1	k
augmented k-simplicial prism		k	$k+1$
2-simplicial prism(-1_{21}) [50, 3.4.1]	$K_3\square K_2$	6	3
3-simplicial prism(-1_{31}) [50, 4.9.2]	$K_4\square K_2$	4	4
5-simplicial prism	$K_6\square K_2$	3	6
triangle-triangle duoprism(-1_{22})[50, 4.10]	$K_3\square K_3$	3	4
tetrahedron-tetrahedron duoprism	$K_4\square K_4$	2	6
triangle-hexahedron duoprism	$K_3\square K_6$	2	7
rectified 4-simplex(0_{21}) [4]	$J_{5,2}$	5	4
rectified 5-simplex(0_{31})	$J_{6,2}$	3	5
rectified 7-simplex	$J_{8,2}$	2	7
birectified 5-simplex(0_{22})	$J_{6,3}$	2	5
birectified 8-simplex	$J_{9,3}$	1	8
trirectified 7-simplex	$J_{8,4}$	1	7
5-demicube(1_{21}) [76, pack.5.16]		4	5
6-demicube(1_{31})		2	6
8-demicube		1	8
1_{22}		1	6
2_{31}		1	7
2_{21} [25, Appendix A]		3	6
3_{21} [6]		2	7
4_{21} [6]		1	8
3p‖refl ortho 3p [50, 4.13]		2	4
3g‖gyro 3p [50, 4.6.2]		5	4
3g‖ortho 4g [50, 4.7.3]		5	4
3p‖ortho line [50, 4.8.2]		5	4
oct‖hex [76, pack.5.14]		4	5

As a last example, since

$$k(d,\alpha) = A\Big(d-\alpha+1, \frac{1}{\alpha+1}\Big).$$

the following fact provides another proof Corollary 2.2.4:

$$k(d,d-1) = A(2,1/d) = \begin{cases} 4 & \text{if } d \geq 4 \\ 5 & \text{if } d = 3 \\ 6 & \text{if } d = 2 \text{(optimal)} \end{cases}$$

Before ending this part, we present the following lemma (see [44, Lemma 2.3]).

Lemma 2.2.9. *A graph in the form of $K_2 \star G$ is d-ball packable if and only if G is $(d-1)$-unit-ball packable.*

For the proof, just use disjoint half-spaces to represent K_2, then G must be representable by a packing of unit balls.

2.2.3 Graphs in the form of $\Diamond_d \star G_m$

Theorem 2.2.10. *A graph in the form of $\Diamond_{d-1} \star P_4$ is not d-ball packable, but $\Diamond_{d+1} = \Diamond_{d-1} \star C_4$ is.*

Proof. The graph $\Diamond_{d-1}$ is the 1-skeleton of the $(d-1)$-dimensional orthoplex. The vertices of a regular orthoplex of edge length $\sqrt{2}$ forms an optimal spherical code of minimal distance $\pi/2$. As in the proof of Theorem 2.2.1, we first construct the ball packing of $\Diamond_{d-1} \star P_2$. The edge P_2 is represented by two disjoint half-spaces. The graph $\Diamond_{d-1}$ is represented by $2(d-1)$ unit balls. Their centers are on a $(d-2)$-dimensional sphere S, otherwise further construction would not be possible. So the centers of these unit balls must be the vertices of a regular $(d-1)$-dimensional orthoplex of edge length 2, and the radius of S is $\sqrt{2}$.

We now construct $\Diamond_{d-1} \star P_3$ by adding the unique ball that is tangent to all the unit balls and also to one half-space. An elementary calculation shows that the radius of this ball is $1/2$. By symmetry, a ball touching the other half-space has the same radius. These two balls must be tangent since their diameters sum up to 2. Therefore, an attempt for constructing a ball packing of $\Diamond_{d-1} \star P_4$ results in a ball packing of $\Diamond_{d+1} = \Diamond_{d-1} \star C_4$. □

For example, $C_4 \star C_4$ is 3-ball packable, as shown in Figure 2.2. This is also observed by Maehara and Oshiro in [60]. By the same argument as in the proof of Corollary 2.2.4, we have

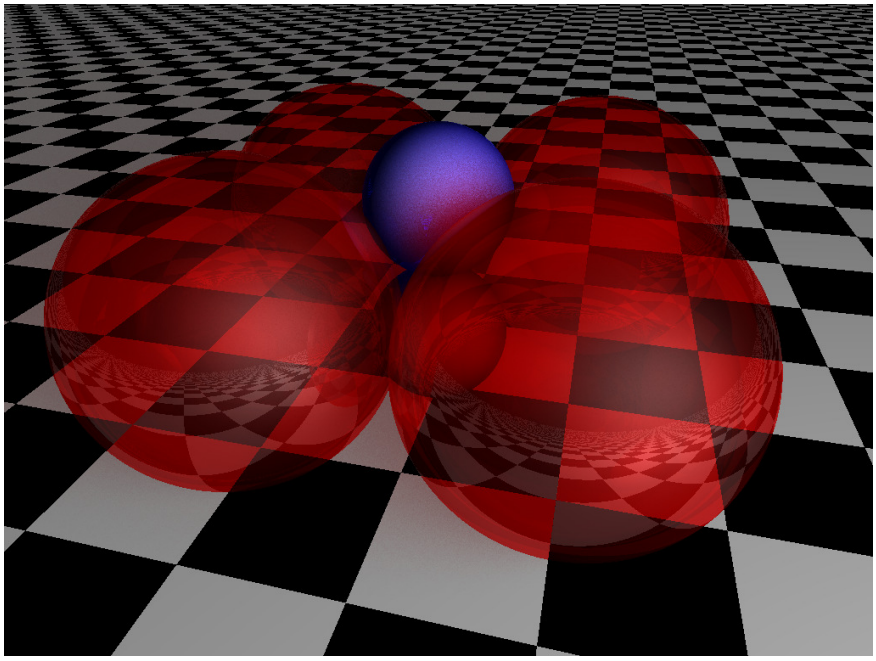

Figure 2.2: A ball packing of $C_4 \star C_4$. The red balls form a cycle, and the blue balls form a cycle with the lower and the upper half-space. The upper half-space is not shown. The image is rendered by POV-Ray.

Corollary 2.2.11. *A graph in the form of $\Diamond_{d-1} \star G_4$ is not d-ball packable, with the exception of $\Diamond_{d+1} = \Diamond_{d-1} \star C_4$.*

2.2.4 Graphs in the form of $G_n \star G_m$

The following is a corollary of Corollary 2.2.4.

Corollary 2.2.12. *A graph in the form of $G_6 \star G_3$ is not 3-ball packable, with the exception of $C_6 \star C_3$.*

Proof. As in the proof of Theorem 2.2.1, up to Möbius transformations, we may represent G_3 by three unit balls. We assume that their centers are not collinear, otherwise further construction is not possible. Let S be the 1-sphere decided by their centers. Every ball representing a vertex of G_6 must center on the straight line passing through the center of S perpendicular to the plane containing S. From the proof of Corollary 2.2.4, the number of disjoint balls touching all three unit balls is at most six, while six balls only happens in the Soddy's hexlet. □

The following corollaries follow from the same argument with slight modification.

Corollary 2.2.13. *A graph in the form of $G_4 \star G_4$ is not 3-ball packable, with the exception of $C_4 \star C_4$.*

Proof. Up to Möbius transformation, we may represent three vertices of the first G_4 by unit balls, whose centers decide a 1-sphere S. Balls representing vertices of the second G_4 must center on the straight line passing through the center of S perpendicular to the plane containing S. Then the remaining vertex of the first G_4 must be represented by a unit ball centered on S, too. We conclude from Corollary 2.2.11 that the only possibility is $C_4 \star C_4$. □

Corollary 2.2.14. *A graph in the form of $G_4 \star G_6$ is not 4-ball packable, with the exception of $C_4 \star \Diamond_3$.*

Proof. Up to Möbius transformation, we represent four vertices of G_6 by unit balls, whose centers decide a 2-sphere S. Balls representing vertices of G_4 must center on the straight line passing through the center of S perpendicular to the hyperplane containing S. Then the two remaining vertices of G_6 must be represented by unit balls centered on S, too. The diameter of S is minimal *only* when $G_6 = \Diamond_3$. In this case, G_4 must be in the form of C_4 by Corollary 2.2.11. If G_6 is in any other form, a ball touching the unit balls must have a larger radius, which is not possible.

Special caution is needed for a degenerate case. It is possible to have the six unit balls centered on a 1-sphere. In this case, the radius of a ball touching all of them is at least 1, which rules out the possibility of further construction. □

Therefore, if a graph is 3-ball packable, any induced subgraph in the form of $G_6 \star G_3$ must be in the form of $C_6 \star K_3$, and any induced subgraph in the form of $G_4 \star G_4$ must be in the form of $C_4 \star C_4$. If a graph is 4-ball packable, every induced subgraph in the form of $G_4 \star G_6$ must be in the form of $C_4 \star \Diamond_3$.

Remark 2.2.15. The argument in these proofs should be used with caution. As mentioned in the proof of Corollary 2.2.14, one must check carefully the degenerate cases. In higher dimensions, we are in general not so lucky, so these results does not generalize.

The following is a corollary of Theorem 2.2.6, for which we omit the simple proof.

Corollary 2.2.16. *A graph in the form of $K_2 \star G_\alpha \star G_{k(d-1,\alpha)+1}$ is not d-ball packable.*

2.3 Apollonian packings and stacked polytopes

In this section, we study the relation between Apollonian ball packings and stacked polytopes. An Apollonian ball packing is constructed from a Descartes' configuration by repeatedly introducing new balls to form new Descartes' configurations. A stacked

polytope is constructed from a simplex by repeatedly gluing new simplices onto facets. There is a 1-to-1 correspondence between 2-dimensional Apollonian ball packings and 3-dimensional stacked polytopes. Namely, a graph can be realised by the tangency relations of an Apollonian disk packing if and only if it is the 1-skeleton of a stacked 3-polytope. However, this relation does not hold in higher dimensions.

On the one hand, the 1-skeleton of a stacked polytope may not be realizable by the tangency relations of any Apollonian ball packing. Our main result, proved in Section 2.3.5, give a condition on stacked 4-polytopes to restore the relation in this direction:

Theorem 2.3.1 (Main result)**.** *The* 1*-skeleton of a stacked* 4*-polytope is* 3*-ball packable if and only if it does not contain six* 4*-cliques sharing a* 3*-clique.*

For higher dimensions, we propose Conjecture 2.3.16 following the pattern of dimension 2 and 3. On the other hand, the tangency graph of an Apollonian ball packing may not be the 1-skeleton of any stacked polytope. We prove in Corollary 2.3.13 and Theorem 2.3.14 that this only happens in dimension 3.

Many proof techniques are inspired by [40].

2.3.1 Apollonian cluster of balls

Definition 2.3.2. A collection of d-balls is said to be *Apollonian* if it can be built from a Descartes' configuration by repeatedly introducing, for $d+1$ pairwise tangent balls, a new ball that is tangent to all of them.

For example, Coxeter's loxodromic sequence is Apollonian. Note that it is possible for a newly added ball to touch more than $d+1$ balls, and may overlap some other balls. In the latter case, the result is not a packing. In the present section, we are interested in (finite) *Apollonian ball packings*.

We reformulate the replacing operation described before (2.3) by inversions. Given a Descartes' configuration $\mathscr{D} = \{\mathsf{B}_1, \cdots, \mathsf{B}_{d+2}\}$, let R_i be the inversion in the sphere that orthogonally intersects the boundary of B_j for all $1 \leq j \neq i \leq d+2$. Then $R_i\mathscr{D}$ forms a new Descartes' configuration, which keeps every ball of $\mathscr{D}$, except that B_i is replaced by $R_i\mathsf{B}_i$. With this point of view, a Coxeter's sequence can be obtained from an initial Descartes' configuration $\mathscr{D}_0$ by recursively constructing a sequence of Descartes' configurations by $\mathscr{D}_{n+1} = R_{j+1}\mathscr{D}_n$ where $j \equiv n \pmod{d+2}$, then taking the union.

The group W generated by $\{R_1, \ldots, R_{d+2}\}$ is called the *Apollonian group*. The union of the orbits $\cup_{\mathsf{B}\in\mathscr{D}_0} W\mathsf{B}$ is called the *Apollonian ball cluster* [40]. The Apollonian cluster is an infinite ball packing in dimensions 2 [39] and 3 [12]. That is, the interiors of any two balls in the cluster are either identical or disjoint. This is not true for higher dimensions. Our main object of study, (finite) Apollonian ball packings, can be seen as special subsets of Apollonian clusters.

Define

$$\mathbf{R}_i := \mathbf{I} + \frac{2}{d-1}\mathbf{e}_i\mathbf{e}^\intercal - \frac{2d}{d-1}\mathbf{e}_i\mathbf{e}_i^\intercal$$

where $\mathbf{e}_i$ is a $(d+2)$-vector whose entries are 0 except for the i-th entry being 1. So $\mathbf{R}_i$ coincides with the identity matrix at all rows except for the i-th row, whose diagonal entry is -1 and off-diagonal entries are $2/(d-1)$. One then verifies that $\mathbf{R}_i$ induces a representation of the Apollonian group. In fact, if $\mathbf{M}$ is the curvature–center matrix of a Descartes' configuration $\mathscr{D}$, then $\mathbf{R}_i\mathbf{M}$ is the curvature–center matrix of $R_i\mathscr{D}$.

2.3.2 Stacked polytopes

For a simplicial polytope, a *stacking operation* glues a new simplex onto a facet.

Definition 2.3.3. A simplicial d-polytope is *stacked* if it can be iteratively constructed from a d-simplex by a sequence of *stacking operations*.

We call the 1-skeleton of a polytope $\mathcal{P}$ the *graph* of $\mathcal{P}$, denoted by $G(\mathcal{P})$. For example, the graph of a d-simplex is the complete graph on $d+1$ vertices. The graph of a stacked d-polytope is a *d-tree*, that is, a chordal graph whose maximal cliques are of a same size $d+1$. Inversely,

Theorem 2.3.4 (Kleinschmidt [49])**.** *A d-tree is the graph of a stacked d-polytope if and only if there is no three $(d+1)$-cliques sharing d vertices.*

A d-tree satisfying this condition will be called *stacked d-polytopal graph*. We then see from Corollary 2.2.7 that a $(d+1)$-tree is d-ball packable only if it is stacked $(d+1)$-polytopal.

A simplicial d-polytope $\mathcal{P}$ is stacked if and only if it admits a triangulation with only interior faces of dimension $(d-1)$. For $d \geq 3$, this triangulation is unique, whose simplices correspond to the maximal cliques of $G(\mathcal{P})$. This implies that stacked polytopes are uniquely determined by their graph (i.e. stacked polytopes with isomorphic graphs are combinatorially equivalent). The *dual tree* [36] of $\mathcal{P}$ takes the simplices of the triangulation as vertices, and connect two vertices if the corresponding simplices share a $(d-1)$-face.

The following correspondence between Apollonian 2-ball packings and stacked 3-polytopes can be easily seen from Theorem 1.3.4 by comparing the construction processes:

Theorem 2.3.5. *If a disk packing is Apollonian, then its tangency graph is stacked 3-polytopal. If a graph is stacked 3-polytopal, then it is disk packable with an Apollonian disk packing, which is unique up to Möbius transformations and reflections.*

The relation between 3-tree, stacked 3-polytope and Apollonian 2-ball packing can be illustrated as in Figure 2.3, where the double-headed arrow $A \twoheadrightarrow B$ emphasizes that every instance of B corresponds to an instance of A satisfying the given condition, and the left-right arrow $A \leftrightarrow B$ emphasizes on the one-to-one correspondence.

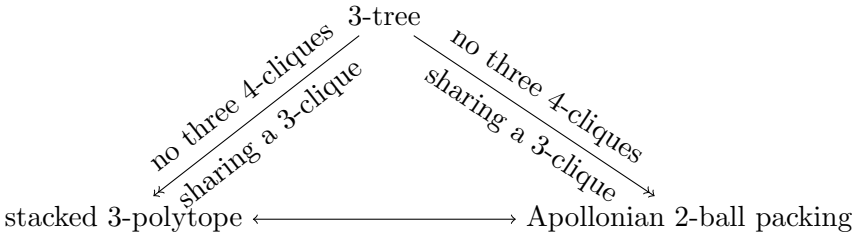

Figure 2.3: Relation between 3-trees, stacked 3-polytopes and 2-ball packings.

Since any graph in the form of $K_d \star P_m$ is stacked $(d+1)$-polytopal, Theorem 2.2.1 provides some examples of stacked $(d+1)$-polytope whose graph is not d-ball packable, and $C_3 \star C_6$ provides an example of Apollonian 3-ball packing whose tangency graph is not stacked 4-polytopal. Therefore, in higher dimensions, the relation between Apollonian ball packings and stacked polytopes is more complicated. The following remains true:

Theorem 2.3.6. *If the graph of a stacked $(d+1)$-polytope is d-ball packable, its ball packing is Apollonian and unique up to Möbius transformations and reflections.*

Proof. The Apollonianity can be easily seen by comparing the construction processes. The uniqueness can be proved by an induction on the construction process. While a stacked polytope is built from a simplex, we construct its ball packing from a Descartes' configuration, which is unique up to Möbius transformations and reflections. For every stacking operation, a new ball representing the new vertex was added into the packing, forming a new Descartes' configuration. We have an unique choice for every newly added ball, so the uniqueness is preserved at every step of construction. □

For a d-polytope $\mathcal{P}$, the *link* of a k-face F is the subgraph of $G(\mathcal{P})$ induced by the common neighbors of the vertices of F. The following lemma will be useful for the proofs later:

Lemma 2.3.7. *For a stacked d-polytope $\mathcal{P}$, the link of a k-face is stacked $(d-k-1)$-polytopal.*

2.3.3 Weighted mass of a word

The following theorem was proved in [40]

Theorem 2.3.8. *The 3-dimensional Apollonian group is a hyperbolic Coxeter group generated by the relations* $\mathbf{R}_i\mathbf{R}_i = \mathbf{I}$ *and* $(\mathbf{R}_i\mathbf{R}_j)^3 = \mathbf{I}$ *for* $1 \le i \ne j \le 5$.

Here we sketch the proof in [40], which is based on the study of reduced words.

Definition 2.3.9. A word $\mathbf{U} = \mathbf{U}_1\mathbf{U}_2\cdots\mathbf{U}_n$ over the generator of the 3-dimensional Apollonian group (i.e. $\mathbf{U}_i \in \{\mathbf{R}_1, \cdots, \mathbf{R}_5\}$) is *reduced* if it does not contain

- subword in the form of $\mathbf{R}_i\mathbf{R}_i$ for $1 \le i \le 5$; or
- subword in the form of $\mathbf{V}_1\mathbf{V}_2\cdots\mathbf{V}_{2m}$ in which $\mathbf{V}_1 = \mathbf{V}_3$, $\mathbf{V}_{2m-2} = \mathbf{V}_{2m}$ and $\mathbf{V}_{2j} = \mathbf{V}_{2j+3}$ for $1 \le j \le 2m-2$.

Notice that $m = 2$ excludes the subwords of the form $(\mathbf{R}_i\mathbf{R}_j)^2$. One verifies that a non-reduced word can be simplified to a reduced word using the generating relations. Then it suffices to prove that no nonempty reduced word, treated as product of matrices, is identity.

To prove this, the authors of [40] studied the sum of entries in the i-th row of $\mathbf{U}$, i.e. $\sigma_i(\mathbf{U}) := \mathbf{e}_i^\intercal\mathbf{U}\mathbf{e}$, and the sum of all the entries in $\mathbf{U}$, i.e. $\Sigma(\mathbf{U}) := \mathbf{e}^\intercal\mathbf{U}\mathbf{e}$. The latter is called the *mass* of $\mathbf{U}$. The quantities $\Sigma(\mathbf{U})$, $\Sigma(\mathbf{R}_j\mathbf{U})$, $\sigma_i(\mathbf{U})$ and $\sigma_i(\mathbf{R}_j\mathbf{U})$ satisfy a series of linear equations, which was used to inductively prove that $\Sigma(\mathbf{U}) > \Sigma(\mathbf{U}')$ for a reduced word $\mathbf{U} = \mathbf{R}_i\mathbf{U}'$. Therefore $\mathbf{U}$ is not an identity since $\Sigma(\mathbf{U}) \ge \Sigma(\mathbf{R}_i) = 7 > \Sigma(\mathbf{I}) = 5$.

We propose the following adaption. Given a weight vector $\mathbf{w}$, we define $\sigma_i^w(\mathbf{U}) = \mathbf{e}_i^\intercal\mathbf{U}\mathbf{w}$ the weighted sum of entries in the i-th row of $\mathbf{U}$, and $\Sigma^w(\mathbf{U}) = \mathbf{e}^\intercal\mathbf{U}\mathbf{w}$ the *weighted mass* of $\mathbf{U}$. The following lemma can be proved with an argument similar as in [40]:

Lemma 2.3.10. *For dimension* 3*, if* $\Sigma^w(\mathbf{R}_i) \ge \Sigma^w(\mathbf{I})$ *for any* $1 \le i \le 5$*, then for a reduced word* $\mathbf{U} = \mathbf{R}_i\mathbf{U}'$*, we have* $\Sigma^w(\mathbf{U}) \ge \Sigma^w(\mathbf{U}')$.

Sketch of proof. It suffices to replace "sum" by "weighted sum", "mass" by "weighted mass", and "$>$" by "$\ge$" in the proof of [40, Theorem 5.1]. It turns out that the following relations hold for $1 \le i, j \le 5$.

$$\sigma_i^w(\mathbf{R}_j\mathbf{U}) = \begin{cases} \sigma_i^w(\mathbf{U}) & \text{if } i \ne j \\ \Sigma^w(\mathbf{U}) - 2\sigma_i^w(\mathbf{U}) & \text{if } i = j \end{cases} \tag{2.7}$$

$$\Sigma^w(\mathbf{R}_i\mathbf{U}) = 2\Sigma^w(\mathbf{U}) - 3\sigma_i^w(\mathbf{U})$$

Then, if we define $\delta_i^w(\mathbf{U}) := \Sigma^w(\mathbf{R}_i\mathbf{U}) - \Sigma^w(\mathbf{U})$, the following relations hold:

$$\begin{aligned}
\delta_i^w(\mathbf{R}_j\mathbf{U}) &= \begin{cases} \delta_i^w(\mathbf{U}) + \delta_j^w(\mathbf{U}) & \text{if } i \neq j \\ -\delta_i^w(\mathbf{U}) & \text{if } i = j \end{cases} \\
\delta_i^w(\mathbf{R}_j\mathbf{U}) &= \delta_j^w(\mathbf{R}_i\mathbf{U}) \text{ if } i \neq j \\
\delta_i^w(\mathbf{R}_j\mathbf{R}_i\mathbf{U}) &= \delta_j^w(\mathbf{U})
\end{aligned}$$

These relations suffice for the induction. The base case is already assumed in the assumption of the theorem, which reads $\delta_i^w(\mathbf{I}) \geq 0$ for $1 \leq i \leq 5$. So the rest of the proof is exactly the same as in the proof of [40, Theorem 5.1]. For details of the induction, we refer the readers to the original proof. The conclusion is $\delta_i^w(\mathbf{U}') \geq 0$, i.e. $\Sigma^w(\mathbf{U}) \geq \Sigma^w(\mathbf{U}')$. □

2.3.4 A generalization of Coxeter's sequence

Let $\mathbf{U} = \mathbf{U}_n \cdots \mathbf{U}_2\mathbf{U}_1$ be a word over the generators of the 3-dimensional Apollonian group (we have a good reason for inverting the order of the indices). Let $\mathbf{M}_0$ be the curvature-center matrix of an initial Descartes' configuration, consisting of five balls $\mathsf{B}_1, \cdots, \mathsf{B}_5$. The curvature-center matrices recursively defined by $\mathbf{M}_i = \mathbf{U}_i\mathbf{M}_{i-1}$, $1 \leq i \leq n$, define a sequence of Descartes' configurations. We take B_{5+i} to be the single ball that is in the configuration at step i but not in the configuration at step $i-1$. This generates a sequence of $5+n$ balls, which generalizes Coxeter's loxodromic sequence in dimension 3. In fact, Coxeter's loxodromic sequence is generated by an infinite word of period 5, e.g. $\mathbf{U} = \cdots \mathbf{R}_2\mathbf{R}_1\mathbf{R}_5\mathbf{R}_4\mathbf{R}_3\mathbf{R}_2\mathbf{R}_1$.

Lemma 2.3.11. *If* $\mathbf{U}$ *is reduced and* $\mathbf{U}_1 = \mathbf{R}_1$*, then in the sequence constructed above,* B_1 *is disjoint from every ball except the first five.*

Proof. We take the initial configuration to be the configuration used in the proof of Theorem 2.2.1. Assume B_1 to be the lower half-space $x_1 \leq 0$, then the initial curvature-center matrix is

$$\mathbf{M}_0 = \begin{pmatrix} 0 & -1 & 0 & 0 \\ 0 & 1 & 0 & 0 \\ 1 & 1 & 1 & \sqrt{1/3} \\ 1 & 1 & -1 & \sqrt{1/3} \\ 1 & 1 & 0 & -2\sqrt{1/3} \end{pmatrix}$$

Every row corresponds to the curvature-center coordinates $\mathbf{m}$ of a ball. The first coordinate m_1 is the curvature κ. If the curvature is not zero, the second coordinate m_2 is the "height" of the center times the curvature, i.e. $x_1\kappa$.

Now take the second column of $\mathbf{M}_0$ to be the weight vector $\mathbf{w}$. That is,

$$\mathbf{w} = (-1, 1, 1, 1, 1)^\intercal.$$

We have $\Sigma^w(\mathbf{R}_1) = 9 > \Sigma^w(\mathbf{I}) = 3$ and $\Sigma^w(\mathbf{R}_j) = 3 = \Sigma^w(\mathbf{I})$ for $j > 1$. By Lemma 2.3.10, we have

$$\Sigma^w(\mathbf{U}_k\mathbf{U}_{k-1}\cdots\mathbf{U}_2\mathbf{R}_1) \geq \Sigma^w(\mathbf{U}_{k-1}\cdots\mathbf{U}_2\mathbf{R}_1)$$

By (2.7), this means that

$$\sigma_j^w(\mathbf{U}_k\cdots\mathbf{U}_2\mathbf{R}_1) \geq \sigma_j^w(\mathbf{U}_{k-1}\cdots\mathbf{U}_2\mathbf{R}_1)$$

if $\mathbf{U}_k = \mathbf{R}_j$, or equality if $\mathbf{U}_k \neq \mathbf{R}_j$.

The key observation is that $\sigma_j^w(\mathbf{U}_k\cdots\mathbf{R}_1)$ is nothing but the second curvature–center coordinate m_2 of the j-th ball in the k-th Descartes' configuration. So at every step, a ball is replaced by another ball with a larger or same value for m_2. Especially, since $\sigma_j^w(\mathbf{R}_1) \geq 1$ for $1 \leq j \leq 5$, we conclude that $m_2 \geq 1$ for every ball.

Four balls in the initial configuration have $m_2 = 1$. Once they are replaced, the new ball must have a *strictly* larger value of m_2. This can be seen from (2.4) and notice that the r.h.s. of (2.4) is at least 4 since the very first step of the construction. We then conclude that $m_2 > 1$ for all balls except the first five. This exclude the possibility of curvature zero, so $x_1\kappa > 1$ for all balls except the first five.

For dimension 3, Equation (2.4) is integral. Therefore the curvature-center coordinates of all balls are integral (see [40] for more details on integrality of Apollonian packings). Since the sequence is a packing (by the result of [12]), no ball in the sequence has a negative curvature. By the definition of the curvature-center coordinates, the fact that $m_2 > 1$ exclude the possibility of curvature 0. Therefore all balls have a positive curvature $\kappa \geq 1$ except the first two.

For conclusion, $x_1\kappa > 1$ and $\kappa \geq 1$ implies that $x_1 > 1/\kappa$, therefore all balls are disjoint from the half-space $x_1 \leq 0$ except the first five. □

2.3.5 Proof of the main result

The "only if" part of Theorem 2.3.1 follows from Theorem 2.2.1 and the following lemma.

Lemma 2.3.12. *Let G be a stacked 4-polytopal graph. If G has an induced subgraph in the form of $G_3 \star G_6$, then G must have an induced subgraph in the form of $K_3 \star P_6$.*

Note that $C_6 \star K_3$ is not an induced subgraph of any stacked polytopal graph.

Proof. Let H be an induced subgraph of G of form $G_3 \star G_6$. Let $v \in V(H)$ be the last vertex of H that is added into the polytope during the construction of the stacked polytope. We have $\deg_H v = 4$, and the neighbors of v induce a complete graph. So the vertex v must be a vertex of G_6. On the other hand, G_3 is an induced subgraph of K_4, therefore must be the complete graph K_3. Hence H is of the form $K_3 \star G_6$.

By Lemma 2.3.7, in the stacked 4-polytope with graph G, the link of every 2-face is stacked 1-polytopal. In other words, the common neighbors of K_3 induce a path P_n where $n \geq 6$. Therefore G must have an induced subgraph of the form $P_6 \star K_3$. □

Proof of the "if" part of Theorem 2.3.1. The complete graph on 5 vertices is clearly 3-ball packable. Assume that every stacked 4-polytope with less than n vertices satisfies this theorem. We now study a stacked 4-polytope $\mathcal{P}$ of $n+1$ vertices that do not have six 4-cliques in its graph with 3 vertices in common, and assume that $G(\mathcal{P})$ is not ball packable.

Let u, v be two vertices of $G(\mathcal{P})$ of degree 4. Deleting v from $\mathcal{P}$ leaves a stacked polytope $\mathcal{P}'$ of n vertices that satisfies the condition of the theorem, so $G(\mathcal{P}')$ is ball packable by the assumption of induction. In the ball packing of $\mathcal{P}'$, the four balls corresponding to the neighbors of v are pairwise tangent. We then construct the ball packing of $\mathcal{P}$ by adding a ball B_v that is tangent to these four balls. We have only one choice (the other choice coincides with another ball), but since $G(\mathcal{P})$ is not ball packable, B_v must overlap some other balls.

However, deleting u also leaves a stacked polytope whose graph is ball packable. Therefore B_v must overlap B_u and only B_u. Now if there is another vertex w of degree 4 different from u and v, deleting w leaves a stacked polytope whose graph is ball packable, which produces a contradiction. Therefore u and v are the only vertices of degree 4.

Let $\mathcal{T}$ be the dual tree of $\mathcal{P}$, its leaves correspond to vertices of degree 4. So $\mathcal{T}$ must be a path, whose two ends correspond to u and v. We can therefore construct the ball packing of $\mathcal{P}$ as a generalised Coxeter's sequence studied in the previous part. The first ball is B_u. The construction word does not contain any subword of form $(\mathbf{R}_i\mathbf{R}_j)^2$ (which produces $C_6 \star K_3$ and violates the condition) or $\mathbf{R}_i\mathbf{R}_i$. One can always simplify the word into a *non-empty* reduced word. This does not change the corresponding matrix, so the curvature-center matrix of the last Descarte configuration remains the same.

Then Lemma 2.3.11 says that B_u and B_v are disjoint, which contradicts our previous discussion. Therefore $G(\mathcal{P})$ is ball packable. □

Corollary 2.3.13 (of the proof)**.** *The tangency graph of an Apollonian 3-ball packing is a 4-tree if and only if it does not contain any Soddy's hexlet.*

Proof. The "only if" part is trivial. We only need to proof the "if" part.

If the tangency graph is a 4-tree, then during the construction, every newly added ball touches exactly 4 pairwise tangent balls. If it is not the case, we can assume B to be the first ball that touches five balls, the extra ball being B'.

Since the tangency graph is stacked 4-polytopal before introducing B, there is a sequence of Descartes' configurations generated by a word, with B' in the first configuration and B in the last one. By ignoring the leading configurations in the sequence if necessary, we may assume that the second Descartes' configuration does not contain B'. We can arrange the first configuration as in the previous proof, taking B' as the lower half-space $x_1 < 0$ and labelling it as the first ball. Therefore the generating word $\mathbf{U}$ ends with $\mathbf{R}_1$.

We may assume that $\mathbf{U}$ does not have any subword of the form $\mathbf{R}_i\mathbf{R}_i$. If $\mathbf{U}$ is reduced, we know in the proof of Theorem 2.3.1 that B and B' are disjoint, contradiction. So $\mathbf{U}$ is non-reduced, but we may simplify $\mathbf{U}$ to a reduced one $\mathbf{U}'$. This will not change the curvature-center matrix of the last Descartes' configuration. After this simplification, the last letter of $\mathbf{U}'$ can not be $\mathbf{R}_1$ anymore, otherwise B and B' are disjoint. If $\mathbf{U}$ ends with $\mathbf{R}_i\mathbf{R}_1$, then $\mathbf{U}'$ ends with $\mathbf{R}_1\mathbf{R}_i$.

In the sequence of balls generated by $\mathbf{U}'$, the only ball that touches B' but not in the initial Descartes' configuration is generated at the first step by $\mathbf{R}_i$. This ball must be B by assumption. This is the only occurrence of $\mathbf{R}_i$ in $\mathbf{U}'$, otherwise B is not contained in the last Descartes' configuration generated by $\mathbf{U}'$. Since B is the last ball generated by $\mathbf{U}$, $\mathbf{R}_i$ must be the first letter of $\mathbf{U}$. The only possibility is then $\mathbf{U} = \mathbf{R}_i\mathbf{R}_1\mathbf{R}_i\mathbf{R}_1$, which implies the presence of Soddy's hexlet. □

By Corollary 2.2.7, the tangency graph of an Apollonian 3-ball packing does not contain three 5-cliques sharing a 4-clique, so being a 4-tree implies that it is stacked 4-polytopal. Therefore, the relation between 4-trees, stacked 4-polytopes and Apollonian 3-ball packings can be illustrated as in Figure 2.4.

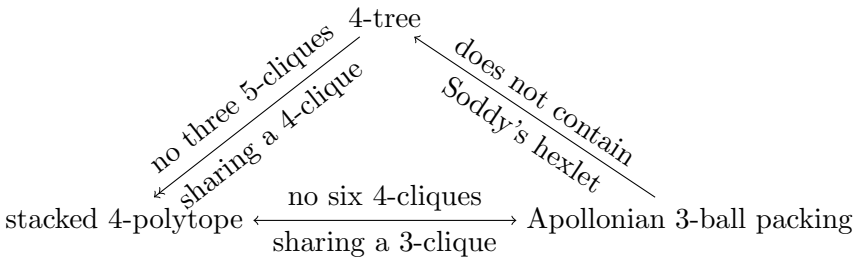

Figure 2.4: Relation between 4-trees, stacked 4-polytopes and 3-ball packings.

2.3.6 Higher dimensions

In dimensions higher than 3, the following relation between Apollonian packing and stacked polytope is restored.

Theorem 2.3.14. *For $d > 3$, if a d-ball packing is Apollonian, then its tangency graph is stacked $(d+1)$-polytopal.*

We will need the following lemma:

Lemma 2.3.15. *If $d \neq 3$, let $\mathbf{w}$ be the $(d+2)$ dimensional vector $(-1, 1, \ldots, 1)^\intercal$, and $\mathbf{U} = \mathbf{U}_n \ldots \mathbf{U}_2\mathbf{U}_1$ be a word over the generators of the d-dimensional Apollonian group (i.e. $\mathbf{U}_i \in \{\mathbf{R}_1, \cdots, \mathbf{R}_{d+2}\}$). If $\mathbf{U}$ ends with $\mathbf{R}_1$ and does not contain any subword of the form $\mathbf{R}_i\mathbf{R}_i$, then $\sigma_i^w(\mathbf{U}) \neq 1$ for $1 \leq i \leq d+2$ as long as $\mathbf{U}$ contains the letter $\mathbf{R}_i$.*

Proof. It is shown in [40, Theorem 5.2] that the j-th row of $\mathbf{U}-\mathbf{I}$ is a linear combination of rows of the matrix $\mathbf{A} = \frac{1}{d-1}\mathbf{e}\mathbf{e}^\intercal - d\mathbf{I}$. However, the weighted row sum $\sigma_i^w(\mathbf{A})$ of the i-th row of $\mathbf{A}$ is 0 except for $i = 1$, whose weighted row sum is $\frac{2}{d-1}$. So $\sigma_i^w(\mathbf{U}-\mathbf{I}) = \frac{2C_i}{d-1}$, where C_i is the coefficient in the linear combination.

According to the calculation in [40], C_i is a polynomial in the variable $x_d = \frac{1}{d-1}$ in the form of

$$C_i(x_d) = \sum_{k=0}^{n_i-1} c_k 2^{k+1} x_d^k$$

where n_i is the length of the longest subword that starts with $\mathbf{R}_i$ and ends with $\mathbf{R}_1$, and c_k are integer coefficients. The leading term is $2^{n_i}x_d^{n_i-1}$ (i.e. $c_{n_i-1} = 1$). Then, by the same argument as in [40], we can show that $C_i(x_d)$ is not zero as long as $\mathbf{U}$ contains $\mathbf{R}_i$. Therefore, for $i \neq 1$,

$$\sigma_i^w(\mathbf{U}) = \frac{2C_i}{d-1} + \sigma_i^w(\mathbf{I}) = \frac{2C_i}{d-1} + 1 \neq 1.$$

For $i = 1$, since $\sigma_1^w(\mathbf{I}) = -1$, what we need to prove is that $C_1 \neq d-1$. So the calculation is slightly different. If $C_1 = d-1$, then x_d is a root of the polynomial $x_dC_1(x_d) - 1$, whose leading term is $(2x_d)^{n_1}$ (note that n_1 is well defined because $\mathbf{U}$ ends with $\mathbf{R}_1$). By the rational root theorem, $d-1$ divides 2^{n_1}. So we must have $d-1 = 2^p$ for some $p > 1$, that is, $x_d = 2^{-p}$. We then have

$$\sum_{k=1}^{n_1} c_{k-1} 2^{k(1-p)} = 1.$$

Multiply both side by $2^{(p-1)n_1}$, we got

$$\sum_{k=1}^{n_1} c_{k-1} 2^{(p-1)(n_1-k)} = 2^{(p-1)n_1}.$$

The right hand side is even since $(p-1)n_1 > 0$. The terms in the summation are even except for the last one since $(p-1)(n_1-k) > 0$. The last term in the summation is $c_{n_1-1}2^0 = 1$ (recall that $c_{n_1-1} = 1$), so the left hand side is odd, which is the desired contradiction. Therefore

$$\sigma_1^w(\mathbf{U}) = \frac{2C_1}{d-1} + \sigma_1^w(\mathbf{I}) \neq 1.$$

□

Proof of Theorem 2.3.14. Consider a construction process of the Apollonian ball packing. The theorem is true at the first step. Assume that it remains true before the introduction of a ball B. We are going to prove that, once added, B touches exactly $d+1$ pairwise tangent balls in the packing.

If this is not the case, assume that B touches a $(d+2)$-th ball B', then we can find a sequence of Descartes' configurations, with B' in the first configuration and B in the last, generated (similar as in Section 2.3.4) by a word over the generators of the d-dimensional Apollonian group with distinct adjacent terms. Without loss of generality, we assume B' to be the lower half-space $x_1 \leq 0$, as in the proof of the Corollary 2.3.11. Then Lemma 2.3.15 says that no ball (except for the first $d+2$ balls) in this sequence is tangent to B', contradicting our assumption.

By induction, every newly added ball touches exactly $d+1$ pairwise tangent balls, so the tangency graph is a $(d+1)$-tree, and therefore $(d+1)$-polytopal. □

So the relation between $(d+1)$-trees, stacked $(d+1)$-polytopes and Apollonian d-ball packings can be illustrated as as in Figure 2.5, where the hooked arrow $A \hookrightarrow B$ emphasizes that every instance of A corresponds to an instance of B.

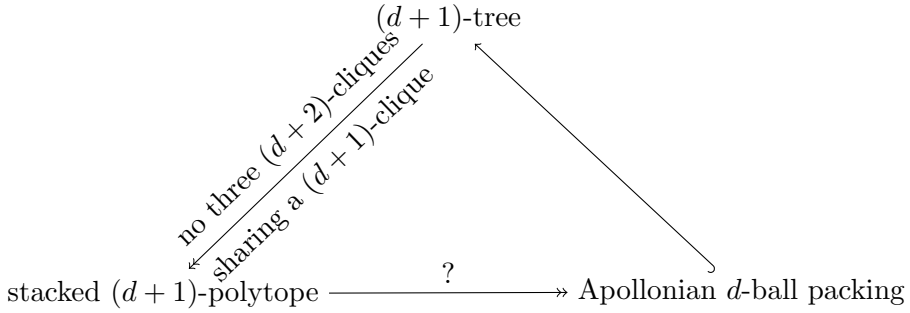

Figure 2.5: Relation between $(d+1)$-trees, stacked $(d+1)$-polytopes and d-ball packings.

Now the remaining problem is to characterise stacked $(d+1)$-polytopal graphs that are d-ball packable. From Corollary 2.2.7, we know that if a $(d+1)$-tree is d-ball

packable, the number of $(\alpha+3)$-cliques sharing a $(\alpha+2)$-clique is at most $k(d-1,\alpha)$ for all $1 \leq \alpha \leq d-1$. Following the patterns in Theorems 2.3.1 and 2.3.4, we propose the following conjecture:

Conjecture 2.3.16. *For an integer $d \geq 2$, there is $d-1$ integers $n_1, \ldots, n_{d-1}$ such that a $(d+1)$-tree is d-ball packable if and only if the number of $(\alpha+3)$-cliques sharing an $(\alpha+2)$-clique is at most n_α for all $1 \leq \alpha \leq d-1$.*

2.4 Discussion

A convex $(d+1)$-polytope is *edge-tangent* if all of its edges are tangent to a d-sphere called *midsphere*. One can derive from the disk packing theorem that[2]:

Theorem 2.4.1. *Every convex 3-polytope has an edge-tangent realization.*

Eppstein, Kuperberg and Ziegler have proved in [33] that no stacked 4-polytopes with more than six vertices has an edge-tangent realization. Comparing to Theorem 2.3.1, we see that ball packings and edge-tangent polytopes are not so closely related in higher dimensions: a polytope with ball packable graph does not, in general, have an edge-tangent realization. In this part, we would like to discuss about this difference in detail.

2.4.1 From ball packings to polytopes

Recall from Section 1.3 that a ball packing $\mathscr{B}$ corresponds to a set of space-like directions X in Lorentz space. By applying a Möbius transformation to the packing if necessary, we may assume that every direction in X is future-directed. With a properly chosen direction of past $\mathbf{z}$, the intersection $\widehat{Q}$ of the affine hyperplane $H^1_{\mathbf{z}} = \{\mathbf{x} \mid \mathcal{B}(\mathbf{x},\mathbf{y}) = 1\}$ with the light cone is a sphere, and the space-like directions in X can be identified to points $\widehat{X}$ on $H^1_{\mathbf{z}}$. Points in $\widehat{X}$ are all outside the projective sphere $\widehat{Q}$.

Let $\widehat{\mathbf{x}}, \widehat{\mathbf{y}} \in \widehat{X}$ be two space-like directions corresponding to a pair of tangent balls in $\mathscr{B}$, the segment $\widehat{\mathbf{x}}\widehat{\mathbf{y}}$ is tangent to the sphere $\widehat{Q}$. Then a $(d+1)$-polytope $\mathcal{P} \subset H^1_{\mathbf{z}}$ is constructed by taking the convex hull of $\widehat{X}$.

Theorem 2.4.2. *The tangency graph $G(\mathscr{B})$ is isomorphic to a spanning subgraph of the 1-skeleton $G(\mathcal{P})$.*

[2] Schramm [75] said that the theorem is first claimed by Koebe [51], who only proved the simplicial and simple cases. He credits the full proof to Thurston [86], but the online version of Thurston's lecture notes only gave a proof for simplicial cases.

Proof. For every $\mathsf{B}_i \in \mathscr{B}$, the corresponding space-like direction $\widehat{\mathbf{x}}_i \in \widehat{X}$ is a vertex of $\mathcal{P}$, since the projective hyperplane $\{\widehat{\mathbf{x}} \mid \mathcal{B}(\mathbf{x}_i, \mathbf{x}) = 0\}$ divides $\widehat{\mathbf{x}}_i$ from other directions in $\widehat{X}$.

For every edge $\mathsf{B}_i\mathsf{B}_j$ in $G(\mathscr{B})$, we now prove that $\widehat{\mathbf{x}}_i\widehat{\mathbf{x}}_j$ is an edge of $\mathcal{P}$. Since $\widehat{\mathbf{x}}_i\widehat{\mathbf{x}}_j$ is tangent to the projective light cone $\widehat{Q}$, $\mathcal{B}(\widehat{\mathbf{x}}, \widehat{\mathbf{x}}) \geq 0$ for all points $\widehat{\mathbf{x}}$ on the segment $\widehat{\mathbf{x}}_i\widehat{\mathbf{x}}_j$. If $\widehat{\mathbf{x}}_i\widehat{\mathbf{x}}_j$ is not an edge of $\mathcal{P}$, some point $\widehat{\mathbf{x}} = \lambda\widehat{\mathbf{x}}_i + (1-\lambda)\widehat{\mathbf{x}}_j$ $(0 \leq \lambda \leq 1)$ can be written as a convex combination of other vertices $\widehat{\mathbf{x}} = \sum_{k\neq i,j} \lambda_k \widehat{\mathbf{x}}_k$, where $\lambda_k \geq 0$ and $\sum \lambda_k \leq 1$. Then we have

$$0 \leq \mathcal{B}(\widehat{\mathbf{x}}, \widehat{\mathbf{x}}) = \mathcal{B}\Big(\lambda\widehat{\mathbf{x}}_i + (1-\lambda)\widehat{\mathbf{x}}_j, \sum_{k\neq i,j} \lambda_k \widehat{\mathbf{x}}_k\Big) < 0$$

because $\mathcal{B}(\widehat{\mathbf{x}}_i, \widehat{\mathbf{x}}_j) \leq -1$ if $i \neq j$. This is a contradiction. □

For an arbitrary d-ball packing $\mathscr{B}$, if a polytope $\mathcal{P}$ is constructed from $\mathscr{B}$ as described above, it is possible that $G(\mathcal{P})$ is not isomorphic to $G(\mathscr{B})$. More specifically, there may be an edge of $\mathcal{P}$ that does not correspond to any edge of $G(\mathscr{B})$. This edge will intersect $\widehat{Q}$, and $\mathcal{P}$ is therefore not edge-tangent. On the other hand, if the graph of a polytope $\mathcal{P}$ is isomorphic to $G(\mathscr{B})$, since the graph does not determine the combinatorial type of a polytope, $\mathcal{P}$ may be different from the one constructed as above. So a polytope whose graph is ball packable may not be edge-tangent.

2.4.2 Edge-tangent polytopes

A polytope is edge-tangent if it can be constructed from a ball packing as described above, and its graph is isomorphic to the tangency relation of this ball packing. Neither condition can be removed. For the other direction, given an edge-tangent polytope $\mathcal{P}$, one can always obtain a ball packing of $G(\mathcal{P})$ by reversing the construction above.

Disk packings are excepted from these problems. In fact, it is easier [74] to derive Theorem 2.4.1 from the following version of the disk packing theorem, which is equivalent but contains more information:

Theorem 2.4.3 (Brightwell and Scheinerman [16])**.** *For every 3-polytope $\mathcal{P}$, there is a pair of disk packings, one consists of* vertex-disks *representing $G(\mathcal{P})$, the other consists of* face-disks *representing the dual graph $G(\mathcal{P}^*)$, such that:*

- *For each edge e of $\mathcal{P}$, the vertex-disks corresponding to the two endpoints of e and the face-disks corresponding to the two faces bounded by e meet at a same point;*
- *A vertex-disk and a face-disk overlap iff the corresponding vertex is on the boundary of the corresponding face, in which case their boundaries intersect orthogonally.*

This representation is unique up to Möbius transformations.

The presence of the face-disks and the orthogonal intersections guarantee the incidence relations between vertices and faces, and therefore fix the combinatorial type of the polytope. We can generalize this statement into higher dimensions:

Theorem 2.4.4. *Given a $(d+1)$-polytope $\mathcal{P}$, if there is a packing of d-dimensional* vertex-balls *representing $G(\mathcal{P})$, together with a collection of $(d-1)$-dimensional* facet-balls *indexed by the facets of $\mathcal{P}$, such that:*

- *For each edge e of $\mathcal{P}$, the vertex-balls corresponding to the two endpoints of e and the boundaries of the facet-balls corresponding to the facets bounded by e meet at a same point;*
- *Either a vertex-ball and a facet-ball are disjoint, or their boundaries intersect at a non-obtuse angle;*
- *The boundary of a vertex-ball and the boundary of a facet-ball intersect* orthogonally *iff the corresponding vertex is on the boundary of the corresponding facet.*

Then $\mathcal{P}$ has an edge-tangent realization.

Again, the convexity is guaranteed by the disjointness and nonobtuse intersections, and the incidence relations are guaranteed by the orthogonal intersections. For an edge-tangent polytope, the facet-balls can be obtained by intersecting the midsphere with the facets. However, they do not form a d-ball packing for $d > 2$. On the other hand, for an arbitrary polytope of dimension 4 or higher, even if its graph is ball packable, the facet-balls satisfying the conditions of Theorem 2.4.4 do not in general exist.

For example, consider the stacked 4-polytope with 7 vertices. The packing of its graph (with the form $K_3 \star P_4$) is constructed in the proof of Theorem 2.2.1. We notice that a ball whose boundary orthogonally intersects the boundary of the three unit balls and the boundary of ball C, have to intersect the boundary of ball D orthogonally (see Figure 2.1), thus violates the last condition of Theorem 2.4.4. One verifies that the polytope constructed from this packing is not simplicial.

2.4.3 Stress freeness

Given a ball packing $\mathscr{B} = \{\mathsf{B}_1, \cdots, \mathsf{B}_n\}$, let $\mathbf{v}_i$ be the vertices of the polytope $\mathcal{P}$ constructed as above. A *stress* of $\mathscr{B}$ is a real function T on the edge set of $G(\mathscr{B})$ such that for all $\mathsf{B}_i \in \mathscr{B}$

$$\sum_{\mathsf{B}_i\mathsf{B}_j \text{ edge of } G(\mathscr{B})} T(\mathsf{B}_i\mathsf{B}_j)(\mathbf{v}_j - \mathbf{v}_i) = 0$$

We can view stress as forces between tangent spherical caps when all caps are in equilibrium. We say that $\mathscr{B}$ is *stress-free* if it has no non-zero stress.

Theorem 2.4.5. *If the graph of a stacked $(d+1)$-polytope is d-ball packable, its ball packing is stress-free.*

Proof. We construct the ball packing as we did in the proof of Theorem 2.3.6, and assume a non-zero stress. The last ball B that is added into the packing has $d+1$ "neighbor" balls tangent to it. Let $\mathbf{v}$ be the vertex of $\mathcal{P}$ corresponding to B. If the stress is not zero on all the $d+1$ edges incident to $\mathbf{v}$, since $\mathcal{P}$ is convex, they can not be of the same sign. So there must be a hyperplane containing $\mathbf{v}$ separating positive edges and negative edges of $\mathbf{v}$. This contradicts the assumption that the spherical cap corresponding to $\mathbf{v}$ is in equilibrium. So the stress must vanish on the edges incident to $\mathbf{v}$. We then remove B and repeat the same argument on the second last ball, and so on, and finally conclude that the stress has to be zero on all the edges of $G(\mathscr{B})$. □

The above theorem, as well as the proof, was informally discussed in Kotlov, Lovász and Vempala's paper on Colin de Verdière number [52, Section 8]. In that paper, the authors defined an graph invariant $\nu(G)$ using the notion of stress-freeness, which turns out to be strongly related to Colin de Verdière number. Their results imply that if the graph G of a stacked $(d+1)$-polytope with n vertices is d-ball packable, then $\nu(G) \leq d+2$, and the upper bound is achieved if $n \geq d+4$. However, Theorem 2.2.1 asserts that graphs of stacked polytopes are in general not ball packable.

Chapter 3

Boyd–Maxwell packings

Most of this chapter is based on a joint work with Jean-Philippe Labbé [22]. Motivated by recent studies on limit roots of infinite Coxeter systems, we revisit Boyd–Maxwell packings, a large class of ball packings that are generated by inversions in the similar way as Apollonian packings (see Section 2.3.1).

A Coxeter group is usually represented as a reflection group in a vector space, which allows to associate a root system to the Coxeter system, see [11] and [47]. For infinite Coxeter systems, Vinberg introduced a more flexible geometric representation that depends on a bilinear form associated to the Coxeter system [53, 91]. In this framework, limit roots are the accumulation points of the directions of the roots. The notion was introduced and studied in [45]. Properties of limit roots of infinite Coxeter systems were investigated in a series of papers. Limit roots lie on the isotropic cone of the bilinear form associated to the geometric representation [45]. The cone over limit roots is the imaginary cone [31]. The relations between limit roots and the imaginary cone are further investigated in [32].

We say that a Coxeter system is Lorentzian if, in the geometric representation mentioned above, the Coxeter group acts on a Lorentz space as a discrete reflection group generated by reflections in the basis, see Section 3.1.1. In many examples of Lorentzian Coxeter systems, fractal patterns of ball packings appear while visualizing limit roots on an affine hyperplane, see [45, Figure 1(b); 46, Figure 1] and Figure 3.1 below. A description of this fractal structure is conjectured in [45, Section 3.2] and proved in [32, Theorem 4.10]. In [46], Hohlweg, Préaux and Ripoll prove that the set of limit roots of a Coxeter group W acting on a Lorentz space is equal to the limit set of W seen as a discrete reflection group of hyperbolic isometries. This explains the pattern of Apollonian disk packing left by the limit roots of the universal Coxeter group of rank 4.

While investigating limit roots, we observed that patterns appearing in these examples are similar to the ball packings studied by Boyd and Maxwell, which generalizes

the renowed Apollonian ball packings. In [14], Boyd proposed a class of infinite ball packings that are generated by inversions, which is later related to Lorentzian Coxeter systems by Maxwell [62]. More specifically, for a Lorentzian Coxeter system, Maxwell proved that the balls correponding to space-like weights form a ball packing if and only if the Lorentzian Coxeter system is of "level 2", see Section 3.1.3.

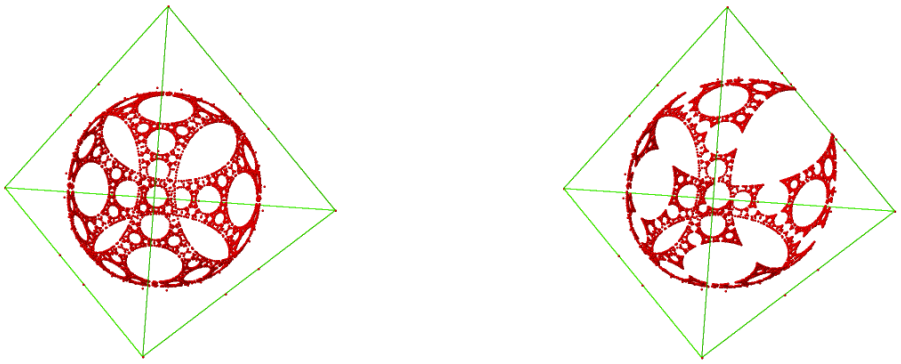

(a) Positive roots of depth ≤ 7 for the Coxeter system of rank 4 with a complete Coxeter graph with all edges labeled by 4. This Coxeter system is of level 2.

(b) Positive roots of depth ≤ 7 for the Coxeter system of rank 4 with a complete Coxeter graph with all edges labeled by 4 except one dotted edge labeled by -1.1. This Coxeter system is of level 3.

Figure 3.1: The pattern of a ball packing and a ball cluster approximated by roots generated by rank-4 Coxeter systems, seen in the affine space spanned by simple roots. The figure is generated by a sage program written by Jean-Philippe Labbé.

In the present chapter, we unify the study of limit roots and the work of Boyd and Maxwell in three steps.

First, if the Lorentzian Coxeter system is of level 2, we show in Section 3.2 that the fractal patterns left by the limit roots are nothing but the corresponding Boyd–Maxwell packings, see Theorem 3.2.1. In Section 3.3, we describe tangency graphs of Boyd–Maxwell packings in terms of the Coxeter complex. Then, in Section 3.4.1, we generalize Maxwell's work to Lorentzian Coxeter systems of level ≥ 3. In this case, the balls corresponding to space-like weights may overlap, and do not form a packing, but many interesting properties still hold. Notably, the set of limit roots is again the residual set of the balls, see Theorem 3.4.3. Finally, in Section 3.4.2, we present geometrically an idea of further generalizing Maxwell's work to degenerate Lorentzian Coxeter systems, which completes the connection between the study of limit roots and Boyd–Maxwell ball packings. In Section 3.5, we summarize the results in [23] about limit directions of Lorentzian Coxeter systems.

3.1 Lorentzian Coxeter systems

Let (W, S) be a finitely generated *Coxeter system*, where S is a finite set of generators and the *Coxeter group* W is generated with the relations $(st)^{m_{st}} = e$ where $s, t \in S$, $m_{ss} = 1$ and $m_{st} = m_{ts} \geq 2$ or $= \infty$ if $s \neq t$. The cardinality $|S| = n$ is the *rank* of the Coxeter system (W, S). For an element $w \in W$, the *length* $\ell(w)$ of w is the smallest natural number k such that $w = s_1 s_2 \dots s_k$ for $s_i \in S$. The readers are invited to consult [11, 47] for more details. We associate a matrix B to (W, S) as follows:

$$B_{st} = \begin{cases} -\cos(\pi/m_{st}) & \text{if} \quad m_{st} < \infty, \\ -c_{st} & \text{if} \quad m_{st} = \infty, \end{cases}$$

for $s, t \in S$, where c_{st} are chosen arbitrarily with $c_{st} = c_{ts} \geq 1$. We say that the Coxeter system (W, S) associated with the matrix B is a *geometric Coxeter system*, and denote it by $(W, S)_B$. To encode geometric Coxeter systems $(W, S)_B$, we adopt Vinberg's convention for Coxeter graphs. That is, if $c_{st} > 1$ the edge st is dotted and labeled by $-c_{st}$. This convention is also used by Abramenko and Brown in [1, Section 10.3.3] and Maxwell in [62, Section 1].

In this chapter, the Lorentz system is always of rank n. The dimension of other objects, such like the Lorentz space and the Boyd–Maxwell packings, vary correspondingly.

3.1.1 Canonical geometric representation

Let V be a real vector space of dimension n, equipped with a basis $\Delta = \{\alpha_s\}_{s \in S}$. The matrix B defines a bilinear form $\mathcal{B}$ on V by $\mathcal{B}(\alpha_s, \alpha_t) = \alpha_s^{\intercal} B \alpha_t$ for $s, t \in S$. For a vector $\alpha \in V$ such that $\mathcal{B}(\alpha, \alpha) \neq 0$, we define the reflection σ_α

$$\sigma_\alpha(\mathbf{x}) := \mathbf{x} - 2\frac{\mathcal{B}(\mathbf{x}, \alpha)}{\mathcal{B}(\alpha, \alpha)}\alpha, \quad \text{for all } \mathbf{x} \in V. \tag{3.1}$$

The homomorphism $\rho : W \to \mathrm{GL}(V)$ that sends $s \in S$ to σ_{α_s} is a faithful *geometric representation* of the Coxeter group W as a discrete subgroup of Lorentz transformations. We refer the readers to [45, Section 1] for more details. In the following, we will write $w(x)$ in place of $\rho(w)(x)$.

If the matrix B is positive definite, we say that $(W, S)_B$ is of *finite type*, in this case W is a finite group, see [47, Theorem 6.4]. If B is positive semidefinite but not definite, we say that $(W, S)_B$ is of *affine type*. In either case, the group W can be represented as a reflection group in Euclidean space. If B has signature $(n-1, 1)$, the pair $(V, \mathcal{B})$ is a n-dimensional *Lorentz space*, and we say that $(W, S)_B$ is of *Lorentzian type*. In the present chapter, Coxeter systems always come with an associated matrix B. Therefore,

we sometimes drop the term "geometric", and simply call $(W, S)_B$ a Coxeter system.

Let $\Phi = W(\Delta)$ be the orbit of Δ under the action of W. The vectors in Δ are called *simple roots*, and the vectors in Φ are called *roots*. The roots Φ are partitioned into *positive roots* $\Phi^+ = \text{cone}(\Delta) \cap \Phi$ and *negative roots* $\Phi^- = -\Phi^+$. Note that in [45] and [32], simple roots only need to be positively independent but not necessarily linearly independent. The *depth* $\mathsf{dp}(\gamma)$ for $\gamma \in \Phi^+$ is the smallest integer k such that $\gamma = s_1 s_2 \dots s_{k-1}(\alpha)$, for $s_i \in S$ and $\alpha \in \Delta$.

Let V^* be the dual vector space of V with dual basis Δ^*. If the bilinear form $\mathcal{B}$ is non-singular, which is the case for Lorentz spaces, V^* can be identified with V, and $\Delta^* = \{\omega_s\}_{s \in S}$ can be identified with a set of vectors in V such that

$$\mathcal{B}(\alpha_s, \omega_t) = \delta_{st}, \tag{3.2}$$

where δ_{st} is the Kronecker delta function. Vectors in Δ^* are called *fundamental weights*, and vectors in the orbit

$$\Omega := W(\Delta^*) = \bigcup_{\omega \in \Delta^*} W(\omega)$$

are called *weights*.

Remark 3.1.1. In the present chapter, we are mainly concerned with Coxeter groups acting on Lorentz space, therefore we use the term "Lorentzian". In the literature, the term *hyperbolic* is used, but with different meanings. In [11, 47], the term *hyperbolic* stands for what we call Lorentzian *of level 1* (see Section 3.1.3 for the definition), while *compact* hyperbolic stand for what we call *strict* Lorentzian of level 1 (see Appendix A for the definition). In [31, Section 9.1] and [32], if the simple roots are linearly independent, the term *weakly hyperbolic* corresponds to what we call Lorentzian. Whereas in [61, 62, 91], the term *hyperbolic* stands for what we call Lorentzian. See [45, Section 3.5] and Remark 3.10 therein for more discussion on terminology.

3.1.2 Limit roots

As observed in [45, Section 2.1], the set of roots $\Phi \subset V$ is discrete and has no limit point. Nevertheless, it is possible to study the asymptotic directions of the roots. For this, we consider the *projective space* $\mathbb{P}V$. The group action of W on V by reflection induces a *projective action* of W on $\mathbb{P}V$:

$$w \cdot \widehat{\mathbf{x}} = \widehat{w(\mathbf{x})}, \quad w \in W, \quad \mathbf{x} \in V.$$

One verifies that this is indeed a group action.

Let $\mathbf{z} = \sum_{s \in S} \omega_s$ be the sum of weights. One verifies that $h(\mathbf{x}) = \mathcal{B}(\mathbf{z}, \mathbf{x})$ is the

sum of the coordinates of $\mathbf{x}$ in the basis Δ. We call it the *height* of the vector $\mathbf{x}$. The hyperplane $H^1_{\mathbf{z}} = \{\mathbf{x} \in V \mid h(\mathbf{x}) = 1\}$ is the affine subspace $\mathsf{aff}(\Delta)$ spanned by the simple roots.

Recall from Section 1.2.1 that $\mathbb{P}V$ can be identified with $H^1_{\mathbf{z}} = \mathsf{aff}(\Delta)$ plus a projective hyperplane added at infinity. If $h(\mathbf{x}) \neq 0$, $\widehat{\mathbf{x}}$ is identified with the intersection of $\mathsf{aff}(\Delta)$ and the straight line passing through $\mathbf{x}$ and the origin. For a simple root $\alpha \in \Delta$, the affine picture of $\widehat{\alpha}$ is α itself. In this sense, the projective roots $\widehat{\Phi}$, projective weights $\widehat{\Omega}$ and projective light cone $\widehat{Q}$ are respectively identified with the intersection of $\mathsf{aff}(\Delta)$ with the 1-subspaces spanned by the roots, weights and light-like vectors. In this affine picture, $\mathsf{conv}(\widehat{\Delta})$ appears as a simplex, and the projective light cone $\widehat{Q}$ is projectively equivalent to a sphere, see for instance [32, Proposition 4.13]. In Figure 3.2, simple roots, fundamental weights and some positive roots are represented in $\mathsf{aff}(\Delta)$.

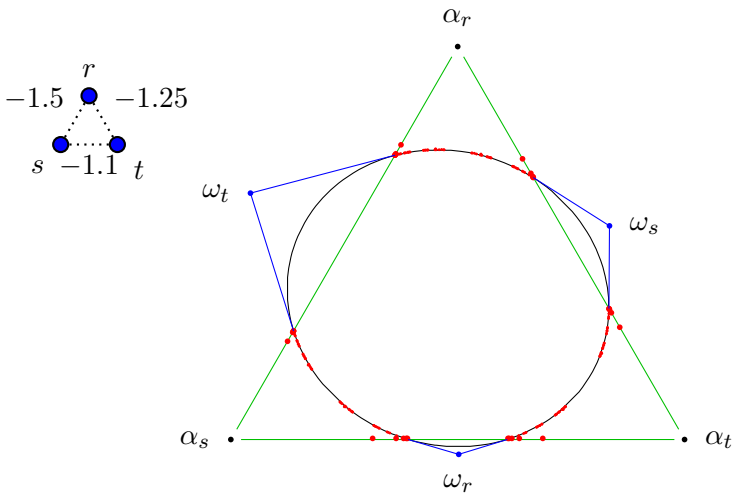

Figure 3.2: Simple roots, fundamental weights, and positive roots of depth ≤ 6 of a geometric Coxeter system of rank 3 seen in the affine space spanned by the simple roots. The Coxeter graph is shown in the upper-left corner.

Definition 3.1.2 (Hohlweg–Labbé–Ripoll [45, Definition 2.12])**.** The set E_Φ of *limit roots* is the set of accumulation points of $\widehat{\Phi}$, in other words,

$$E_\Phi = \{\widehat{\mathbf{x}} \in \mathbb{P}V \mid \text{ there is an injective sequence } (\gamma_i)_{i\in\mathbb{N}} \in \Phi \text{ such that } \lim_{i\to\infty} \widehat{\gamma}_i = \widehat{\mathbf{x}}\}. \quad (3.3)$$

[45, Theorem 2.7] asserts that

$$E_\Phi \subseteq \widehat{Q} \cap \mathsf{conv}(\widehat{\Delta}),$$

see also [31, Proposition 5.3]. Consequently, there is no limit root in the set $\widehat{Q} \setminus \mathsf{conv}(\widehat{\Delta})$. If the set $\widehat{Q} \setminus \mathsf{conv}(\widehat{\Delta})$ consists of open balls (spherical caps), it was conjectured that E_Φ is equal to the complement of the W-orbit of these balls, see [45, Section 3.2]. This conjecture is proved in [43, Theorem 1.2] for Lorentzian Coxeter systems, and more generally in [32, Theorem 4.10] for Δ positively independent. The present chapter relates this result, presented in Theorem 3.1.3, to the result of Maxwell.

Theorem 3.1.3 ([32, Theorem 4.10], [43, Theorem 1.2])**.** *Let $(W, S)_B$ be an irreducible Lorentzian Coxeter system. Then*

$$E_\Phi = \widehat{Q} \setminus (W \cdot (\widehat{Q} \setminus \mathsf{conv}(\widehat{\Delta}))).$$

In particular, if $\widehat{Q} \subset \mathsf{conv}(\widehat{\Delta})$, then $E_\Phi = \widehat{Q}$.

Remark 3.1.4. In [32], the group W acts on the affine space $\mathsf{aff}(\Delta)$, but the action is not defined everywhere. For this reason, Theorem 4.10 of [32] is stated in terms of $\widehat{Q}_{\mathrm{act}}$, the part of $\widehat{Q}$ where W acts. This is however not necessary in our setting, because the action of W is well defined on the projective space $\mathbb{P}V$.

The following theorem is useful for the proofs.

Theorem 3.1.5 ([32, Theorem 3.1])**.** *The set of limit roots E_Φ is a minimal set under the action of W. That is, for any limit root $\widehat{\mathbf{x}} \in E_\Phi$, the orbit $W \cdot \widehat{\mathbf{x}}$ is dense in E_Φ.*

3.1.3 Boyd–Maxwell packing

Recall from Section 2.3.1 that Apollonian packings can be constructed by inversions. In [14], Boyd proposed a new class of infinite ball packings generalizing this construction. The building block still consists of $d+2$ non-overlapping balls. But these balls are not necessarily tangent to each other, hence do not form a Descartes' configuration. Recall from Section 2.1.2 that Descartes–Soddy–Gossett Theorem has a generalisation to arbitrary $d+2$ balls. Similar to Apollonian packings (see Section 2.3.1), an inversion in a sphere that orthogonally intersects the boundary of $d+1$ balls replaces the remaining one with another ball, forming a new building block with the same separation matrix. Boyd then proves that [14, Theorem 4.4] the inversions produce an infinite ball packing if the separation matrix of the building block satisfies certain conditions. Boyd explicitly constructed 13 examples up to dimension nine. Moreover, he noticed a connection to reflection groups.

In [62], Maxwell revisits these packings, and interprets them using Lorentzian Coxeter groups. A Coxeter graph G is said to be *of level* 0 if it represents a finite or affine Coxeter system. The list of level-0 Coxeter graphs can be found in [47, Chapter 2]. A graph is *of level* $\leq r$ if every induced subgraph of G on $n-r$ vertices is of level 0.

A graph is *of level* r if it is of level $\leq r$ but not of level $\leq r-1$. Correspondingly, a Coxeter system $(W,S)_B$ with a Coxeter graph of level r is said to be *of level* r.

For a Lorentzian Coxeter system $(W,S)_B$, while the roots are all space-like, a weight can be space-like, time-like or light-like. Let Ω_r be the set of *space-like weights*. We call the set of balls corresponding to the space-like weights

$$\{\mathsf{B}(\omega) \mid \omega \in \Omega_r\}$$

the *Boyd–Maxwell ball cluster* generated by $(W,S)_B$ (recall from Section 1.2.2 for definition of $\mathsf{B}(\mathbf{x})$). Maxwell proved that Coxeter systems of level 2 are Lorentzian [62, Proposition 1.6] and the following theorem.

Theorem 3.1.6 (Maxwell [62, Theorem 3.2])**.** *Let $(W,S)_B$ be a Lorentzian Coxeter system. The Boyd–Maxwell ball cluster generated by $(W,S)_B$ is a ball packing if and only if $(W,S)_B$ is of level* 2*.*

For example, the Apollonian disk packing is the Boyd–Maxwell ball packing generated by the universal Coxeter system of rank 4. Maxwell manually enumerated connected Coxeter graphs of level 2, and suggested a computer verification. This was completed by the author with the computer algebra system Sage [80] in the joint work with Labbé [22]. The algorithm, presented in Appendix A, is inspired by Chein's enumeration of level-1 Coxeter graphs. The complete list is given in the appended figures.

Remark 3.1.7. If the level-2 Coxeter system is reducible, the Coxeter graph is the union of a level-1 graph and an isolated vertex [62]. In this case, there are only two space-like weights in opposite directions, and the Boyd–Maxwell ball packing consists of two balls that is complement to each other. In the following, we shall focus on irreducible Coxeter systems.

Comparing to Boyd's work, given a Lorentzian Coxeter system, the boundary of the balls corresponding to roots are inversion spheres, and the reflections with respect to roots correspond to inversions. The building block, consisting of the balls corresponding to space-like fundamental weights, may have less than $d+2$ balls. In this sense, Maxwell's approach generalizes Boyd's packing. Figure 3.3 shows an image of a 3-dimensional Boyd–Maxwell ball packing.

The *residual set* of a Boyd–Maxwell ball cluster is the complement of the interiors of all balls in the cluster. The Hausdorff dimension of the residual set of Apollonian disk packing was studied in [12] and calculated in [65], see also [38]. The Hausdorff dimension of the residual set of Apollonian 3-ball packings was calculated in [10].

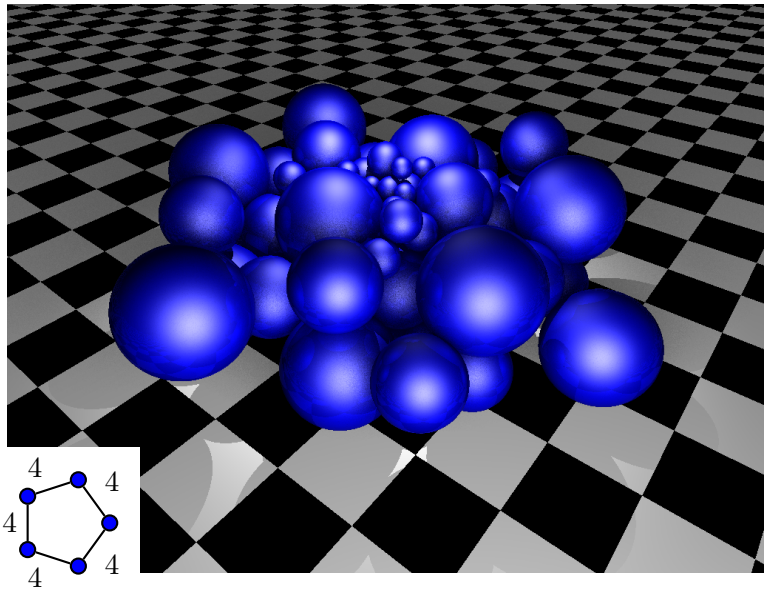

Figure 3.3: Some balls in the ball packing generated by the level-2 Lorentzian Coxeter group whose Coxeter graph is a 5-cycle with all edges labeled by 4. The coordinates are calculated by Sage [80] with the help of CHEVIE package [35], the image is rendered by POV-Ray.

3.2 Boyd–Maxwell packings and limit roots

In this Section, we prove the following theorem, which is the first step for connecting limit roots to Boyd–Maxwell packings.

Theorem 3.2.1. *The set E_Φ of limit roots of an irreducible Lorentzian Coxeter system $(W, S)_B$ of level 2 is equal to the residual set of the Boyd-Maxwell ball packing $\mathscr{B}$ generated by $(W, S)_B$.*

The proof is based on the study of limit weights, which turn out to coincide with limit roots for Lorentzian Coxeter systems. The theorem then follows directly from Maxwell's work.

3.2.1 Limit weights

Let $(W, S)_B$ be a (not necessarily Lorentzian) geometric Coxeter system as described in Section 3.1.1. When the bilinear form $\mathcal{B}$ is non-singular, we define the set of limit weights E_Ω analogously to limit roots.

Definition 3.2.2. The set of *limit weights* E_Ω is the set of accumulation points of the projective weights $\widehat{\Omega}$. That is

$$E_\Omega = \{\widehat{\mathbf{x}} \in \mathbb{P}V \mid \text{there is an injective sequence } (\omega_i)_{i\in\mathbb{N}} \in \Omega \text{ such that } \lim_{i\to\infty} \widehat{\omega}_i = \widehat{\mathbf{x}}\}. \quad (3.4)$$

We recall the following facts about limit roots.

Theorem 3.2.3 ([45, Theorem 2.7])**.** *Consider an injective sequence of roots $(\gamma_k)_{k\in\mathbb{N}}$ and suppose that $(\widehat{\gamma}_k)_{k\in\mathbb{N}}$ converges to a limit $\widehat{\beta}$. Then*

(i) $h(\gamma_k)$ tends to $+\infty$,

(ii) $\widehat{\beta}$ lies in $\widehat{Q}$.

Remark 3.2.4. Theorem 3.2.3(i) is not in the statement of [45, Theorem 2.7], but mentioned in its proof. It is proved in [45, Lemma 2.10] that the squared Euclidean norm of a positive root grows at least linearly with its depth. Then, since the height of a positive root is nothing but its L_1-norm, Theorem 3.2.3(i) follows from the equivalence of the norms.

Here is an analogous result for limit weights.

Theorem 3.2.5. *Consider an injective sequence of weights $(\omega_k)_{k\in\mathbb{N}}$ and suppose that $(\widehat{\omega}_k)_{k\in\mathbb{N}}$ converges to a limit $\widehat{\psi}$. Then*

(i) $h(\omega_k)$ tends to $-\infty$,

(ii) $\widehat{\psi}$ lies in $\widehat{Q}$.

In preparation for the proof, we make the following observations. For $\alpha_t \in \Delta$ and $\omega_s \in \Delta^*$, we have from Equation (3.2) that

$$\sigma_{\alpha_t}(\omega_s) = \begin{cases} \omega_s & \text{if } s \neq t, \\ \omega_s - 2\alpha_s & \text{if } s = t. \end{cases} \quad (3.5)$$

Let $s \in S$ and $w = s_1 s_2 \dots s_k \in W$ where $k = \ell(w)$. Define the set

$$\mathsf{pre}^s(w) := \{s_1 s_2 \dots s_m \mid s_{m+1} = s\}.$$

For any $w' \in \mathsf{pre}^s(w)$, since the expression $w = s_1 s_2 \dots s_k$ is reduced, we have $\ell(w') < \ell(w's)$ and $w'(\alpha_s) \in \Phi^+$, see for example [47, Theorem 5.4]. From Equation (3.5) we have

$$w(\omega_s) = \omega_s - 2 \cdot \sum_{w' \in \mathsf{pre}^s(w)} w'(\alpha_s). \quad (3.6)$$

Proof of Theorem 3.2.5. Every weight in the sequence can be written in the form of an element of W acting on a fundamental weight. By passing to a subsequence if necessary, we may assume that $\omega_k = w_k(\omega_s)$ for a fixed fundamental weight $\omega_s \in \Delta^*$ and an injective sequence of elements $(w_k)_{k\in\mathbb{N}}$ with increasing length.

(i) Using the linearity of h in Equation (3.6), we get

$$h(\omega_k) = h(w_k(\omega_s)) = h(\omega_s) - 2 \cdot \sum_{w' \in \mathsf{pre}^s(w_k)} h(w'(\alpha_s)) \tag{3.7}$$

While $h(\omega_s)$ remains constant, we claim that the summation in (3.7) diverges as k tends to $+\infty$. To prove this claim, we first notice that all the summands are positive. Since S is finite, there are only finitely many positive roots with a bounded depth. As the height of a positive root grows with depth (see Remark 3.2.4), there are only finitely many positive roots with a bounded height. If the summation in (3.7) is bounded by a positive number for infinitely many $k \in \mathbb{N}$, the summation in (3.6) contains a bounded number of items chosen from finitely many positive roots for these k. Consequently, the sequence (ω_k) is not injective as assumed. This contradiction proves our claim.

(ii) Since w_k preserves the bilinear form, $\mathcal{B}(\omega_k, \omega_k) = \mathcal{B}(\omega_s, \omega_s)$ is constant. Using (i), we get

$$\mathcal{B}(\widehat{\psi}, \widehat{\psi}) = \lim_{k\to\infty} \mathcal{B}(\widehat{w_k(\omega_s)}, \widehat{w_k(\omega_s)}) = \lim_{k\to\infty} \frac{\mathcal{B}(\omega_s, \omega_s)}{h(\omega_k)^2} = 0.$$

□

Theorem 3.2.6. *The set of limit weights of a Lorentzian Coxeter system $(W, S)_B$ is equal to its set of limit roots. That is, $E_\Omega = E_\Phi$.*

Proof. We only prove one inclusion, namely $E_\Phi \subseteq E_\Omega$. The proof for the other inclusion works similarly.

Consider an injective sequence of projective roots $(\widehat{\gamma}_k)_{k\in\mathbb{N}}$ that converges to a limit root $\widehat{\beta}$. By Theorem 3.2.3, $\widehat{\beta} \in \widehat{Q}$. By passing to a subsequence, we may assume that $\gamma_k = w_k(\alpha)$ for a fixed simple root $\alpha \in \Delta$ and an injective sequence $(w_k)_{k\in\mathbb{N}}$ of elements of W with increasing length. For each $k \in \mathbb{N}$, we can choose a fundamental weight ω_k, such that $(w_k(\omega_k))_{k\in\mathbb{N}}$ is an injective sequence of weights. This is more clear on Coxeter complex using the notion of gallery distance (see Section 3.3.1): a sequence of chambers with increasing gallery distance from the fundamental chamber guarantees an injective sequence of vertices. By passing again to a subsequence, we may assume that $\omega_k = \omega$ for a fixed fundamental weight $\omega \in \Delta^*$, and that the sequence $(w_k(\omega))_{k\in\mathbb{N}}$ converges to a limit $\widehat{\psi} \in \widehat{Q}$. By Theorem 3.2.5, one has $\widehat{\psi} \in \widehat{Q}$. The bilinear form $\mathcal{B}(\alpha, \omega)$ equals 0 or 1, $h(w_k(\alpha))$ tends to $+\infty$ by Theorem 3.2.3(i), and $h(w_k(\omega))$ tends

to $-\infty$ by Theorem 3.2.5(i). Consequently, we have:

$$\mathcal{B}(\widehat{\beta},\widehat{\psi}) = \lim_{k\to\infty} \mathcal{B}(\widehat{w_k(\alpha)},\widehat{w_k(\omega)}) = \lim_{k\to\infty} \frac{\mathcal{B}(\alpha,\omega)}{h(w_k(\alpha))h(w_k(\omega))} = 0.$$

Since both $\widehat{\beta}$ and $\widehat{\psi}$ lie in the projective light-cone $\widehat{Q}$, we must have $\widehat{\beta} = \widehat{\psi}$ by Proposition 1.2.1. Thus, $E_\Phi \subseteq E_\Omega$. □

Figure 3.4 illustrates the result of the previous theorem.

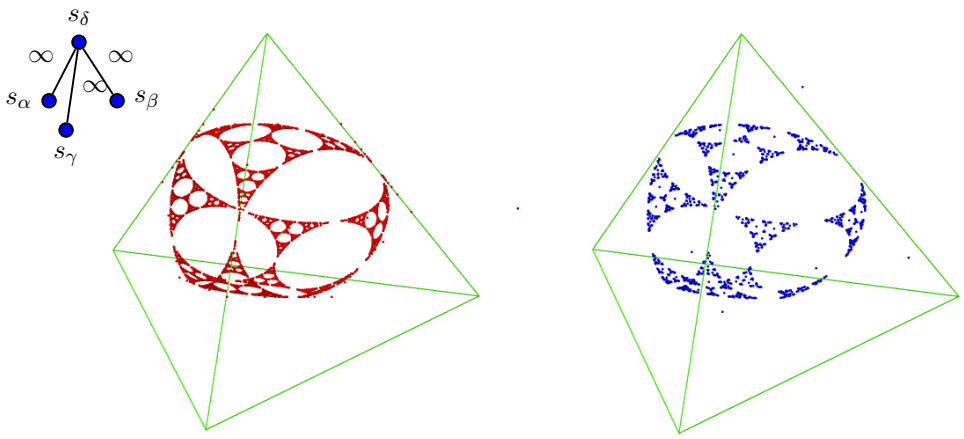

(a) Roots of depth ≤ 9. (b) Weights of "depth" ≤ 9.

Figure 3.4: Positive roots and space-like weights for a Lorentzian Coxeter system of rank 4 seen in the affine space spanned by the simple roots. The Coxeter graph is shown on the upper-left corner. The figure is generated by a sage program written by Jean-Philippe Labbé [45].

Remark 3.2.7. It is natural to ask whether the previous result holds for non-singular geometric Coxeter systems in general. The property that distinguish Lorentz spaces is Proposition 1.2.1, which asserts that a totally isotropic subspace of a Lorentz space is at most of dimension 1. Indeed, it would be interesting to know if the equality $E_\Omega = E_\Phi$ holds in general.

For this, an answer to [32, Question 4.9] would be helpful. In fact, $E_\Omega = E_\Phi$ holds under the assumption that $\mathsf{conv}(E_\Phi) \cap \widehat{Q} = E_\Phi$. Here is a sketch of proof: From the definition, limit weights are on the boundary of the projective Tits cone $\widehat{T}$ [1, Exercise 2.90] (see Section 3.3.1 for definition of Tits cone). We have seen in Theorem 3.2.5(ii) that limit weights are on the projective isotropic cone $\widehat{Q}$. Consequently, limit weights are in the dual of $\widehat{T}$, which is $\mathsf{conv}(E_\Phi)$ by [31, Theorem 5.1(a)]. By assumption, we have proved that $E_\Omega \subseteq E_\Phi$, and the equality follows from Theorem 3.1.5.

3.2.2 Proof of Theorem 3.2.1

Recall from Section 3.1.3 that Ω_r denotes the set of space-like weights. It is the union of the orbits of space-like fundamental weights. Space-like weights in Ω_r correspond to balls in the Boyd–Maxwell ball packing $\mathscr{B}$ generated by $(W, S)_B$. This correspondence allows us to prove Theorem 3.2.1.

Proof of Theorem 3.2.1. The set E_Φ is a minimal set under the action of W by Theorem 3.1.5. Therefore $E_\Phi = E_\Omega$ is the set of accumulation points of $\widehat{\Omega}_r$. Since limit roots are light-like, $E_\Phi = E_\Omega$ is disjoint from $\widehat{\Omega}_r$. By Theorem 3.1.6, E_Φ is disjoint from the interiors of the balls in the Boyd–Maxwell packing $\mathscr{B}$. This proves that E_Φ is contained in the residual set of $\mathscr{B}$.

The other inclusion follows from the fact that $\mathscr{B}$ is maximal, i.e. it is impossible to add any ball into the complement of $\mathscr{B}$ to form a bigger packing. In other words, for a point p in the residual set of $\mathscr{B}$, every neighborhood of p contains some ball in $\mathscr{B}$. So p is an accumulation point of $\widehat{\Omega}_r$, therefore a limit root. The maximality of $\mathscr{B}$ is guaranteed by [62, Theorem 3.3] and [63, Theorem 6.1]. □

Let us now explain the relation between ball packings studied by Boyd and Maxwell and ball packings observed in the study of limit roots. Maxwell's condition of "level 2" can be interpreted as follows. Consider a Coxeter system $(W, S)_B$ of level 2 with Coxeter graph G. Then $(W, S)_B$ is of level ≤ 2, i.e. removing any two vertices from G leaves an affine or finite Coxeter graph. In the affine picture, this means that every $(n-2)$-face of the simplex $\mathsf{conv}(\widehat{\Delta})$ is disjoint from, or tangent to the projective light cone $\widehat{Q}$. Furthermore, $(W, S)_B$ is not of level ≤ 1, i.e. there exists a vertex of G whose removal does not yield an affine or finite Coxeter graph. In the affine picture, this means that some facet of the simplex $\mathsf{conv}(\widehat{\Delta})$ intersects the projective light cone $\widehat{Q}$ transversally. In other words, there is at least one space-like weight. In the point of view of [45] and [32], $(W, S)_B$ is of level 2 if and only if $\widehat{Q} \setminus \mathsf{conv}(\widehat{\Delta})$ is not empty and consists of a union of disjoint open balls. Then we notice from Equation (3.2) that

$$\mathsf{aff}(\Delta \setminus \{\alpha_s\}) = \mathsf{aff}(\Delta) \cap H_{\omega_s}, \quad \forall s \in S,$$

In other words, the supporting hyperplane $\mathsf{aff}(\Delta \setminus \{\alpha_s\})$ of the simplex $\mathsf{conv}(\widehat{\Delta})$ is exactly the intersection of $\mathsf{aff}(\Delta)$ and the orthogonal hyperplane for the fundamental weight ω_s. Therefore, the closed balls obtained by the space-like fundamental weights are exactly the closure of the open balls in $\widehat{Q} \setminus \mathsf{conv}(\widehat{\Delta})$. Consequently, if the Coxeter system is Lorentzian of level 2, the fractal structure described in Theorem 3.1.3 is the Boyd–Maxwell ball packing described in Theorem 3.1.6.

3.3 Tangency graph and Coxeter complex

In this section, we study the tangency graph of Boyd–Maxwell ball packings. This investigation incorporates Apollonian packings as a special case, but the flavor is different from Chapter 2. In Chapter 2, we study finite ball packings, and give a forbidden induced graph characterisation. In this section, the Boyd–Maxwell packings are infinite. We describe the tangency graph in terms of the Coxeter complex, but do not give any characterisation.

3.3.1 Coxeter complex

For a Lorentzian Coxeter system $(W, S)_B$, let $C = \text{cone}(\Delta^*)$ be the closed cone over fundamental weights. Equivalently, C is the intersection of the half-spaces $\{\mathbf{x} \in V \mid \mathcal{B}(\mathbf{x}, \alpha) \geq 0\}$ for simple roots $\alpha \in \Delta$. The *Tits cone*

$$T = \text{cone}(\Omega) = \bigcup_{w \in W} w(C)$$

is the closed cone spanned by weights. It contains one component of the light cone [62, Corollary 1.3]. By abuse of language, we consider $\widehat{C}$ in the affine picture of $\mathbb{P}V$ as a $(n-1)$-dimensional simplex supported by projective hyperplanes

$$\widehat{H}_\alpha = \{\widehat{\mathbf{x}} \in \mathbb{P}V \mid \mathcal{B}(\mathbf{x}, \alpha) = 0\}$$

with $\alpha \in \Delta$. Its vertices are the projective fundamental weights. We call $\widehat{C}$ the *fundamental chamber*. The simplices $w \cdot \widehat{C}$ with $w \in W$ are called *chambers*. The facets of a chamber are called *panels*. For $w \in W$ and $\alpha \in \Delta$, the projective hyperplane $w \in \widehat{H}_\alpha$ is called a *wall*. The *Coxeter complex* $\mathscr{C}$ associated to the Lorentzian Coxeter system $(W, S)_B$ is the simplicial complex whose maximal simplices correspond to the chambers. The Coxeter complex $\mathscr{C}$ is a simplicial decomposition of the projective Tits cone $\widehat{T}$ whose vertices correspond to the projective weights. It is pure of dimension $n-1$, where n is the rank of the Coxeter system.

Remark 3.3.1. This definition of Coxeter complex is adapted for our purpose. It applies to Lorentzian Coxeter systems because the Tits cone is strictly convex and does not contain any line through the origin [1, Section 2.6.3]. This is however not true for finite or affine Coxeter groups. We refer the readers to [1, Chapter 3] for combinatorial definition in term of cosets, which applies to general Coxeter systems.

The group W acts simply transitively on the chambers of $\mathscr{C}$. The *dual graph* of $\mathscr{C}$ is the Cayley graph of (W, S). Two chambers are *adjacent* if they share a panel. A *gallery* is a sequence of chambers $(\widehat{C}_0, \dots, \widehat{C}_k)$ such that consecutive chambers are adjacent, and k is the *length* of the gallery. We say that a gallery $(\widehat{C}_0, \dots, \widehat{C}_k)$

connects two simplices $\widehat{A}$ and $\widehat{A}'$ of $\mathscr{C}$ if $\widehat{A} \subseteq \widehat{C}_0$ and $\widehat{A}' \subseteq \widehat{C}_k$. The *gallery distance* $d(\widehat{A}, \widehat{A}')$ between two simplices $\widehat{A}$ and $\widehat{A}'$ is the minimum length of a gallery connecting $\widehat{A}$ and $\widehat{A}'$. A gallery connecting $\widehat{A}$ and $\widehat{A}'$ with length $d(\widehat{A}, \widehat{A}')$ is called a *minimal gallery*. For an element $w \in W$, its length $\ell(w) = d(\widehat{C}, w \cdot \widehat{C})$. We refer the readers to [1, Section 1.4.9] for more details. A pure simplicial complex of dimension $n-1$ is *vertex-colorable* if there is a set of n colors and a *type function* τ that assigns to each vertex of $\mathscr{C}$ a color such that vertices of each chamber have different colors. The following property of $\mathscr{C}$ is useful for our purpose [1, Theorem 3.5]:

Theorem 3.3.2. *The simplicial complex $\mathscr{C}$ is vertex-colorable, and the action of W on $\mathscr{C}$ is type-preserving.*

In the previous theorem, we can use the fundamental weights Δ^* as the colors. A vertex v is assigned the color $\omega \in \Delta^*$ if and only if v is in the orbit $W \cdot \widehat{\omega}$. Correspondingly, every simplex is assigned a type, which is the set of the colors of its vertices. For a panel of type $\Delta^* \setminus \{\omega\}$, we say instead that it is of type ω, to lighten the text.

3.3.2 Tangency graph

In Section 2.3, we compare the tangency graphs of Apollonian packings to 1-skeletons of stacked polytopes, and give a forbidden subgraph characterisation for 3-dimensional Apollonian packings. In this part, we interpret the tangency graph of a Boyd–Maxwell ball packing in terms of the Coxeter complex of the associated Coxeter system.

Recall that the vertices of a Coxeter complex can be colored by fundamental weights. Vertices with time- or light-like colors are called *imaginary vertices*, and vertices with space-like colors are called *real vertices*. Real vertices correspond to balls in the Boyd–Maxwell packing. For a Lorentzian Coxeter system of level 2, $\mathcal{B}(\omega, \omega) \leq 1$ for all fundamental weights $\omega \in \Delta^*$, see [62, Proposition 1.6]. A vertex colored by ω, such that $\mathcal{B}(\omega, \omega) = 1$, is called *surreal*, and a panel of type ω is called *surreal*. Two surreal vertices are said to be *adjacent* if they are of the same color and belong to two adjacent chambers of the Coxeter complex $\mathscr{C}$ sharing a surreal panel. By Equation (3.1), a pair of adjacent surreal vertices correspond to a pair of tangent balls. Finally, an edge uv of type $\{\omega_u, \omega_v\}$ is called a *real edge* if and only if $\mathcal{B}(\overline{\omega}_u, \overline{\omega}_v) = -1$ (recall from Section 1.2.2 that $\overline{\mathbf{x}}$ is the normalized vector). One verifies that the vertices of a real edge correspond to a pair of tangent balls.

We can now describe the tangency graph in term of the Coxeter complex.

Theorem 3.3.3. *Let $\mathscr{B}$ be a Boyd–Maxwell ball packing generated by a Coxeter system $(W, S)_B$ of level 2. Let $\mathscr{C}$ be the Coxeter complex of $(W, S)_B$, then the vertices of the tangency graph $G(\mathscr{B})$ are the real vertices of $\mathscr{C}$, and uv is an edge of $G(\mathscr{B})$ if and only if one of the following condition is fulfilled,*

- *The edge uv of $\mathscr{C}$ is real, in which case u and v are of different colors,*
- *The vertices u and v are surreal and adjacent, in which case u and v are of the same color.*

Edges connecting pairs of adjacent surreal vertices are not present in the Coxeter complex $\mathscr{C}$, we call them *surreal edges*. So the tangency graph $G(\mathscr{B})$ can be constructed by taking the real vertices and real edges from the 1-skeleton of $\mathscr{C}$, and add surreal edges.

Proof. We have seen that real vertices represent balls in the Boyd–Maxwell packing, while real edges and surreal edges represent pairs of tangent balls. This was first observed by Maxwell in [62]. It remains to prove that every pair of tangent balls must be represented by a real edge or a surreal edge.

For two real vertices u and v such that $d(u,v) \geq 2$, we will prove that the balls represented by u and v are not tangent. The proof is by induction on the gallery distance. The inductive step is exactly the same as in the proof of Equation (1.5) in [62], but we need to establish different base cases for proving strict inequalities.

Let u be a vertex of $\mathscr{C}$, $\omega_u \in \Delta^*$ be its color, and $s_u \in S$ and $\alpha_u \in \Delta$ be the corresponding generator and simple root, that is $s_u(\omega_u) = \omega_u - 2\alpha_u$. Without loss of generality, we assume that $u = \widehat{\omega}_u$. Let v be another vertex of $\mathscr{C}$ and $(C_0, \ldots, C_{d(u,v)})$ be a minimal gallery connecting u and v. We may assume that C_0 is the fundamental chamber. Let ω_i $(1 \leq i \leq d(u,v))$ be the type of the panel shared by C_i and C_{i-1}, we define $w = s_1 w' = s_1 \ldots s_{d(u,v)}$ where s_i is the generator corresponding to ω_i. Note that $s_1 = s_u$ and $s_{d(u,v)} = s_v$. Then $C_{d(u,v)} = w \cdot C_0$, and $v = w \cdot \widehat{\omega}_v$. Maxwell proved that [62, Equation (1.6) et seq.]

$$\begin{aligned} \mathcal{B}(\omega_u, w(\omega_v)) &= \mathcal{B}(\omega_u, w'(\omega_v)) - 2\mathcal{B}(\alpha_u, w'(\omega_v)), && (3.8)\\ &\leq -\sqrt{\mathcal{B}(\omega_u,\omega_u)\mathcal{B}(\omega_v,\omega_v)} && (3.9) \end{aligned}$$

for any $u \neq v$. We now prove, by induction on $d(u,v)$, that the inequality (3.9) is strict for $d(u,v) \geq 2$. First, we establish the base cases.

If u and v are of different colors, $\omega_u \neq \omega_v$, the base case for the induction is $d(u,v) = 2$. We may assume that $w = s_u s_v$, where s_u and s_v do not commute (otherwise $d(u,v) = 0$), then

$$\begin{aligned} \mathcal{B}(\omega_u, w(\omega_v)) &= \mathcal{B}(s_u(\omega_u), s_v(\omega_v)) = \mathcal{B}(\omega_u - 2\alpha_u, \omega_v - 2\alpha_v),\\ &= \mathcal{B}(\omega_u,\omega_v) + 4\mathcal{B}(\alpha_u,\alpha_v) - 2\mathcal{B}(\omega_u,\alpha_v) - 2\mathcal{B}(\alpha_u,\omega_v). \end{aligned}$$

In the last line, the last two terms are 0, the second term is *strictly* negative since s_u and s_v do not commute, and the first term $\leq -\sqrt{\mathcal{B}(\omega_u,\omega_u)\mathcal{B}(\omega_v,\omega_v)}$ by (3.9). We

conclude that

$$\mathcal{B}(\omega_u, w(\omega_v)) < -\sqrt{\mathcal{B}(\omega_u,\omega_u)\mathcal{B}(\omega_v,\omega_v)}.$$

Therefore, $\mathcal{B}(\overline{\omega}_u, \overline{w(\omega_v)}) < -1$, and the balls represented by u and v are not tangent.

If u and v are of the same color $\omega = \omega_u = \omega_v$, the base case for the induction is $d(u,v) = 3$. Let $s = s_u = s_v$ and $\alpha = \alpha_u = \alpha_v$. We may assume that $w = ss's$, where $s \neq s' \in S$ and the order of ss' is bigger than 3 (otherwise $d(u,v) \leq 1$). Then

$$\begin{aligned}\mathcal{B}(\omega, w(\omega)) &= \mathcal{B}(s(\omega), s's(\omega)) = \mathcal{B}(s(\omega), s(\omega)) - 2\mathcal{B}(s(\omega), \alpha')^2 \\ &= \mathcal{B}(\omega,\omega) - 2\mathcal{B}(\omega - 2\alpha, \alpha')^2 = \mathcal{B}(\omega,\omega) - 8\mathcal{B}(\alpha,\alpha')^2,\end{aligned}$$

where α' is the simple root corresponding to s'. In the last line, the first term is ≤ 1 by [62, Proposition 1.6]. As for the second term, since the order of ss' is bigger than 3, we have $\mathcal{B}(\alpha,\alpha') < -1/2$, so $8\mathcal{B}(\alpha,\alpha')^2 > 2$. We conclude that $\mathcal{B}(\omega, w(\omega)) < -1$, so $\mathcal{B}(\overline{\omega}, \overline{w(\omega)}) < -1$, therefore the balls represented by u and v are not tangent.

In Equation (3.8), the second term $\mathcal{B}(\alpha_u, w'(\omega_v))$ is non-negative [62, Corollary 1.8]. We then use Equation (3.8) for the induction, and conclude that if $d(u,v) \geq 2$, the corresponding balls are not tangent, so uv does not correspond to any edge of $G(\mathscr{B})$. Therefore, the only possible edges are the real and the surreal edges. □

Corollary 3.3.4. *For an irreducible Lorentzian Coxeter system $(W,S)_B$ of level 2, the projective Tits cone $\widehat{T} \subset \mathbb{P}V$ is an edge-tangent infinite polytope. That is, every edge of $\widehat{T}$ is tangent to the projective light-cone $\widehat{Q}$. Furthermore, the 1-skeleton of $\widehat{T}$ is the tangency graph of the Boyd–Maxwell packing $\mathscr{B}$ generated by $(W,S)_B$.*

Proof. Vertices of $\widehat{T}$ are projective weights. No edge of $\widehat{T}$ is disjoint from $\widehat{Q}$, otherwise two balls in the packing $\mathscr{B}$ would overlap. No edge of $\widehat{T}$ intersect $\widehat{Q}$ transversally because $\widehat{Q} \subset \widehat{T}$ by [62, Corollary 1.3]. Finally, an edge of $\widehat{T}$ that is tangent to $\widehat{Q}$ correspond to a pair of tangent balls in $\mathscr{B}$. □

3.4 Further generalization

In this section, we generalise Boyd–Maxwell packings in two different directions.

On the one hand, we consider Lorentzian Coxeter systems of level ≥ 3. The Boyd–Maxwell cluster is no longer a packing, but many properties remains. Consequently, with similar techniques, we can extend Theorem 3.2.1 to any Boyd–Maxwell cluster.

On the other hand, we consider geometric Coxeter systems whose associated matrices have signature $(d-1, 1, n-d)$. They can also be represented as reflection subgroups of Lorentz group, as long as we do not insist the simple roots to form a basis. Maxwell's Theorem 3.1.6 then generalizes with a different definition of "level".

3.4.1 Limit roots and Boyd–Maxwell ball clusters

For a Lorentzian Coxeter system of level ≤ 1, every facet of $\mathsf{conv}(\widehat{\Delta})$ is disjoint from, or tangent to Q. Since there are no space-like weights, the Boyd–Maxwell ball cluster is empty. Therefore $E_\Phi = \widehat{Q}$, as observed in [32, 45]. In this case, the boundary of the Tits cone is the light cone.

For a Lorentzian Coxeter system of level ≥ 3, the space-like weights still represent $(n-2)$-dimensional balls, but some balls may overlap, see Figure 3.1(b) for an example. To generalize Theorem 3.2.1 to Boyd–Maxwell ball clusters, most of the arguments and discussions in Section 3.2.2 apply. However, slight modifications are necessary.

First of all, we say that two balls *intersect deeply* if one is contained in the other, or if their boundary intersect at an obtuse angle, in which case the bilinear form of the corresponding space-like weights is positive. In a Boyd–Maxwell ball cluster, we claim that no two balls *intersect deeply*. This is a consequence of the following lemma, taken from the proof of Theorem 1.9 in [62].

Lemma 3.4.1 ([62, Equation (1.5)])**.** *Let $\omega, \omega' \in \Omega$ be two distinct weights of a Lorentzian Coxeter group. Then $\mathcal{B}(\omega, \omega') \leq 0$.*

Correspondingly, we say that a ball cluster is *maximal* if it is impossible to add any additional ball into the cluster without deeply intersecting any other ball. The maximality of Boyd–Maxwell packings is again guaranteed by the following generalized version of [62, Theorem 3.3].

Lemma 3.4.2. *Let $(W, S)_B$ be a Lorentzian Coxeter system of level 2 or higher. If $\mathrm{cone}(\Omega) = \mathrm{cone}(\Omega_r)$, then the Boyd–Maxwell ball cluster generated by $(W, S)_B$ is maximal.*

Maxwell's proof of [62, Theorem 3.3] applies directly to this generalized version, and the assumption of this lemma is verified by [63, Theorem 6.1]. All other arguments in the proof of Theorem 3.2.1 generalize directly. We then obtain the following result, which completes the connection between Theorem 3.1.3 and 3.1.6 in the Lorentzian case.

Theorem 3.4.3. *The set E_Φ of limit roots of an irreducible Lorentzian Coxeter system $(W, S)_B$ is equal to the residual set of the Boyd-Maxwell ball cluster generated by $(W, S)_B$.*

3.4.2 Positively independent simple roots

In the previous sections, we assume that the simple roots form a basis of the representation space, whereas in [32, 45], the simple roots are defined to be a set of *positively independent* vectors $\Delta = \{\alpha_s\}_{s \in S}$ such that $\mathcal{B}(\alpha_s, \alpha_t) = B_{st}$. Theorem 3.1.3 holds in

this more general framework. However, if the simple roots are not linearly independent, we can not defined the weights to be the dual basis, so Maxwell's approach does not work. To complete the connection between limit roots and Boyd–Maxwell packings, we propose an idea of extending Maxwell's work.

Let V be a d-dimensional vector space associated with a non-singular bilinear form $\mathcal{B}$. Assume that a geometric Coxeter system $(W,S)_B$ is represented in V as a Coxeter system generated by reflections in a set of simple roots $\Delta \in V$. Then the nullity of the matrix B is $n-d$, where n is the rank of $(W,S)_B$. If $n=d$, this is exactly the representation in Section 3.1.1. Otherwise, we say that $(W,S)_B$ is *degenerate*. In this case, the representation can be obtained from the one in Section 3.1.1 by projecting the simple roots onto the quotient space over the $(n-d)$-dimensional radical.

For a subset $I \subset S$, we say that the Coxeter system generated by I is a *k-facial subsystem* if $\mathsf{conv}\{\widehat{\alpha}_s \in \widehat{\Delta} \mid s \in I\}$ is a k-face of $\mathsf{conv}(\widehat{\Delta})$ in the projective representation space (compare "facial subgroup" in [31, 32]). We now generalize Maxwell's definition of "level". We say that a finite or affine geometric Coxeter system is *of level* 0. A geometric Coxeter system is said to be *of level* $\leq r$ if its $(d-r)$-facial subsystems are all of level 0, and *of level* r if it is of level $\leq r$ but not of level $\leq r-1$. In the case where $n=d$, our definition coincides with Maxwell's.

In the projective space, the dual polytope of $\mathsf{conv}(\widehat{\Delta})$, defined as

$$\widehat{C} = \{\widehat{\mathbf{x}} \in \mathbb{P}V \mid \mathcal{B}(\mathbf{x},\mathbf{y}) \geq 0 \text{ for all } \widehat{\mathbf{y}} \in \mathsf{conv}(\widehat{\Delta})\},$$

is called the *fundamental chamber*. The vertices of $\widehat{C}$ are analogous to the *projective weights*. Then the notions of *chambers*, *weights* and *Tits cone* can be defined similarly as before. Assume that $(V,\mathcal{B})$ is a Lorentz space, we can now repeat the discussion in Section 3.2.2: If the geometric Coxeter system is of level 2, then every codimension-2 face of $\mathsf{conv}(\widehat{\Delta})$ is disjoint from or tangent to the projective light cone $\widehat{Q}$, and at least one facet of $\mathsf{conv}(\widehat{\Delta})$ intersects $\widehat{Q}$ transversally. It is then clear that space-like vertices of the Tits cone correspond to a ball packing.

Regard the interior of $\widehat{Q}$ as the Klein model of hyperbolic space, then the fundamental chamber corresponds to the *Vinberg polytope*, i.e. the fundamental domain of a hyperbolic reflection group. We say that a Vinberg polytope is *of level* r if the reflections in its facets generate a Coxeter system of level r. Vinberg polytopes of level 1 are of finite volume. We have seen that Vinberg polytopes of level 2 correspond to infinite ball packings generated by inversions. As in our enumeration of level-2 Coxeter graphs (see Appendix A), level-2 Vinberg polytopes can be constructed from level-1 Vinberg polytopes. As a consequence, level-2 Vinberg polytopes may exist in very high dimensions, but a complete enumeration or classification is challenging. On the one hand, level-1 Vinberg polytopes do not exist in arbitrarily high dimension, see [71, 92]. In particular, Prokhorov's result [71] implies that level-2 Vinberg polytopes do not exist

in dimension 997. On the other hand, there are infinitely many Vinberg polytopes in low dimensions, see [2]. However, it is possible to enumerate level-2 Vinberg polytopes with few vertices, in the line of [87, 88, 89]. Furthermore, it would be nice to reformulate the argument above in an algebraic way, similar to the approach of Maxwell in [62].

3.5 Limit direction of Coxeter systems

In this part, we summarise the main results in a joint work with Jean-Philippe Labbé [23]. This is independent of the study on Boyd–Maxwell packings.

Limit directions of a geometric Coxeter system $(W, S)_B$ are accumulation points of the orbit $W \cdot \mathbf{x}_0$ for some base point $\mathbf{x}_0 \in \mathbb{P}V$. In other words, let E_V denote the set of limit directions,

$$E_V = \{\widehat{\mathbf{x}} \in \mathbb{P}V \mid \text{there is a vector } \mathbf{x}_0 \in V \text{ and an injective sequence } (w_i \cdot \widehat{\mathbf{x}}_0)_{i\in\mathbb{N}} \\ \text{in the orbit } W \cdot \widehat{\mathbf{x}}_0 \text{ such that } \lim_{i\to\infty} w_i \cdot \widehat{\mathbf{x}}_0 = \widehat{\mathbf{x}}\}.$$

In the previous sections, we have seen that limit roots of a geometric Coxeter system $(W, S)_B$ are limit directions arising from

(i) simple roots [45, Definition 2.12],

(ii) limit roots [32, Theorem 3.1(b)],

(iii) projective roots [32, Theorem 3.1(c)].

Moreover, if $(W, S)_B$ is Lorentzian, limit roots are limit directions arising from

(iv) time-like directions [46, Theorem 3.3],

(v) projective weights [22, Theorem 3.4],

These results motivate us to investigate limit directions of Coxeter groups arising from *any* vector of the representation space, not necessarily roots, weights, or time-like vectors.

In [23], we initiate this investigation for Lorentzian Coxeter systems. By regarding the Coxeter group as a Kleinian group, it is clear that there is no time-like limit direction. It turns out that every light-like limit direction is a limit root [23, Theorem 2.5], so limit roots also arise from light-like directions. In addition, we also prove that limit roots arising from different base points through a same sequence are the same [23, Corollary 2.6]. Then, based on the classification of Lorentzian transformations according to their eigenvalues, we introduce a spectral perspective for limit roots

Theorem 3.5.1. *Let E_∞ be the set of directions of non-unimodular eigenvectors for infinite-order elements of a Lorentzian Coxeter system $(W, S)_B$. Then the set of limit roots E_Φ of $(W, S)_B$ is the closure of E_∞, that is*

$$E_\Phi = \overline{E_\infty}.$$

However, for non-Lorentzian Coxeter systems, there may be isotropic limit directions that are not limit roots, see [23, Example 3.11].

Furthermore, we observed space-like limit directions, and describe the set of limit directions for Lorentzian Coxeter systems in terms of the projective Coxeter arrangement, i.e. the infinite arrangement of reflecting hyperplanes in the projective representation space.

Theorem 3.5.2. *Let E_V be the set of limit directions of a Lorentzian Coxeter system $(W, S)_B$ and $\mathscr{L}_{\text{hyp}}$ be the union of codimension-2 space-like intersections in the projective Coxeter arrangement associated to $(W, S)_B$. Then E_V is "sandwiched" between $\mathscr{L}_{\text{hyp}}$ and its closure, that is*

$$\mathscr{L}_{\text{hyp}} \subset E_V \subseteq \overline{\mathscr{L}_{\text{hyp}}}.$$

The hyperplane arrangement $\mathscr{L}_{\text{hyp}}$ involved in Theorem 3.5.2 is infinite and not discrete. Figure 3.5 shows part of the Coxeter arrangement of a universal Coxeter group and some intersections in $\mathscr{L}_{\text{hyp}}$.

While Theorem 3.5.2 has a combinatorial flavour, a stronger relation holds. Let $\mathscr{U}_{\text{hyp}}$ be the set of space-like unimodular eigendirections of infinite-order elements. Then the set of limit directions satisfies

$$\mathscr{U}_{\text{hyp}} \sqcup E_\Phi \subseteq E_V \subseteq \overline{\mathscr{U}_{\text{hyp}}}.$$

Notably, space-like weights are all limit directions, as marked by diamonds in Figure 3.5, and roots may also be limit directions.

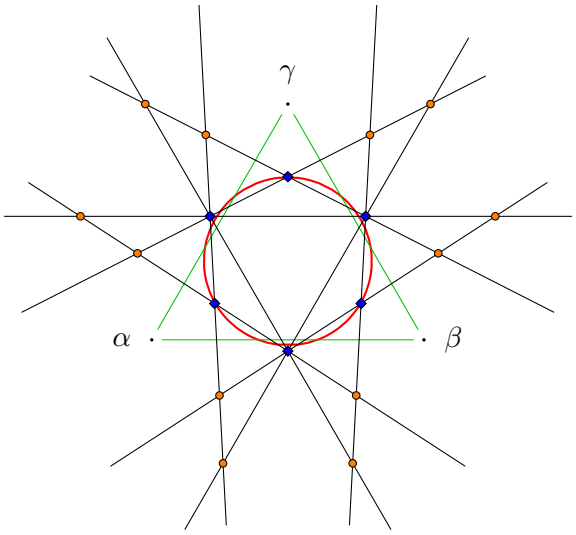

Figure 3.5: Some reflecting hyperplanes in the projective Coxeter arrangement of the universal Coxeter group of rank 3. The associated bilinear form has $c_{ij} = 1.1$ whenever $i \neq j$. Codimension-2 space-like intersections are marked with dots. By Theorem 3.5.2, the intersections in $\mathscr{L}_{\text{hyp}}$ are limit directions. The six intersections marked with diamonds are also weights.

Chapter 4

Packing of grid graphs

This chapter is independent of previous chapters. We study the ball packing of grid graphs, which is motivated by a problem proposed by Benjamini and Schramm [7], which asks for the minimal size of a $(d+1)$-dimensional grid that can not be realised as the tangency graph of a d-ball packing.

In this Chapter, a unit ball is a ball of *curvature* 2, therefore of diameter 1. This is different from Chapter 2. A unit ball centered at the origin will simply be denoted by B_0.

4.1 Grid graphs

Let $\mathbb{Z}$ be the set of integers. For $a \in \mathbb{Z} \cup \{\infty\}$, we use the notation

$$\mathbb{Z}_a = \begin{cases} \{k \mid 0 \leq x < a\} & \text{if } a < \infty, \\ \mathbb{Z} & \text{if } a = \infty. \end{cases}$$

For d integers $a_1, \ldots, a_d \in \mathbb{Z} \cup \{\infty\}$, the *$d$-dimensional grid graph* of size $a_1 \times \cdots \times a_d$ is denoted by $Z_{a_1} \times Z_{a_2} \times \cdots \times Z_{a_d}$. It takes the points in $\mathbb{Z}_{a_1} \times \cdots \times \mathbb{Z}_{a_d}$ as vertices, and two vertices are connected whenever the corresponding points are at distance 1. The ∞ in the subscript are usually omitted. The graph $Z_{a_1} \times Z_{a_2} \times \cdots \times Z_{a_d}$ can also be regarded as the Cartesian product of d paths respectively on $a_1, \ldots, a_d$ vertices. We therefore denote the path graph on n vertices by Z_n. Again ∞ in the subscript will be omitted, so Z denotes the infinite path graph. If the grid has a same size a in k coordinates, we will simply write Z_a^k for short. For example, $Z_2^2 \times Z_3^2$ denotes the $2 \times 2 \times 3 \times 3$ grid graph, Z_2^d denotes the d-dimensional hypercube graph, and Z^d denotes the d-dimensional integer lattice graph.

A grid graph of dimension d is clearly d-ball packable. A standard ball packing of the graph Z^d can be constructed by centering a unit d-ball at each integer point

$\mathbb{Z}^d$. For two sets $X, Y \in \mathbb{R}^d$, the Minkowski sum $X + Y = \{\mathbf{x} + \mathbf{y} \mid \mathbf{x} \in X, \mathbf{y} \in Y\}$. Therefore the standard packing above can be written as

$$\mathsf{B}_0 + \mathbb{Z}^d.$$

Benjamini and Schramm [7] proved that Z^{d+1} is not d-ball packable. They noticed that a sufficiently large $(d+1)$-dimensional grid graph is not d-ball packable, and asked for the size of such a grid. In this chapter, we give a loose upper bound for this size, and construct ball packings explicitly for some grid graphs.

For a vector $\mathbf{x} \in \mathbb{R}^d$, we denote by $\hat{\mathbf{x}}$ the unit vector $\mathbf{x}/\|\mathbf{x}\|$. A *binary combinition* of a set of vectors $\mathbf{x}_1, \ldots, \mathbf{x}_n \in \mathbb{R}^d$ is a point of the form $\sum_{i=1}^n b_i \mathbf{x}_i$ where $b_i \in \mathbb{Z}_2$. We denote by $\mathrm{bin}\{\mathbf{x}_1, \ldots, \mathbf{x}_n\}$ the set of all binary combinations of $\mathbf{x}_1, \ldots, \mathbf{x}_n$. If the vectors are linear independent, $\mathrm{bin}\{\mathbf{x}_1, \ldots, \mathbf{x}_n\}$ is the set of the vertices of the parallelotope spanned by $\mathbf{x}_1, \ldots, \mathbf{x}_n$.

4.2 Packing of $Z^d \times Z_k$

We first construct d-ball packings for the infinite graph $Z^d \times Z_2$. The idea of construction is to interlace two copies of the standard packing $\mathsf{B}_0 + \mathbb{Z}^d$ of Z^d. More specifically, we are looking for a packing in the form of

$$\mathsf{B}_0 + \mathbb{Z}^d + \{0, \hat{\mathbf{x}}\}$$

for some vector $\mathbf{x}$. Since one copy is the translation of the other by an unit vector, the tangency graph is indeed $Z^d \times Z_2$.

However, such a construction does not work for $d \leq 4$. Consider 2^d balls centered at the vertices of the hypercube $\mathbb{Z}_2^d$. If $d < 4$, the space within the hypercube $\mathbb{Z}_2^d$ is too small, in the sense that any unit ball centered within the hypercube has to overlap some balls at the corners. If $d = 4$, only an unit ball centered at the center of the hypercube can avoid overlaps, but it is then tangent to every ball at the corners, so the tangency graph is not correct.

The volume of the unit hypercube is large enough for the construction only if $d > 4$. Let $\mathbf{e} = (\underbrace{1, 1, \ldots, 1}_{d})$, one verifies that

$$\mathsf{B}_0 + \mathbb{Z}^d + \{0, \hat{\mathbf{e}}\}. \tag{4.1}$$

is a d-ball packing for the graph $Z^d \times Z_2$ if $d \geq 5$.

As the dimension increases, the space within the hypercube can become large enough for more balls. In fact, the volumn within the hypercube $\mathbb{Z}_2^d$ is always 1, while

the volume of an unit d-ball is

$$V_d = \frac{(\pi/4)^{d/2}}{\Gamma((d/2)+1)},$$

the fraction of space occupied by the balls at the corners tends to 0 as d tends to infinity. This allows us to interlace more copies of the standard packing of Z^d. For example, by translating the standard packing by integer multiple of $\hat{\mathbf{e}}$, we obtain a d-ball packing

$$\mathsf{B}_0 + \mathbb{Z}^d + \{k\hat{\mathbf{e}} \mid k \in \mathbb{Z}_{\lfloor\sqrt{d}\rfloor-1}\} \tag{4.2}$$

whose tangency graph is $Z^d \times Z_{\lfloor\sqrt{d}\rfloor-1}$.

4.3 Size of packable grids

Theorem 4.3.1. *There is an integer K such that Z_k^{d+1} is not d-ball packable for any $k > K$.*

This is already known to Benjamini and Schramm [7]. Our proof is based on the separation property of ball packings.

Proof. Miller et al. proved in [66] that if a graph $G(V, E)$ is d-ball packable, it has an $O(|V|^{(d-1)/d})$ separator that $(\frac{d+1}{d+2})$-splits. This means that there are two positive real constants C_d and N_d such that, for all $|V| > N_d$, it is possible to remove $C_d|V|^{(d-1)/d}$ vertices from G to partition G into connected components of size at most $\frac{d+1}{d+2}|V|$. We call C_d the *separator bound*. However, the size of a separator of Z_k^{d+1} is at least $k^d = |V|^{d/(d+1)}$. If we take $K = C_d^d$, then for all $k > K$, the size of the separator

$$k^d > C_d k^{(d^2-1)/d} = C_d|V|^{(d-1)/d}.$$

Z_k^{d+1} is therefore not d-ball packable. □

This proof gives C_d^d as an upper bound for the minimal size of a Z_k^{d+1} to be d-ball packable. To the knowledge of the author, the best separator bound C_d is [79]

$$C_d = \frac{2A_{d-1}}{A_d^{1-1/d}V_d^{1/d}} = 2d\left(\frac{V_d}{A_d}\right)^{1-1/d}$$

where A_d is the surface area of a d-sphere of *radius* 1, and V_d is the volume of a d-ball of *radius* 1.

We define $\rho(d)$ to be the maximum number of points in the unit hypercube $\mathbb{Z}_2^d$ such that the minimum distance between any two points, calculated with periodic boundary condition, is at least 1. An upper bound for $\rho(d)$ is $\lfloor 2^n\delta(d)\rfloor$, where $\delta(d)$ is

the *center density* (number of ball centers per unit volume) of the densest unit d-ball packing [27]. The construction in the previous section does not work for $Z^d \times Z_{\rho(d)+1}$ since, by definition, there is no space for $\rho(d)+1$ unit balls within a unit hypercube. This does not prove that $Z^d \times Z_{\rho(d)+1}$ is not d-ball packable, but the intuition strongly leads to the following conjecture.

Conjecture 4.3.2. *The graphs $Z^d \times Z_{\rho(d)+1}$ and $Z^{d+1}_{\rho(d)+1}$ are not d-ball packable.*

4.4 Packing of $Z^d \times Z_2^k$

We now construct a d-ball packing for the graph $Z^d \times Z_2^k$. The idea of construction is the following: Assume that $d = 5k$. We start with the standard packing $\mathsf{B}_0 + \mathbb{Z}^d$ of Z^d. Its projection onto the first five coordinates is the standard packing $\mathsf{B}_0 + Z^5$ of Z^5. Therefore one can safely place a translation $\mathsf{B}_0 + \mathbb{Z}^d + \{\hat{\mathbf{x}}_0\}$ of the standard packing where $\mathbf{x}_0$ points to the diagonal of the first five coordinates. That is,

$$\mathbf{x}_0 = \mathbf{e}_1 + \mathbf{e}_2 + \mathbf{e}_3 + \mathbf{e}_4 + \mathbf{e}_5 = (1, 1, 1, 1, 1, 0, \ldots, 0)$$

where $\mathbf{e}_i$ is the unit vector whose entries are zeros except the i-th entry being 1. Repeat for every five coordinates. Then for the i-th five coordinates ($1 \le i \le k$), a copy of the standard packing $\mathsf{B}_0 + \mathbb{Z}^d$ of Z^d is placed at $\hat{\mathbf{x}}_i$, where $\mathbf{x}_i = \sum_{j=1}^{5} \mathbf{e}_{5(i-1)+j}$. These $\hat{\mathbf{x}}_i$'s are orthogonal and span a unit k-hypercube. One verifies that the copies of the standard packing placed at the vertices of this k-hypercube do not overlap. We have then constructed the following d-ball packing with the tangency graph $Z^d \times Z_2^k$ for $d \ge 5k$:

$$\mathsf{B}_0 + \mathbb{Z}_d + \mathrm{bin}\{\hat{\mathbf{x}}_i \mid 1 \le i \le k\}.$$

This can be slightly improved as follows. Assume that $d = 4k$. We start again with the standard packing $\mathsf{B}_0 + \mathbb{Z}^d$ of Z^d. Its projection onto the first four coordinates is the standard packing $\mathsf{B}_0 + \mathbb{Z}^4$ of Z^4. For any $\varepsilon > 0$, one can place a translation $\mathsf{B} + \mathbb{Z}^d + \hat{\mathbf{x}}_0$ of the standard packing where $\mathbf{x}_0 = \mathbf{e}_1 + \cdots + \mathbf{e}_4 + \varepsilon\mathbf{e}$. Recall that $\mathbf{e}$ is an all-one vector. Since $\varepsilon > 0$, there is no extra tangency relation except those indicated by the edges in $Z^d \times Z_2^k$. Repeat for every four coordinates. Then for the i-th four coordinates ($1 \le i \le k$), a copy of the standard packing is placed at $\hat{\mathbf{x}}_i$ where $\mathbf{x}_i = \sum_{j=1}^{4} \mathbf{e}_{4(i-1)+j} + \varepsilon\mathbf{e}$. One then notice that there exists an $\varepsilon > 0$ such that $\langle \hat{\mathbf{x}}_i - \hat{\mathbf{x}}_j, \hat{\mathbf{x}}_i - \hat{\mathbf{x}}_j \rangle > 1$ for all $i \ne j$, implying that copies placed at the vertices of the parallelotope spanned by $\hat{\mathbf{x}}_i$ ($1 \le i \le k$) do not overlap. We have then constructed the following d-ball packing of the graph $Z^d \times Z_2^k$ for $d \ge 4k$.

$$\mathsf{B}_0 + \mathbb{Z}_d + \mathrm{bin}\{\hat{\mathbf{x}}_i \mid 1 \le i \le k\}.$$

For an integer $k > 0$, let $\Delta(k)$ be the smallest integer such that $Z^{\Delta(k)} \times Z_2^k$ is $\Delta(k)$-ball packable. Our construction gave an upperbound

Theorem 4.4.1.

$$\Delta(k) \leq 4k$$

At this point, we would like to mention a result by [48]. A *d-dimensional dot-product representation* of a graph $G(V, E)$ is a map $f : V \to \mathbb{R}^d$ such that $uv \in E$ if and only if $\langle f(u), f(v) \rangle \geq 1$. It is proved in [48] that

Theorem 4.4.2. *If a graph is d-ball packable, then it has a $(d + 2)$-dimensional dot-product representation.*

It then follows from our construction that

Corollary 4.4.3. *$Z^{d-2} \times Z_2^k$ has a d-dimensional dot-product representation if $d - 2 \geq 4k$.*

This disproves a conjecture, communicated to the author by Prof. Y. WU at a conference in Shanghai [94], and recently also appeared in [56], asserting that a $(d+1)$-cube graph has no d-dot product representation. A first counter-example is obtained by taking $k = 3$ and $d = 14$ in the corollary, which yields a 15-dimensional grid graph that admits a 14-dimensional dot-product representation.

4.5 Packing of $Z_2^{d-1} \times Z_3^2$

All the constructions in the previous sections are unit ball packings. It does not work for a 4-ball packing for the graph $Z_2^3 \times Z_3^2$. In this section, we construct d-ball packings for the graphs $Z_2^{d-1} \times Z_3^2$.

The idea of construction is to find balls of radius r centered at the 2^{d-1} points $(x_1, \underbrace{\pm r, \ldots, \pm r}_{d-1})$. For the last $d - 1$ coordinates, the tangency relations already form a $(d - 1)$-hypercube graph. By the symmetry of the unit hypercube Z_2^{d-1}, we need only to focus on the 2-dimensional half-space $x_2 = x_3 = \cdots = x_d > 0$. If a ball packing of $Z_2^{d-1} \times Z_3^2$ exists, its restriction on this subspace is a disk packing of Z_3^2, in which a circle of radius r is at the coordinate $(x_1, r\sqrt{d-1})$. The calculation is then realized by computer. It turns out that such disk packing exists for $d > 3$. Figure 4.1 shows the results for $d = 4$ and $d = 5$.

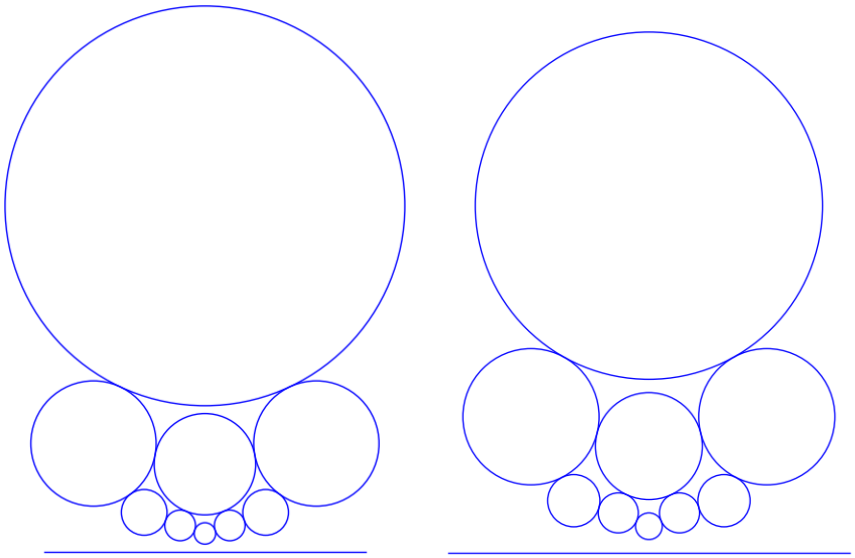

(a) $d = 4$ (b) $d = 5$

Figure 4.1: The packing of $Z_2^{d-1} \times Z_3^2$ restricted to the half-space $x_2 = \cdots = x_d > 0$.

Appendix A

Enumeration of level-2 Coxeter graphs

The list of level-0 Coxeter graphs can be found in [47, Chapter 2]. As observed by Maxwell [62], a graph of level 2 is either connected, or obtained by adding an isolated vertex to a graph of level 1. Coxeter graphs of level 1 are necessarily connected. A complete list is given by Chein in [19] using a FORTRAN program, see also [47, Section 6.9].

Connected Coxeter graphs of level 2 are manually enumerated by Maxwell in [62]. He finds 323 Coxeter graphs of level 2, some of which correspond to the same packing. He then gives a list of 165 graphs, representing different packings generated by these graphs. We follow the suggestion of Maxwell and realize a computer verification of the list along the lines of [19]. The list of level 2 Coxeter graphs is given in the appendix. The current section is dedicated to the description of the algorithm. The algorithm consists of two parts:

Nomination A reasonably short list of candidates covering all the possible Coxeter graphs of level 2 is generated. This is to avoid checking all the graphs with less than 11 vertices.

Recognition Every nominated candidate is passed to a recognition algorithm, and is eliminated if it is not a Coxeter graph of level 2.

A.1 Recognition algorithm

It is used to eliminate false candidates, and to generate the list of level-1 Coxeter graphs, which helps nominating candidates. Instead of following the combinatorial algorithm described in [19], our algorithm takes advantage of developments in computer science. To tell if a matrix M is positive-semidefinite, we use the computer algebra

system Sage to calculate the eigenvalues of M, and look at the sign of the smallest eigenvalue λ. If $\lambda \geq 0$, then M is positive-semidefinite. Since the considered matrices are quite small (size at most 10×10), this process is done fast.

Now consider a Coxeter graph G with its associated matrix B. Checking if G is of finite or affine type is equivalent to checking the positive-semidefiniteness of B as described above. Checking if G is of level $\leq r$ asks to check the positive-semidefiniteness for all the $(n-r) \times (n-r)$ principle minors of B. Consequently, checking if G is of level 2 requires to check if it is of level $\leq$ 2 but not of level ≤ 1.

Remark A.1.1. Sage can numerically calculate the eigenvalues in double precision, which gives 15-17 significant decimal digits. Since the calculation is not in arbitrary precision, it may happen that, for an eigenvalues that equals zero, the program finds a non-zero eigenvalue that is very close to 0. This is however not a problem. In fact, for every finite or affine Coxeter graph with at most 10 vertices, the non-zero eigenvalues of its bilinear form are all bigger than 0.003 according to our test. Therefore, double precision suffices, if all output with absolute value < 0.001 are regarded as zero.

A.2 Nomination of candidates

The nomination of candidates is more technical. In the spirit of [19], we first do some graph theoretical analysis.

As observed by Maxwell [62], a graph of three vertices is of level 2 if it contains a dotted edge, a graph of four vertices is of level ≤ 2 if and only if it contains no dotted edge. It remains to consider graphs of five or more vertices. A level-2 graph with at least five vertices does not contain any dotted edge, and the only admissible labels for an edge is 3, 4, 5 or 6.

Consider a Coxeter graphs G of level 2. Since G is not of level ≤ 1, the deletion of some vertex u from G leaves a graph $G-u$ that is neither finite nor affine. Then $G-u$ is necessarily of level 1. As mentioned before, $G-u$ must be connected. Therefore, a Coxeter graph of level 2 can be obtained by connecting a vertex to a Coxeter graph of level 1. Now let v be any vertex of G. Every connected component of $G-v$ must be of level ≤ 1, therefore in Liste I, Liste II or the list in Appendice of [19]. All these Coxeter graph of level ≤ 1 have at most one cycle, except for three graphs of level 1, namely the complete graph K_4, complete graph minus an edge $K_4 - e$ and the complete bipartite graph $K_{2,3}$.

A.2.1 Graphs constructed from special graphs

If one component of $G-v$ contains more than one cycle, then G is obtained by adding a vertex to K_4, $K_4 - e$ or $K_{2,3}$, putting any admissible label (3, 4, 5 or 6) to the new

edges. This forms our first class of candidates. After passing through the recognition algorithm, Coxeter graphs of level 2 constructed in this way are listed in Figure A.4.

A.2.2 Graphs with two cycles

If $G - v$ contains none of the three special graphs, the argument in [19, Section 3.2] applies and we conclude the following. If G has at least 5 vertices, it has at most 2 cycles. If the number of cycles is exactly 2, the degree of a vertex of G is at least 2. Therefore, for a Coxeter graph with 2 cycles, we have the three possibilities shown in Figure A.1.

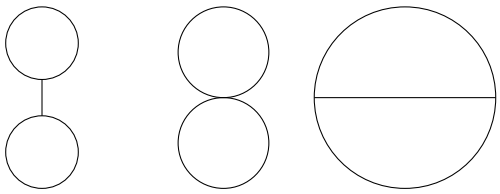

Figure A.1: The three possible forms for a level-2 Coxeter graph with 2 cycles.

We rule out the case on the left, since deletion of two vertices from one of the two cycles leaves a graph that is not of level 0. For the case in the middle, if any of the two cycles contains more than three vertices, deletion of two vertices on that cycle leaves a graph that is not of level 0. The only nominated candidate is therefore the butterfly graph, i.e. two cycles of length 3 sharing a vertex. The butterfly graph is then confirmed by the recognition algorithm as a level-2 graph. For the case on the right, if any of the three paths contains more than two vertices, not counting the ends, deletion of two vertices on that path leaves a graph that is not of level 0. Furthermore, at least two of the three paths contains at least one vertex, otherwise the graph is not simple. Graphs satisfying these two conditions, with any admissible label (3, 4, 5 or 6), are nominated as candidates. After passing through the recognition algorithm, Coxeter graphs of level 2 with two cycles are listed in Figure A.5.

A.2.3 Graphs with one cycle

A graph with only one cycle is either a cycle itself, or formed by attaching some paths to the cycle, i.e., connecting one end of the path to a vertex on the cycle. In the second case, we call the pending paths "tails", and the length of the tail is one plus the length of the path.

If a Coxeter graph of level 1 has at most one cycle, there are three possibilities: a tree, a cycle, or a cycle with one tail of length 1. If a Coxeter graph of level 2 has exactly one cycle, there are four possibilities: a cycle, a cycle with one tail of length 1,

a cycle with two tails of length 1, or a cycle with one tail of length 2. One verifies that a graph can not be of level 2 if it has more or longer tails.

A Coxeter graph of level 2 can be formed in the following ways:

1. Take a tailed cycle of level 1, then append an edge to the tail, with any admissible label (3, 4, 5 or 6). The result is a cycle with a tail of length two.

2. Take a tailed cycle of level 1, then attach an edge to any vertex on the cycle, with any admissible label. The result is a cycle with two pending edges.

3. Take a cycle of level 1, and attach an edge to any vertex on the cycle, with any admissible label. The result is a cycle with a tail of length 1.

4. Take a tree of level 1, then add a new vertex and connect it to any two leaves (vertices of degree 1) of the tree, putting any admissible label to the new edges. It suffices to consider trees with three leaves, since cycles with more than two tails are not of level 2, and cycles with two tails are all considered in the previous case. Among cycles with one tail, we only nominate those with a tail of length one, since cycles with a tail of length two are all considered in the second case, and a longer tail length is not allowed.

5. Take a path of level 1, then add a new vertex and connect it to the two ends of the path, putting any admissible label to the new edges. The result is a cycle.

6. Take a path of level 1, then add a new vertex and connect it to the second and the last vertex on the path, putting any admissible label to the new edges. The result is a cycle with a tail of length 1. However, it turns out that all level 2 Coxeter graphs of this form have been previously nominated, and we find no new graph by this method.

After passing through the recognition algorithm, Coxeter graphs of level 2 in form of a cycle are listed in Figure A.6; those in form of a cycle with one tail of length 1 are listed in Figure A.7 and A.8; those in form of a cycle with one tail of length 2 are listed in Figure A.9; those in form of a cycle with two tails of length 1 are listed in Figure A.10.

A.2.4 Graphs in form of a tree

A tree can be formed by attaching an edge to any vertex on a tree of level 1, with any admissible label (3, 4, 5 or 6). After passing through the recognition algorithm, Coxeter graphs of level 2 in form of a tree are listed in Figures A.11 to A.15.

A.3 Comment on the list

All Coxeter graphs of level 2 found by our algorithm, up to graph isomorphism, are listed in the appended figures. They are grouped according to the nomination method described above, and then subgrouped by number of vertices. The figures are generated using the graph plotting function of Sage [80].

The list given by Maxwell in [62] only includes graphs corresponding to the (group theoretical) maximal elements in each family of Coxeter systems that yield the same packing. Two methods for embedding a Coxeter group as a subgroup of finite index in another Coxeter group can be found in [64]. For checking the result, these embeddings are implemented in the program, and successfully reproduced every graph in Maxwell's list. There are 326 graphs in the present list, while Maxwell's list contains 323 Coxeter graphs of level 2. There are three more rank 5 Coxeter graphs of level 2 in the new list. However, since Maxwell did not list all the graphs that he found, we can not specify which graphs are new.

Finite and affine Coxeter graphs with at most nine vertices are manually input into the program, then level-1 Coxeter graphs are enumerated following Chein's algorithm [19], from which we generate our candidates for Coxeter graphs of level 2. For some graphs in the list, this process can be seen from the arrangement of the edges. For example, for trees, the diagonal edges are from the original level-0 Coxeter graphs, vertical edges are added for constructing level-1 graphs, and horizontal edges are added for constructing level-2 graphs. For cycles with two tails, the cycles are from the original level-0 graphs, edges outside the cycle are added for constructing level-1 graphs, and edges in the cycle are added for constructing level-2 graphs. Colors of vertices indicate its role in the tangency graph: white vertices correspond to imaginary vertices, black and gray vertices correspond to real vertices, and gray vertices are surreal vertices. Some graphs are framed. These graphs of level 2 are *strict* [62, Section 1], meaning that deletion of any two vertices leaves a finite Coxeter graph. In the ball packing generated by a strict Coxeter graph of level 2, no two balls are tangent, i.e. the tangency graph is an empty graph. One can verify that the ball packing generated by a non-strict Coxeter graph of level 2 always contains a pair of tangent balls.

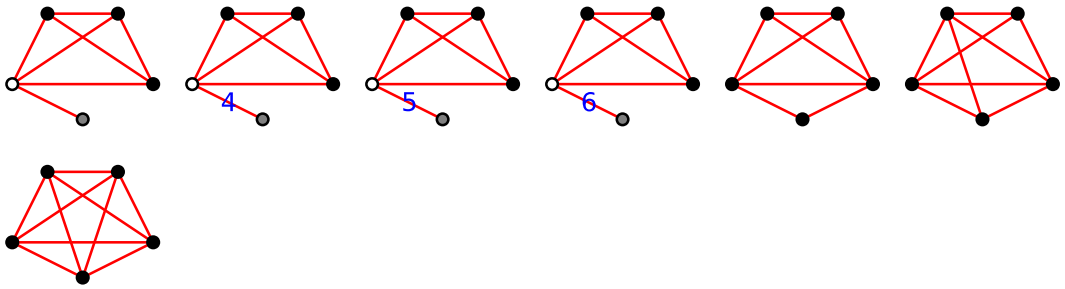

Figure A.2: Graphs constructed from K_4.

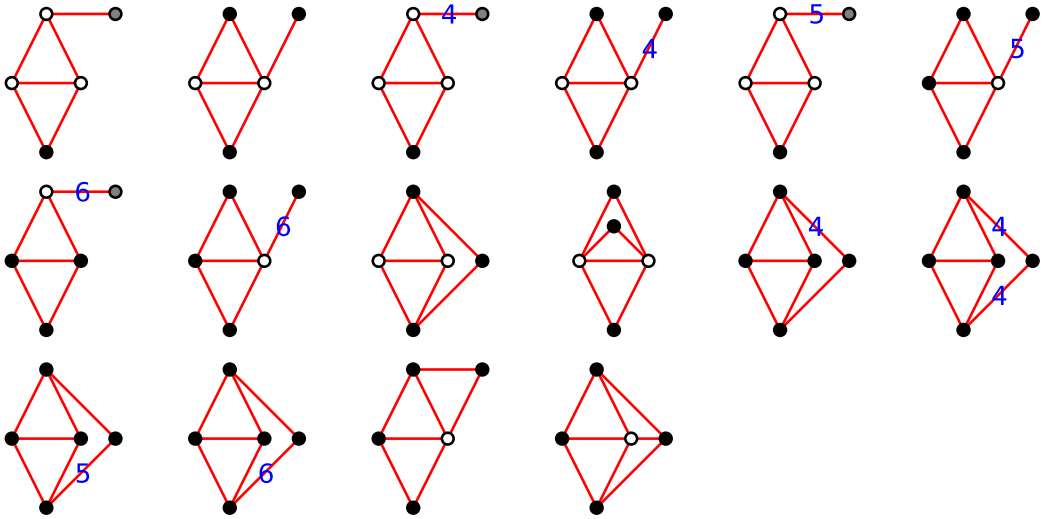

Figure A.3: Graphs constructed from $K_4 - e$.

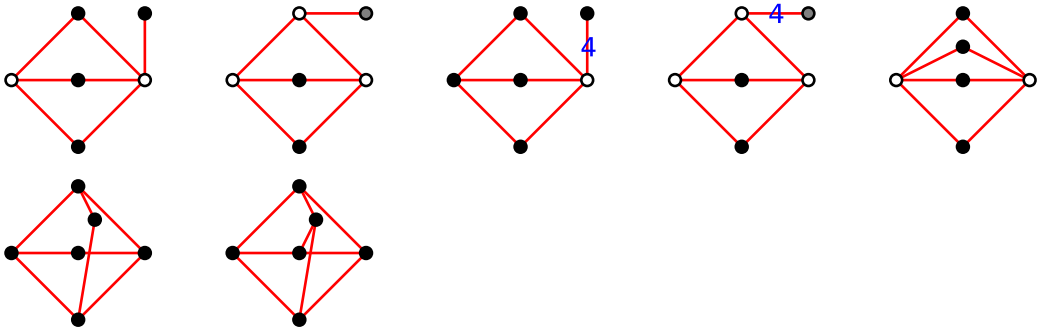

Figure A.4: Graphs constructed from K_{23}.

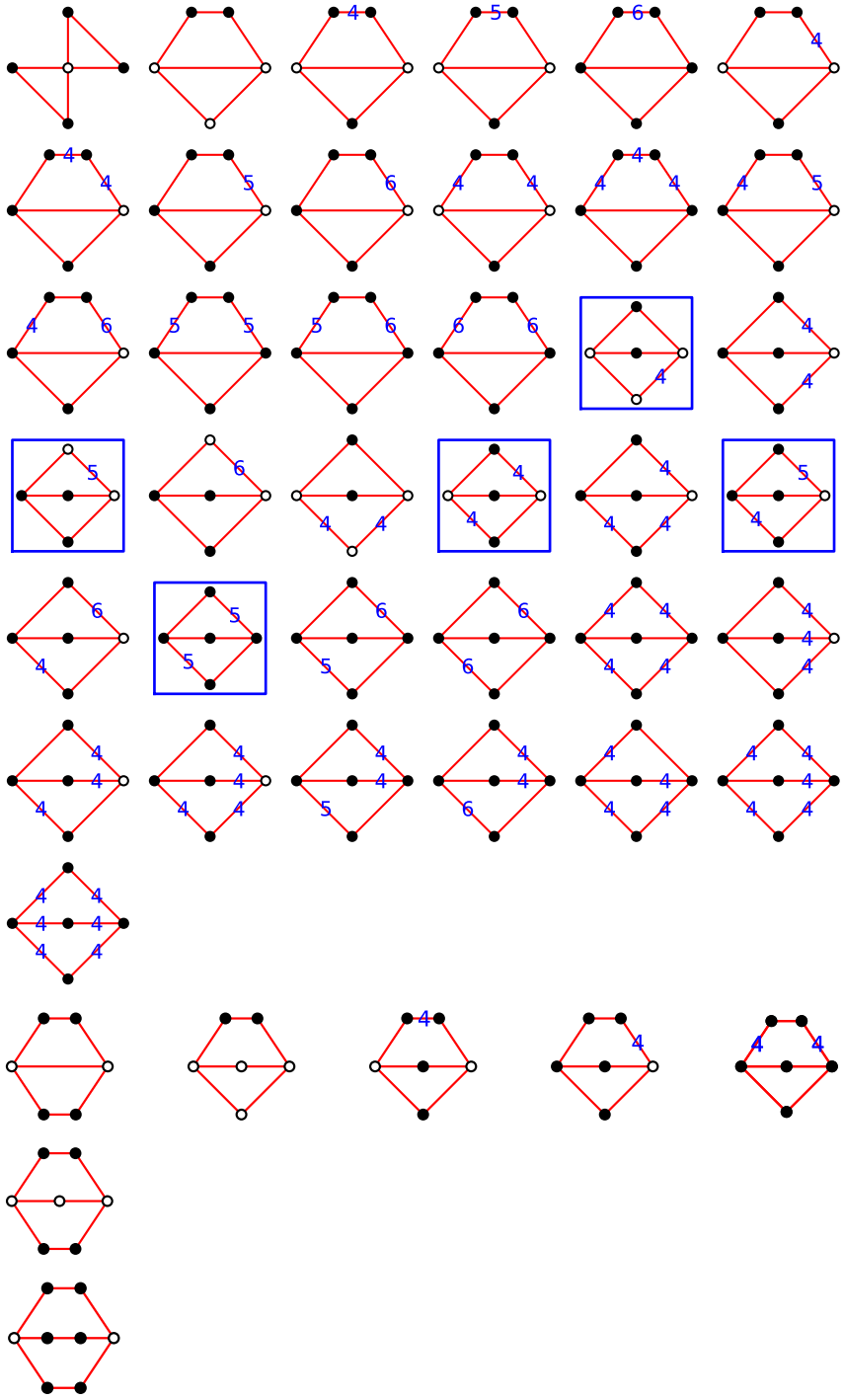

Figure A.5: Graphs with two cycles.

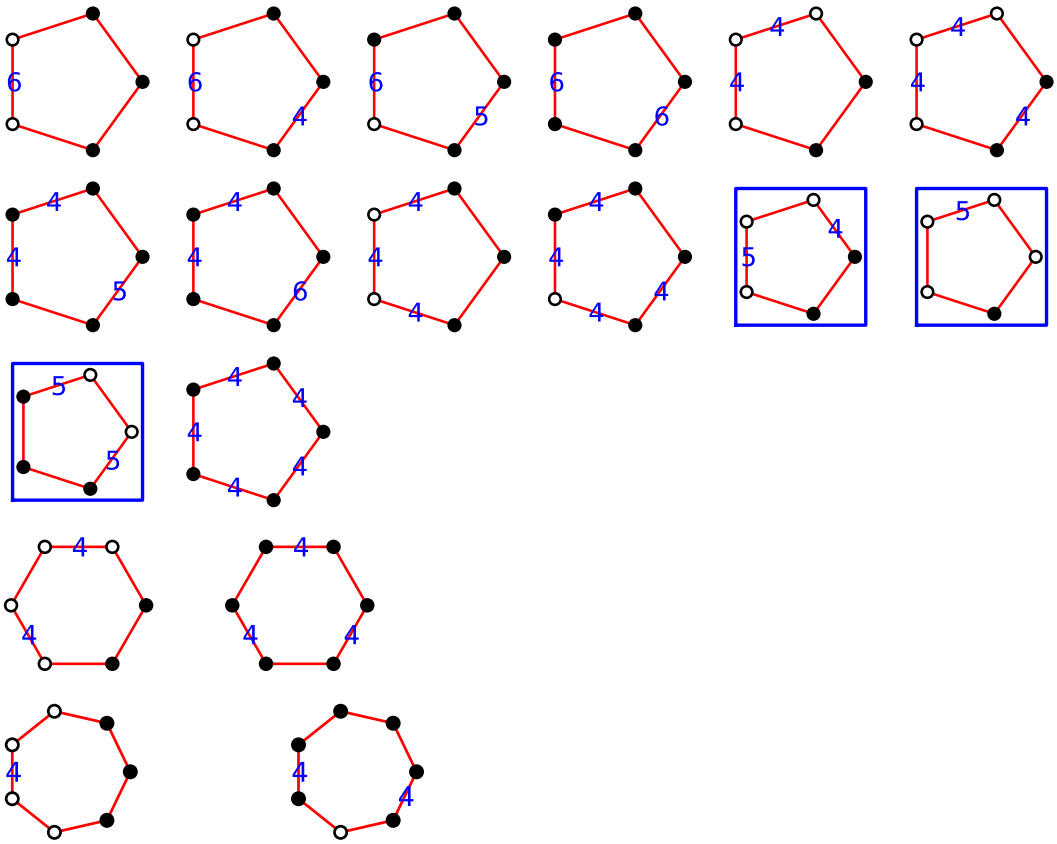

Figure A.6: Cycles

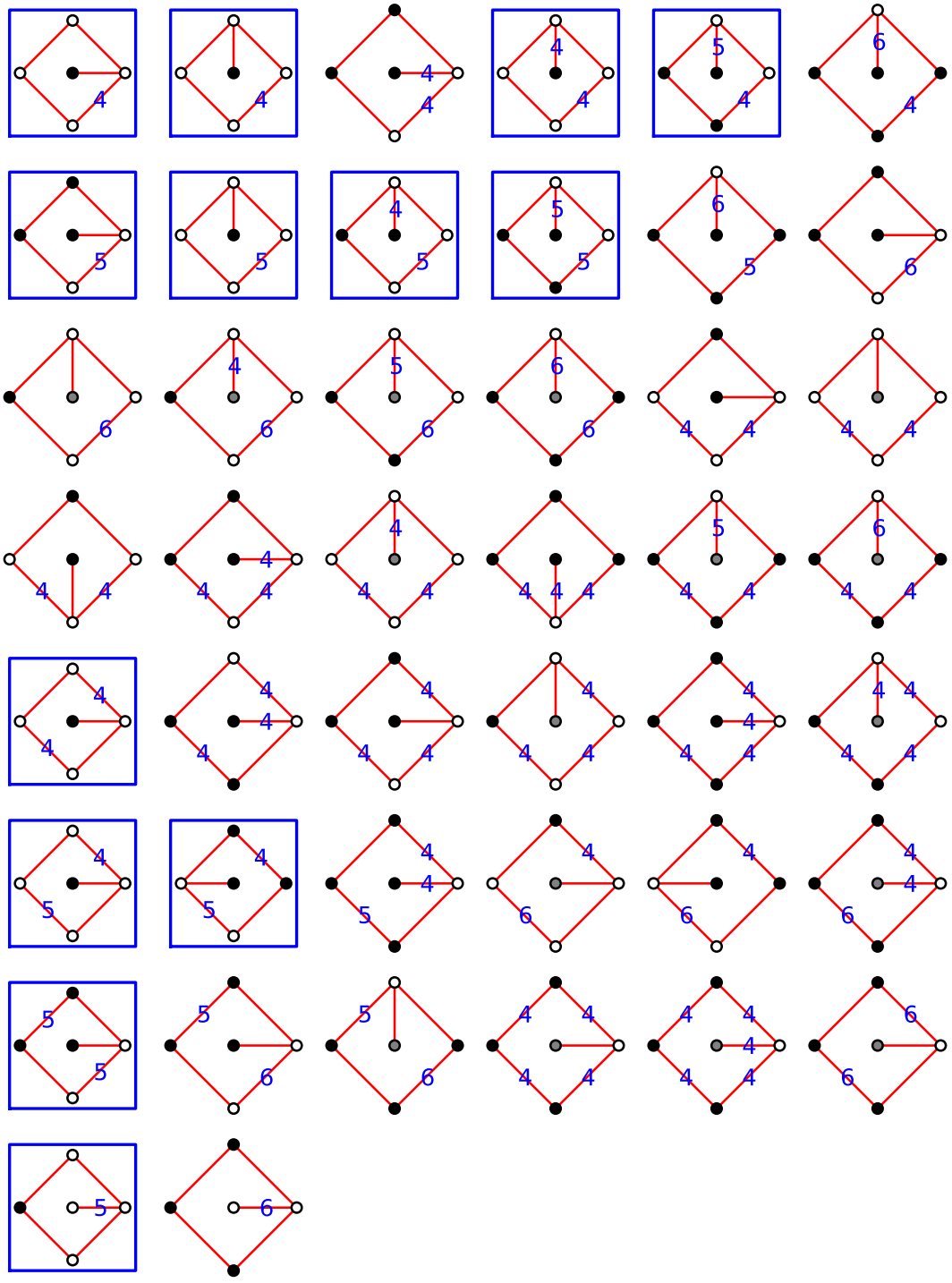

Figure A.7: Cycles with one tail of length 1 (5 vertices)

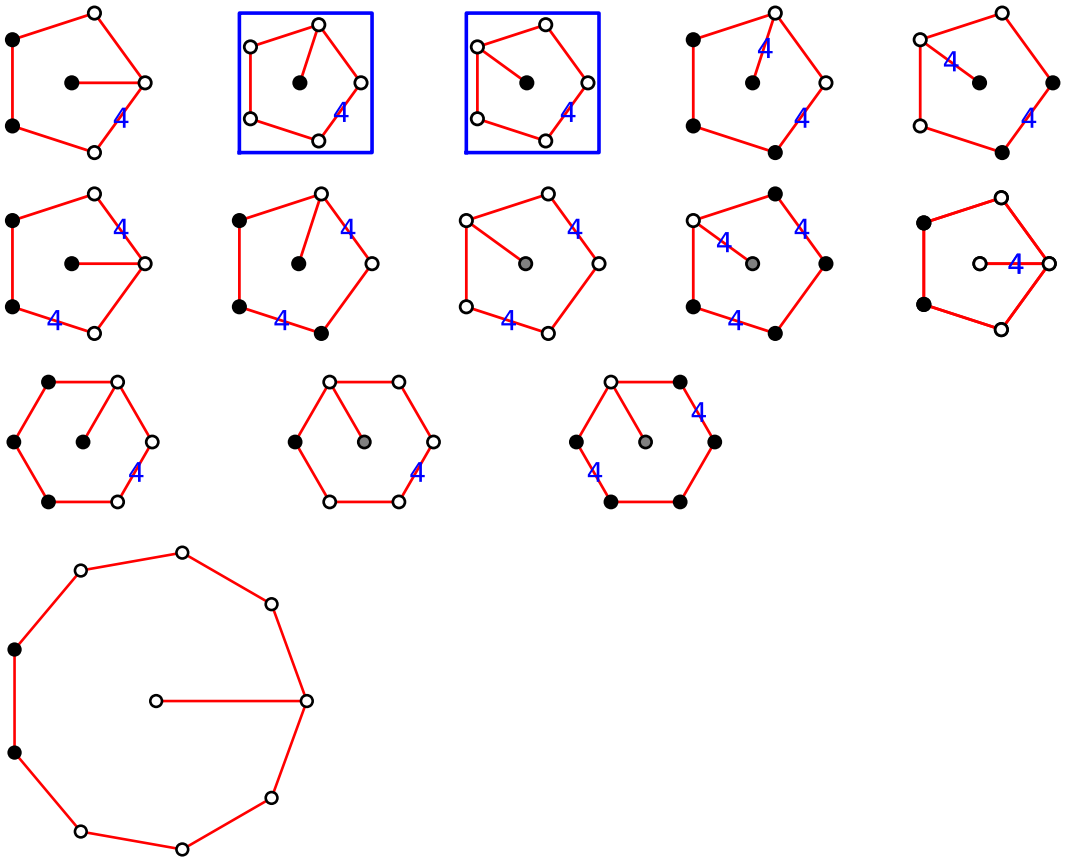

Figure A.8: Cycles with one tail of length 1 (> 5 vertices)

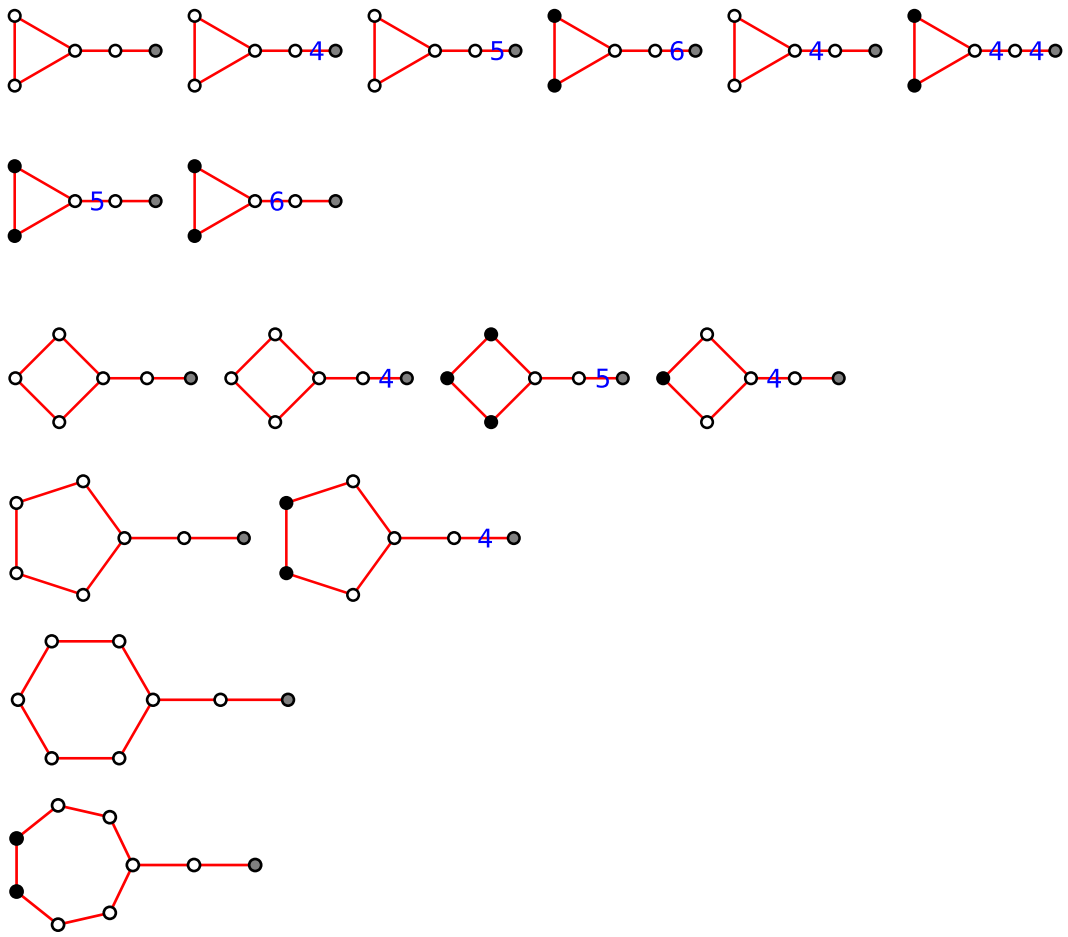

Figure A.9: Cycles with one tail of length 2.

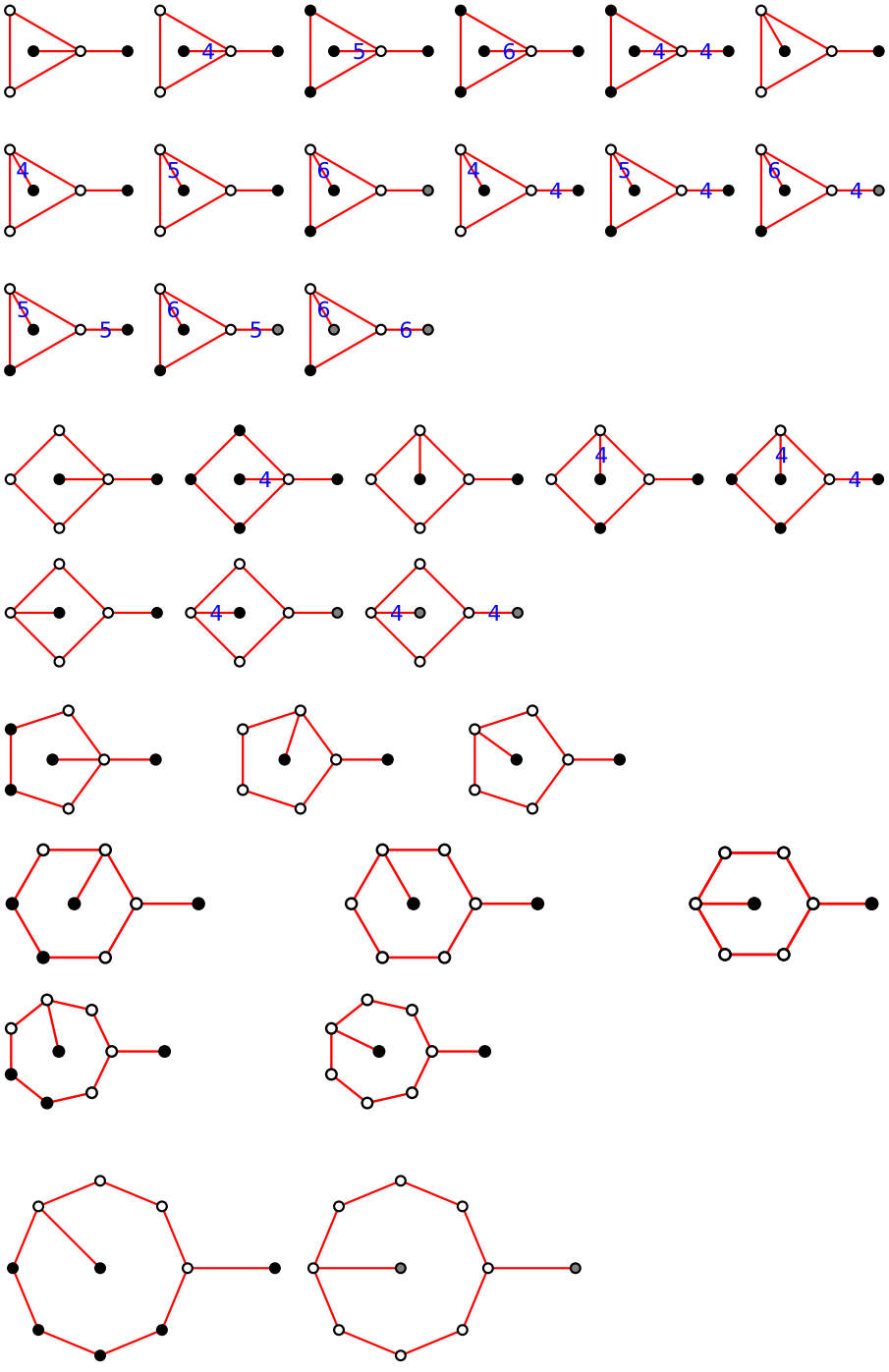

Figure A.10: Cycles with two tails of length 1.

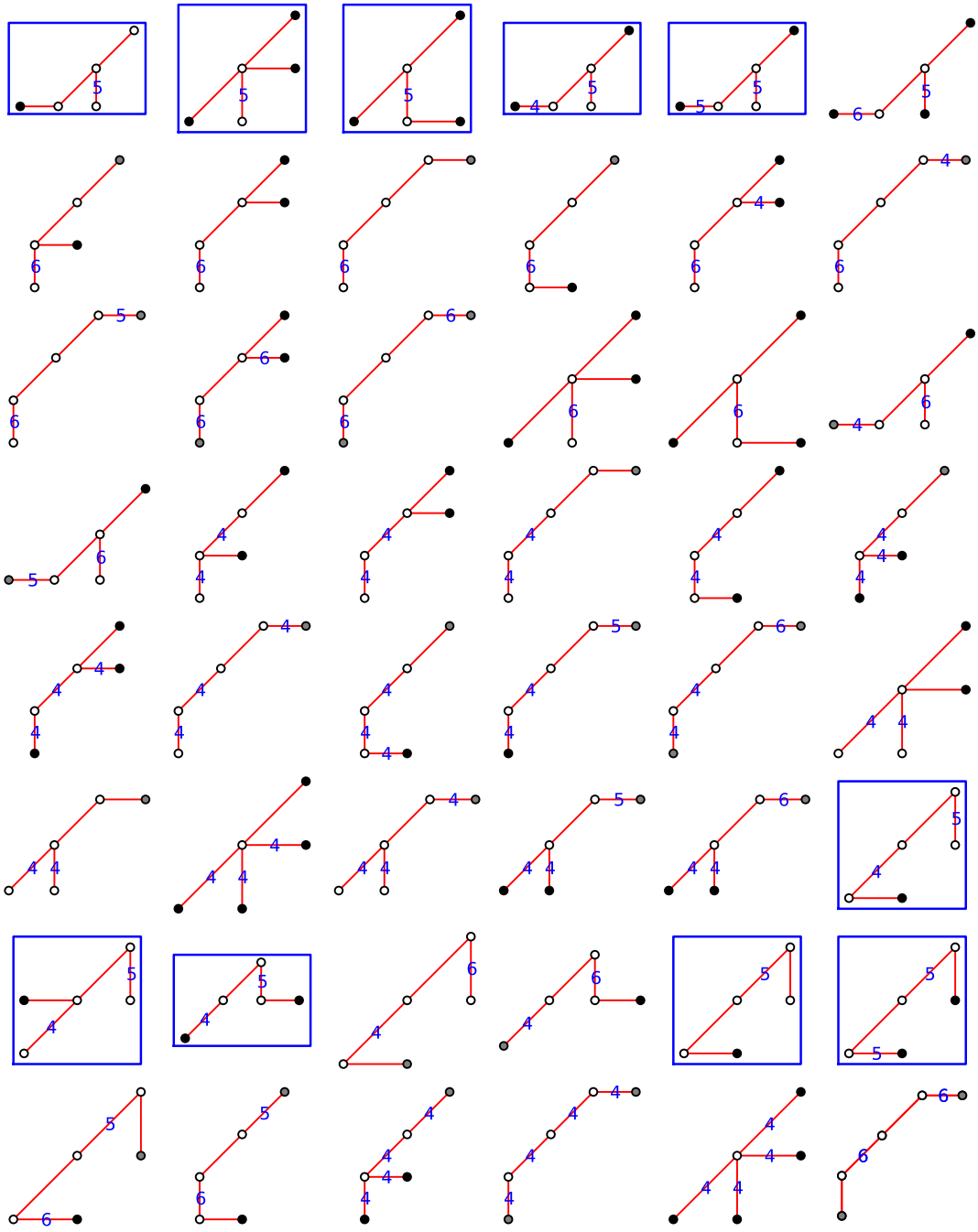

Figure A.11: Trees (5 vertices)

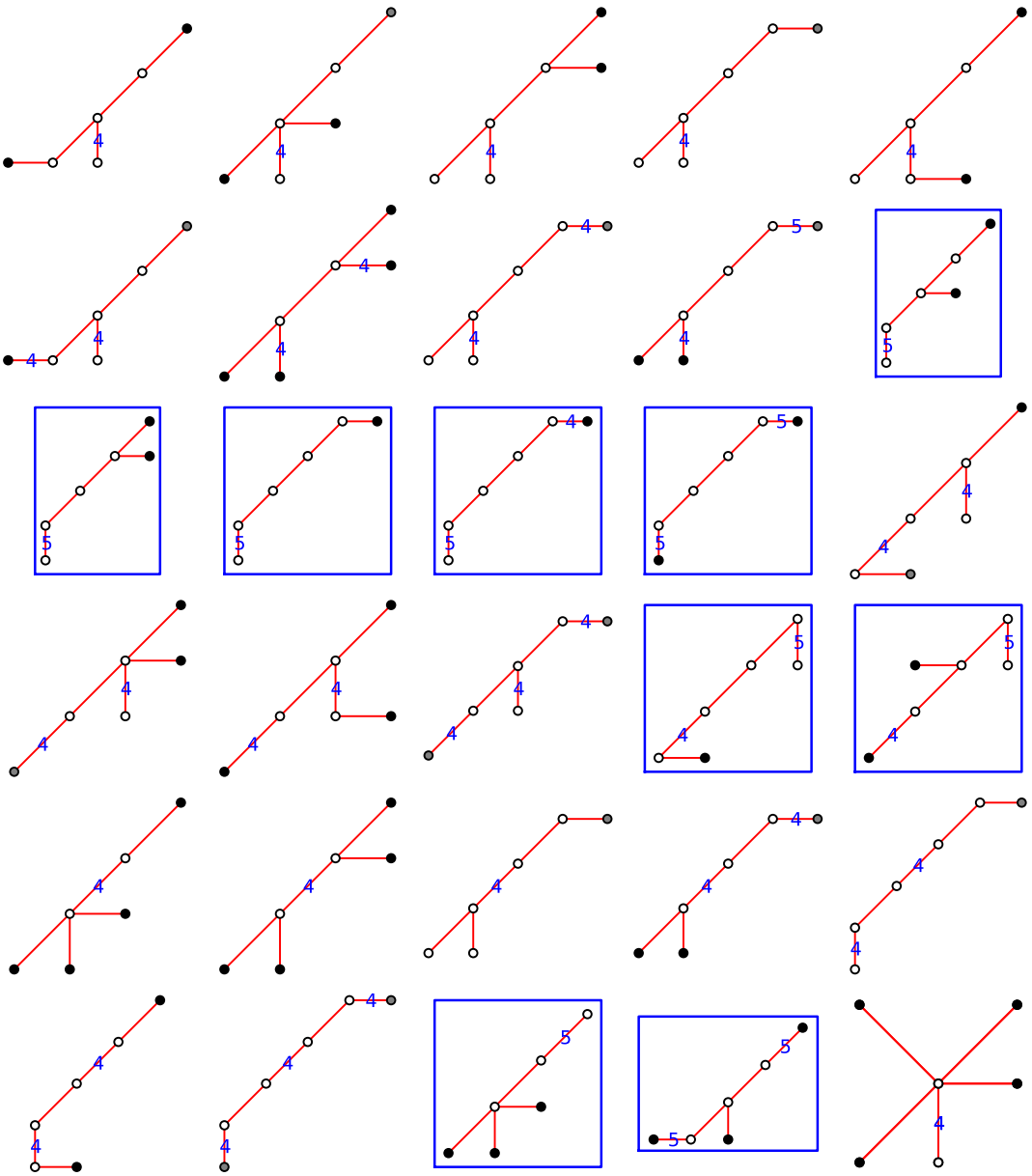

Figure A.12: Trees (6 vertices)

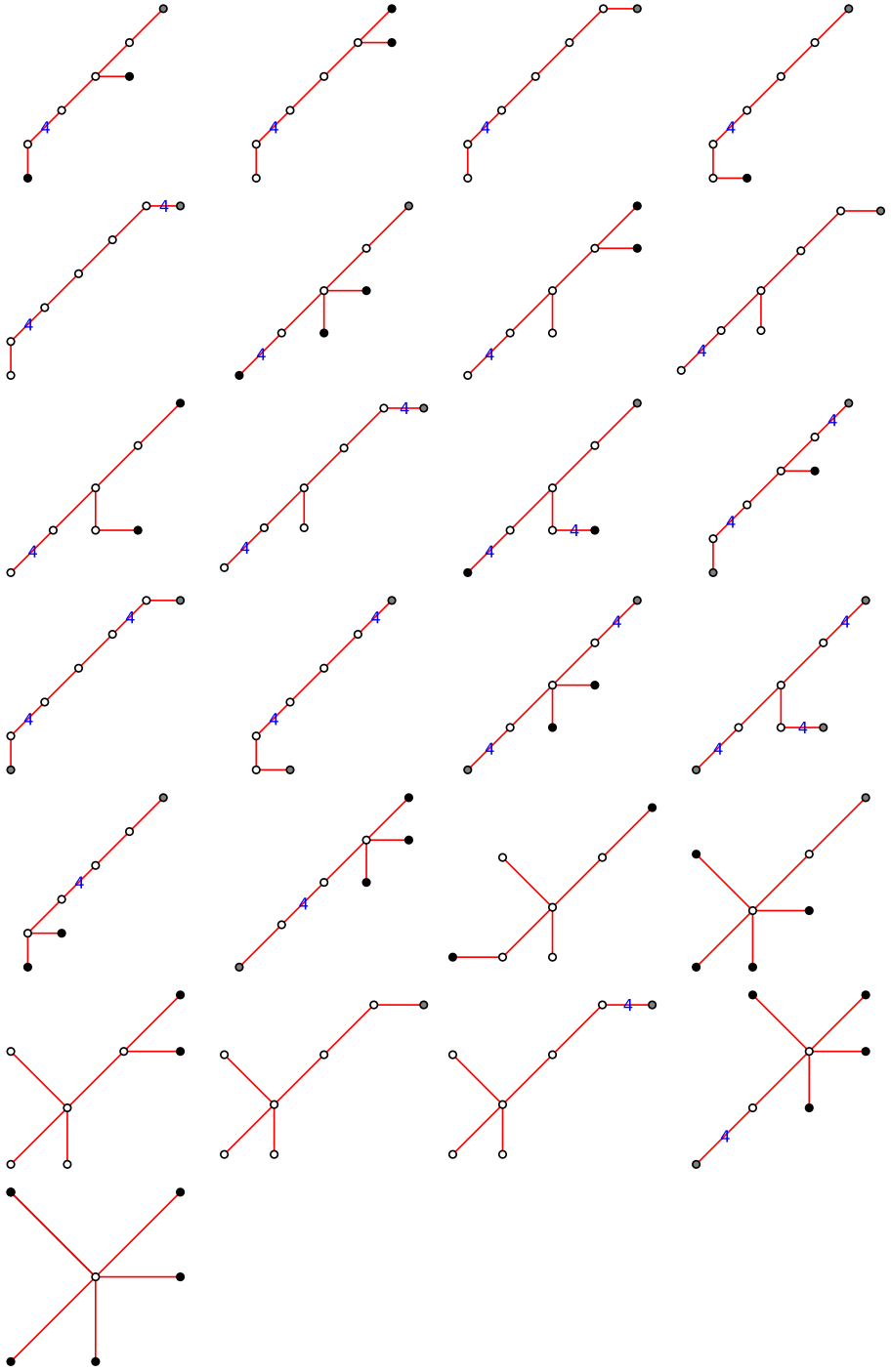

Figure A.13: Trees (7 vertices)

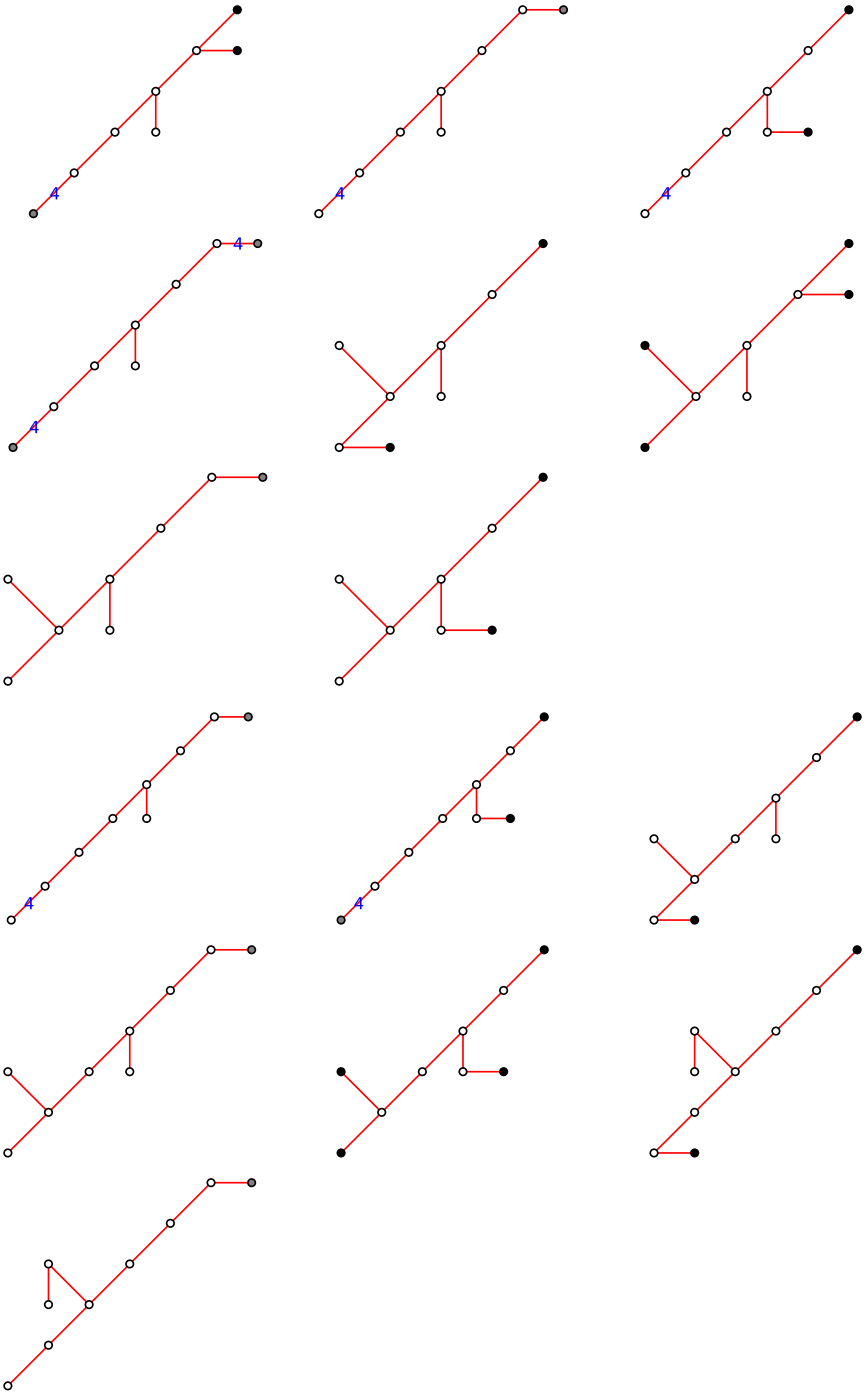

Figure A.14: Trees (8 or 9 vertices)

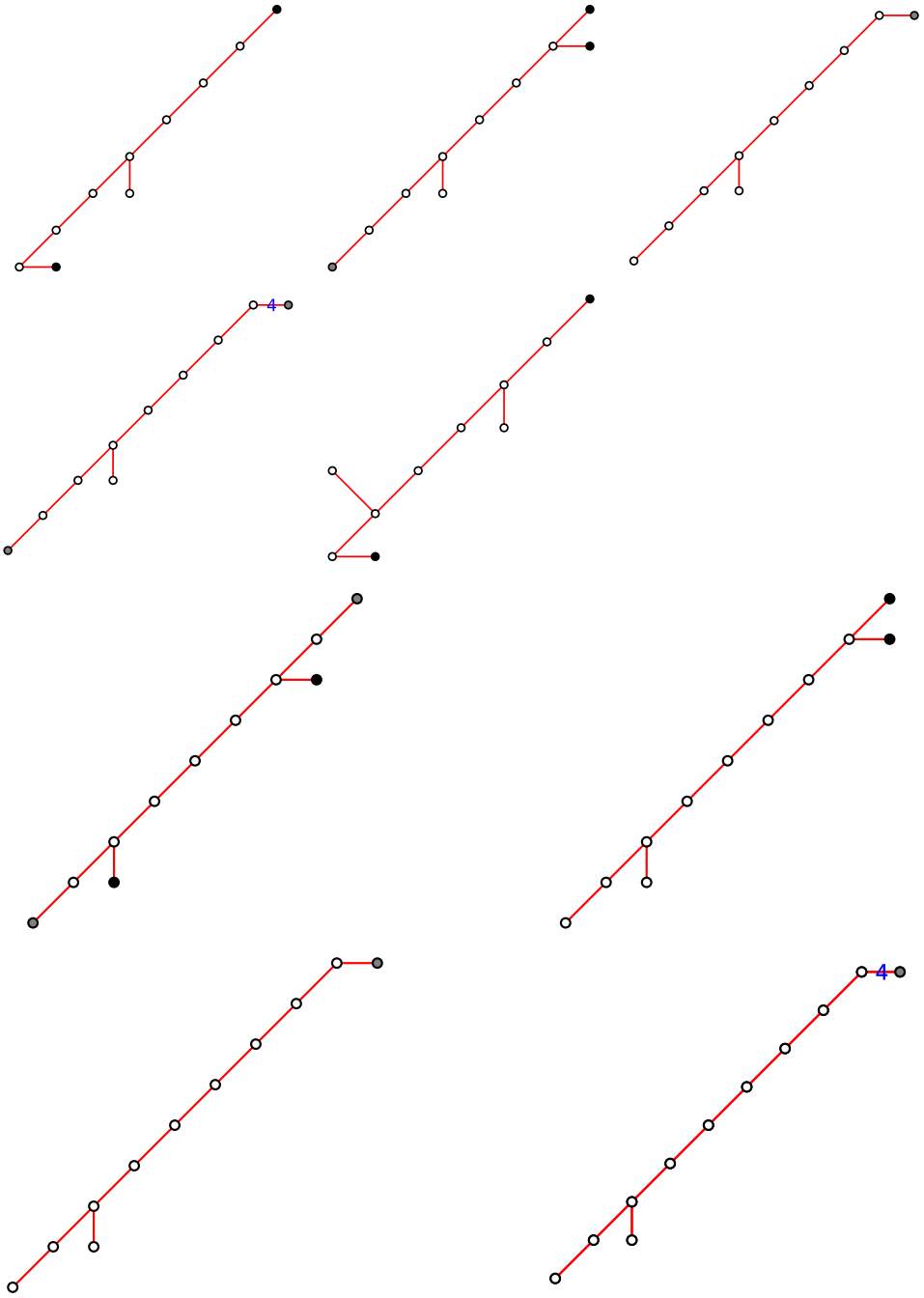

Figure A.15: Trees (10 or 11 vertices)

Zusammenfassung

Während die Kontaktgraphen von Kreispackungen vollständig durch den Satz von Koebe–Andreev–Thurston beschrieben sind, ist weniger über die Kombinatorik von Kugelpackungen in höheren Dimensionen bekannt. Diese Arbeit möchte einen Beitrag zu der Untersuchung von einigen höherdimensionalen Kugelpackungen liefern.

Der Kerngedanke dieser Arbeit ist die Korrespondez zwischen Kugelpackungen im Euklidischen Raum und raumartigen Richtungen im Lorentzraum. Das ermöglicht es uns Kugelpackungen als Punktmengen im projektiven Lorentzraum aufzufassen.

Unsere Untersuchung beginnt mit Descartes–Konfigurationen, der einfachsten Kugelpackung in dieser Arbeit. Sie dient als Grundelement für weitere Konstruktionen. Dann konstruieren wir explizit einige kleine Packungen, dessen Kontaktgraph sich als Join von Graphen darstellen lassen und finden Joins von Graphen, die sich nicht als Kontaktgraph einer Kugelpackung darstellen lassen. Mithilfe dieser Beispiele beschreiben wir die "tangency graphen" von Apollonischen Kugelpackungen in der Dimension 3 durch 1-Skelette von Stapelpolytopen. Für höhere Dimensionen werden Teilresultate erreicht.

Boyd–Maxwell Packungen bilden eine große Klasse von Kugelpackungen, welche von Inversionen erzeugt werden; eine Verallgemeinerung von Apollonischen Packungen. Motiviert durch ihr auftreten in neueren Arbeiten über Grenzwerte von Wurzeln unendlicher Coxetersysteme betachten wir nochmals Boyd–Maxwell Packungen. Außerdem beschreiben wir den Kontaktgraph einer Boyd–Maxwell Packung durch den korrespondierende Coxeterkomplex und vervollständigen die Aufzählung von Coxetergruppen welche diese Packungen erzeugen. Dann schlagen wir weitere Verallgemeinerungen vor, die in viel höheren Dimensionen existieren könnten.

Motiviert durch ein Ergebnis von Benjamini and Schramm untersuchen wir Kugelpackungen dessen Kontaktgraph ein höherdimensionaler Gittergraph ist. Wir bringen eine unscharfe Schranke der Größer solcher Gittergraphen welche eine Kugelpackung zulassen.

Index

Bibliography

[1] Peter Abramenko and Kenneth S. Brown, *Buildings*, GTM, vol. 248, Springer, New York, 2008.

[2] Daniel Allcock, *Infinitely many hyperbolic Coxeter groups through dimension 19*, Geom. Topol. **10** (2006), 737–758. (electronic).

[3] Noga Alon, *Packings with large minimum kissing numbers*, Discrete Math. **175** (1997), no. 1-3, 249–251.

[4] Christine Bachoc and Frank Vallentin, *Optimality and uniqueness of the* $(4, 10, 1/6)$ *spherical code*, J. Combin. Theory Ser. A **116** (2009), no. 1, 195–204.

[5] Bhaskar Bagchi and Basudeb Datta, *Higher-dimensional analogues of the map coloring problem*, Amer. Math. Monthly **120** (2013), no. 8, 733–737.

[6] Eiichi Bannai and Neil J. A. Sloane, *Uniqueness of certain spherical codes*, Canad. J. Math. **33** (1981), no. 2, 437–449.

[7] Itai Benjamini and Oded Schramm, *Lack of sphere packing of graphs via non-linear potential theory* (2010). preprint, available at `arXiv:0910.3071v2 [math.MG]`.

[8] Károly Bezdek and Samuel Reid, *Contact graphs of unit sphere packings revisited*, J. Geom. **104** (2013), no. 1, 57–83.

[9] Alexander I. Bobenko and Boris A. Springborn, *Variational principles for circle patterns and Koebe's theorem*, Trans. Amer. Math. Soc. **356** (2004), no. 2, 659–689.

[10] Michal Borkovec, Walter de Paris, and Ronald Peikert, *The fractal dimension of the Apollonian sphere packing*, Fractals **2** (1994), no. 4, 521–526.

[11] Nicolas Bourbaki, *Groupes et algèbres de Lie. Chapitre 4-6*, Hermann, Paris, 1968 (French).

[12] David W. Boyd, *The osculatory packing of a three dimensional sphere*, Canad. J. Math. **25** (1973), 303–322.

[13] David W. Boyd, *The residual set dimension of the Apollonian packing*, Mathematika **20** (1973), 170–174.

[14] David W. Boyd, *A new class of infinite sphere packings*, Pacific J. Math. **50** (1974), 383–398.

[15] Heinz Breu and David G. Kirkpatrick, *On the complexity of recognizing intersection and touching graphs of disks*, Graph Drawing (Passau, 1995), 1996, pp. 88–98.

[16] Graham R. Brightwell and Edward R. Scheinerman, *Representations of planar graphs*, SIAM J. Discrete Math. **6** (1993), no. 2, 214–229.

[17] Kristal Cantwell, *Chromatic number of graphs of tangent closed balls*, 2010. available at `http://mathoverflow.net/q/8232` (version: 2010-03-12).

[18] Thomas E. Cecil, *Lie Sphere Geometry*, 2nd ed., Universitext, Springer, New York, 2008.

[19] Michel Chein, *Recherche des graphes des matrices de Coxeter hyperboliques d'ordre* ≤ 10, Rev. Française Informat. Recherche Opérationnelle **3** (1969), no. Ser. R-3, 3–16 (French).

[20] Hao Chen, *Distance geometry for kissing spheres* (2012). preprint, available at `arXiv:1203.2131v3 [math.MG]`.

[21] Hao Chen, *Apollonian ball packings and stacked polytopes* (2013). preprint, available at `arXiv:1306.2515v2 [math.MG]`.

[22] Hao Chen and Jean-Philippe Labbé, *Lorentzian Coxeter groups and Boyd-Maxwell Packings* (2013). preprint, available at `arXiv:1310.8608v2 [math.MG]`.

[23] Hao Chen and Jean-Philippe Labbé, *Limit Directions for Lorentzian Coxeter Systems* (2014). preprint, available at `arXiv:1403.1502v1 [math.GR]`.

[24] Henry Cohn and Abhinav Kumar, *Uniqueness of the* $(22, 891, 1/4)$ *spherical code*, New York J. Math. **13** (2007), 147–157.

[25] Henry Cohn and Abhinav Kumar, *Universally optimal distribution of points on spheres*, J. Amer. Math. Soc. **20** (2007), no. 1, 99–148.

[26] Yves Colin de Verdière, *Un principe variationnel pour les empilements de cercles*, Invent. Math. **104** (1991), no. 3, 655–669 (French).

[27] John H. Conway and Neil J. A. Sloane, *Sphere Packings, Lattices and Groups*, 3rd ed., Grundlehren der Mathematischen Wissenschaften, vol. 290, Springer-Verlag, New York, 1999.

[28] Daryl Cooper and Igor Rivin, *Combinatorial scalar curvature and rigidity of ball packings*, Math. Res. Lett. **3** (1996), no. 1, 51–60.

[29] Harold S. M. Coxeter, *Loxodromic sequences of tangent spheres*, Aequationes Math. **1** (1968), 104–121.

[30] René Descartes, *Oeuvres de Descartes, Correspondance IV* (Charles Adam and Paul Tannery, eds.), Léopold Cerf, Paris, 1901 (French).

[31] Matthew Dyer, *Imaginary cone and reflection subgroups of Coxeter groups* (2013). preprint, available at `arXiv:1210.5206v2 [math.RT]`.

[32] Matthew Dyer, Christophe Hohlweg, and Vivien Ripoll, *Imaginary cones and limit roots of infinite Coxeter groups* (2013). preprint, available at `arXiv:1303.6710v2 [math.GR]`.

[33] David Eppstein, Greg Kuperberg, and Günter M. Ziegler, *Fat 4-polytopes and fatter 3-spheres*, Discrete Geometry, 2003, pp. 239–265.

[34] David B. A. Epstein and Robert C. Penner, *Euclidean decompositions of noncompact hyperbolic manifolds*, J. Differential Geom. **27** (1988), no. 1, 67–80.

[35] Meinolf Geck, Gerhard Hiss, Frank Lübeck, Gunter Malle, and Götz Pfeiffer, *CHEVIE—a system for computing and processing generic character tables*, Appl. Algebra Engrg. Comm. Comput. **7** (1996), no. 3, 175–210.

[36] Bernd Gonska and Günter M. Ziegler, *Inscribable stacked polytopes*, Adv. Geom. **13** (2013), no. 4, 723–740.

[37] Thorold Gosset, *"The kiss precise"*, Nature **139** (1937), 62.

[38] Ronald L. Graham, Jeffrey C. Lagarias, Colin L. Mallows, Allan R. Wilks, and Catherine H. Yan, *Apollonian circle packings: number theory*, J. Number Theory **100** (2003), no. 1, 1–45.

[39] Ronald L. Graham, Jeffrey C. Lagarias, Colin L. Mallows, Allan R. Wilks, and Catherine H. Yan, *Apollonian circle packings: geometry and group theory. I. The Apollonian group*, Discrete Comput. Geom. **34** (2005), no. 4, 547–585.

[40] Ronald L. Graham, Jeffrey C. Lagarias, Colin L. Mallows, Allan R. Wilks, and Catherine H. Yan, *Apollonian circle packings: geometry and group theory. III. Higher dimensions*, Discrete Comput. Geom. **35** (2006), no. 1, 37–72.

[41] Thomas Hales and Samuel Ferguson, *The Kepler Conjecture*: *The Hales-Ferguson Proof* (Jeffrey C. Lagarias, ed.), Springer, New York, 2011. Including papers reprinted from Discrete Comput. Geom. **3**6 (2006), no. 1.

[42] Udo Hertrich-Jeromin, *Introduction to Möbius Differential Geometry*, London Mathematical Society Lecture Note Series, vol. 300, Cambridge University Press, Cambridge, 2003.

[43] Akihiro Higashitani, Ryosuke Mineyama, and Norihiro Nakashima, *An analysis of infinite Coxeter groups: the case of type* $(n-1,1)$ *Coxeter matrices* (2013). preprint, available at `arXiv:1212.6617v4 [math.GR]`.

[44] Petr Hliněný, *Touching graphs of unit balls*, Graph Drawing (Rome, 1997), 1997, pp. 350–358.

[45] Christophe Hohlweg, Jean-Philippe Labbé, and Vivien Ripoll, *Asymptotical behaviour of roots of infinite Coxeter groups*, Canad. J. Math. **66** (2014), no. 2, 323–353.

[46] Christophe Hohlweg, Jean-Philippe Préaux, and Vivien Ripoll, *On the limit set of root systems of Coxeter groups and Kleinian groups* (2013). preprint, available at `arXiv:1305.0052v2 [math.GR]`.

[47] James E. Humphreys, *Reflection Groups and Coxeter Groups*, Cambridge Studies in Advanced Mathematics, vol. 29, Cambridge University Press, 1992.

[48] Ross J. Kang, László Lovász, Tobias Müller, and Edward R. Scheinerman, *Dot product representations of planar graphs*, Electron. J. Combin. **18** (2011), no. 1, Paper 216, 14.

[49] Peter Kleinschmidt, *Eine graphentheoretische Kennzeichnung der Stapelpolytope*, Arch. Math. (Basel) **27** (1976), no. 6, 663–667 (German).

[50] Richard Klitzing, *Convex segmentochora*, Symmetry Cult. Sci. **11** (2000), no. 1-4, 139–181. Polyhedra.

[51] Paul Koebe, *Kontaktprobleme der konformen Abbildung*, Ber. Verh. Sächs. Akad. Leipzig **88** (1936), 141–164 (German).

[52] Andrew Kotlov, László Lovász, and Santosh Vempala, *The Colin de Verdière number and sphere representations of a graph*, Combinatorica **17** (1997), no. 4, 483–521.

[53] Daan Krammer, *The conjugacy problem for Coxeter groups*, Group. Geom. Dynam. **3** (2009), no. 1, 71–171.

[54] Greg Kuperberg and Oded Schramm, *Average kissing numbers for non-congruent sphere packings*, Math. Res. Lett. **1** (1994), no. 3, 339–344.

[55] Jeffrey C. Lagarias, Colin L. Mallows, and Allan R. Wilks, *Beyond the Descartes circle theorem*, Amer. Math. Monthly **109** (2002), no. 4, 338–361.

[56] Bo-Jr Li and Gerard Jennhwa Chang, *Dot product dimensions of graphs*, Discrete Appl. Math. **166** (2014), 159–163.

[57] Hiroshi Maehara, *On configurations of solid balls in 3-space: chromatic numbers and knotted cycles*, Graphs Combin. **23** (2007), no. suppl. 1, 307–320.

[58] Hiroshi Maehara and Hiroshi Noha, *On the graph represented by a family of solid balls on a table*, Ryukyu Math. J. **10** (1997), 51–64.

[59] Hiroshi Maehara and Ai Oshiro, *On knotted necklaces of pearls*, European J. Combin. **20** (1999), no. 5, 411–420.

[60] Hiroshi Maehara and Ai Oshiro, *On Soddy's hexlet and a linked 4-pair.*, Discrete and Computational Geometry. Japanese conference, JCDCG '98. Tokyo, Japan, December 9–12, 1998. Proceedings, 2000, pp. 188–198.

[61] George Maxwell, *Hyperbolic trees*, J. Algebra **54** (1978), no. 1, 46–49.

[62] George Maxwell, *Sphere packings and hyperbolic reflection groups*, J. Algebra **79** (1982), no. 1, 78–97.

[63] George Maxwell, *Wythoff's construction for Coxeter groups*, J. Algebra **123** (1989), no. 2, 351–377.

[64] George Maxwell, *Euler characteristics and imbeddings of hyperbolic Coxeter groups*, J. Austral. Math. Soc. Ser. A **64** (1998), no. 2, 149–161.

[65] Curtis T. McMullen, *Hausdorff dimension and conformal dynamics. III. Computation of dimension*, Amer. J. Math. **120** (1998), no. 4, 691–721.

[66] Gary L. Miller, Shang-Hua Teng, William P. Thurston, and Stephen A. Vavasis, *Separators for sphere-packings and nearest neighbor graphs*, J. ACM **44** (1997), no. 1, 1–29.

[67] Oleg Rustumovich Musin, *The problem of the twenty-five spheres*, Russian Math. Surveys **58** (2003), no. 4, 794–795. Translated from Uspekhi Mat. Nauk **58** (2003), no. 4(352), 153–154 (Russian).

[68] Arnold Neumaier and Johan J. Seidel, *Discrete hyperbolic geometry*, Combinatorica **3** (1983), no. 2, 219–237.

[69] Andrew M. Odlyzko and Neil J. A. Sloane, *New bounds on the number of unit spheres that can touch a unit sphere in n dimensions*, J. Combin. Theory Ser. A **26** (1979), no. 2, 210–214.

[70] Florian Pfender and Günter M. Ziegler, *Kissing numbers, sphere packings, and some unexpected proofs*, Notices Amer. Math. Soc. **51** (2004), no. 8, 873–883.

[71] Mikhail N. Prokhorov, *Absence of discrete groups of reflections with a noncompact fundamental polyhedron of finite volume in a Lobachevskiĭ space of high dimension*, Math. USSR Izv. **28** (1987), no. 2, 401–411. Traslated from Izv. Akad. Nauk SSSR Ser. Mat. **50** (1986), no. 2, 413–424 (Russian).

[72] Burt Rodin and Dennis Sullivan, *The convergence of circle packings to the Riemann mapping*, J. Differential Geom. **26** (1987), no. 2, 349–360.

[73] Steffen Rohde, *Oded Schramm: from circle packing to SLE*, Ann. Probab. **39** (2011), no. 5, 1621–1667.

[74] Horst Sachs, *Coin graphs, polyhedra, and conformal mapping*, Discrete Math. **134** (1994), no. 1-3, 133–138. Algebraic and topological methods in graph theory (Lake Bled, 1991).

[75] Oded Schramm, *How to cage an egg*, Invent. Math. **107** (1992), no. 3, 543–560.

[76] Neil J. A. Sloane, Ronald H. Hardin, Warren D. Smith, et al., *Tables of Spherical Codes*. published electronically at `www.research.att.com/~njas/packings/`.

[77] Frederick Soddy, *The hexlet*, Nature **138** (1936), 958.

[78] Frederick Soddy, *The kiss precise*, Nature **137** (1936), 1021.

[79] Daniel A. Spielman and Shang-Hua Teng, *Disk packings and planar separators*, Proceedings of the Twelfth Annual Symposium on Computational Geometry, 1996, pp. 349–358.

[80] William A. Stein et al., *Sage Mathematics Software (Version 6.1.1)*, The Sage Development Team, 2014. `http://www.sagemath.org`.

[81] Kenneth Stephenson, *Circle packing: a mathematical tale*, Notices Amer. Math. Soc. **50** (2003), no. 11, 1376–1388.

[82] Kenneth Stephenson, *Introduction to Circle Packing*: *The theory of discrete analytic functions*, Cambridge University Press, Cambridge, 2005.

[83] Jenő Szirmai, *The optimal ball and horoball packings of the Coxeter tilings in the hyperbolic 3-space*, Beiträge zur Algebra und Geometrie. Contributions to Algebra and Geometry **46** (2005), no. 2, 545–558.

[84] Jenő Szirmai, *The optimal ball and horoball packings to the Coxeter honeycombs in the hyperbolic d-space*, Beiträge Algebra Geom. **48** (2007), no. 1, 35–47.

[85] Jenő Szirmai, *Horoball packings and their densities by generalized simplicial density function in the hyperbolic space*, Acta Math. Hungar. **136** (2012), no. 1-2, 39–55.

[86] William P. Thurston and John W. Milnor, *The Geometry and Topology of Three-Manifolds*, Princeton University Princeton, 1979.

[87] Pavel Tumarkin, *Hyperbolic Coxeter n-polytopes with $n + 2$ facets*, Math. Notes **75** (2004), no. 6, 848–854. Translated from Mat. Zametki **75** (2004), no. 6, 909–916 (Russian).

[88] Pavel Tumarkin, *Compact hyperbolic Coxeter n-polytopes with $n + 3$ facets*, Electron. J. Combin. **14** (2007), no. 1, Research Paper 69, 36 pp. (electronic).

[89] Pavel Tumarkin and Anna Felikson, *On bounded hyperbolic d-dimensional Coxeter polytopes with $d + 4$ hyperfaces*, Trans. Moscow Math. Soc. (2008), 105–151. Translated from Tr. Mosk. Mat. Obs. **69** (2008), 126–181 (Russian).

[90] Jonatan Vasilis, *The ring lemma in three dimensions*, Geom. Dedicata **152** (2011), 51–62.

[91] Èrnest B. Vinberg, *Discrete linear groups that are generated by reflections*, Math. USSR Izv. **5** (1971), no. 5, 1083–1119. Translated from Izv. Akad. Nauk SSSR Ser. Mat. **35** (1971), no. 5, 1072–1112 (Russian).

[92] Èrnest B. Vinberg, *The non-exitence of crystallographic groups of reflections in Lobachevskij spaces of large dimension.*, Trans. Moscow Math. Soc. (1985), 75–112. Translated from Trudy Moskov. Mat. Obshch. **47** (1984), 68–102 (Russian).

[93] John B. Wilker, *Circular sequences of disks and balls*, Notices Amer. Math. Soc. **19** (1972), A.193.

[94] Yaokun Wu. private communication, Shanghai Conference on Algebraic Combinatorics (2012).

[95] Günter M. Ziegler, *Convex polytopes: extremal constructions and f-vector shapes*, Geometric Combinatorics, 2007, pp. 617–691.

Declaration of Authorship

I, Hao Chen, declare that this thesis titled "Ball packings and Lorentzian discrete geometry", and the work presented in it, are my own. I confirm that:

- This work was done wholly or mainly while in candidature for a research degree at Freie Universität Berlin.
- Where any part of this thesis has previously been submitted for a degree or any other qualification at Freie Universität Berlin or any other institution, this has been clearly stated.
- Where I have consulted the published work of others, this is always clearly attributed.
- Where I have quoted from the work of others, the source is always given. With the exception of such quotations, this thesis is entirely my own work.
- I have acknowledged all main sources of help.
- Where the thesis is based on work done by myself jointly with others, I have made clear exactly what was done by others and what I have contributed myself.

Signed: _____

Date: _____